

OWTNM 2018

OWTNM

2018

Bad Sassendorf, Germany

XXVI International Workshop on Optical Wave & Waveguide Theory and Numerical Modelling

Bad Sassendorf, Germany
April 13 – 14, 2018

Proceedings

Proceedings

owtnm2018.uni-paderborn.de

Contact

E-mail: owtnm2018@uni-paderborn.de

Web: owtnm2018.uni-paderborn.de

Dirk Schulz

TU Dortmund University
High Frequency Institute
Friedrich-Wöhler-Weg 4
D-44221 Dortmund
Germany

Phone: ++49(0)231/755-3909

Fax: ++49(0)231/755-4631

E-mail: dirk2.schulz@tu-dortmund.de

Stefan Helfert

FernUniversität Hagen
Lehrgebiet Mikro- und Nanophotonik
Universitätsstraße 27
58084 Hagen
Germany

Phone: ++49(0)2331/987-1144

Fax: ++49(0)2331/987-352

E-mail: Stefan.Helfert@FernUni-Hagen.de

Manfred Hammer

University of Paderborn
Theoretical Electrical Engineering
Warburger Straße 100
33098 Paderborn
Germany

Phone: ++49 (0)5251/60-3560

Fax: ++49 (0)5251/60-3524

E-mail: manfred.hammer@uni-paderborn.de

Proceedings

XXVI International Workshop on Optical Wave & Waveguide Theory and Numerical Modelling,
Bad Sassendorf, April 13 – 14, 2018.

2018 TU Dortmund University, Dortmund, Germany

ISBN 10: 3-921823-98-6 ISBN 13: 978-3-921823-98-9

OWTNM 2018

XXVI International Workshop on Optical
Wave & Waveguide Theory and Numerical Modelling

Bad Sassendorf, Germany, April 13–14, 2018

Proceedings

Acknowledgements

The organizers thank the following institute and companies for their interest and support:



Transregional Collaborative Research Center TRR 142
Warburger Straße 100, D-33098 Paderborn, Germany



Phoenix Software, Software for Micro- and Nano Technologies
P.O. Box 545, 7500 AM Enschede, The Netherlands



JCMwave GmbH
Bolivarallee 22, 14050 Berlin, Germany



CST – Computer Simulation Technology GmbH
Bad Nauheimer Straße 19, 64289 Darmstadt, Germany

Preface

The 26th edition of the International Workshop on Optical Wave & Waveguide Theory and Numerical Modelling (OWTNM) will be held in Bad Sassendorf, Germany, on April 13 & 14, 2018. Since 1992, the annual workshop has been a forum for enthusiastic scientists to exchange ideas, and to discuss problems related to theoretical optics/photonics, computational modelling, and novel device concepts. The organizers hope and expect that the 26th OWTNM will be just as successful as the previous meetings.

Since 2001, for every second year, the yearly OWTNM workshop has been co-located with the European Conference on Integrated Optics (ECIO). Regular attendees experienced the attraction of the larger, then bi-annual ECIO, just as well as they enjoyed the more informal “workshop atmosphere” in the non-ECIO years. In 2016 it was decided to organize the ECIO on a yearly basis, and in 2016 and 2017 the workshop was co-located and partly co-organized with that conference. It was felt, however, that there was a danger that the OWTNM workshop would lose originality and independence, if that arrangement would continue. Respective deliberations of the OWTNM technical committee during the 2017 event in Eindhoven led to the decision to disassociate, at least in 2018, the theory workshop from the ECIO (certainly with mixed feelings). This discussion needs to be continued.

For 2018, however, to tie in with past locations like Saint-Etienne (1999), Eringerfeld / Paderborn (2001), Varese (2006), or Sitges (2012), we decided for a venue that — as we hope — will emphasize the “workshop atmosphere” again. *Bad Sassendorf* in the federal state of North Rhine-Westphalia, Germany, is located roughly midway between Dortmund or Hagen, and Paderborn. The prefix “Bad” indicates a spa town. Since the 10th century, Sassendorf is noted for its salt springs. The workshop will be held on the premises of a converted farmstead, with the former barn serving as our lecture hall. We are fully aware that this constitutes some change with respect to the more recent previous locations in Eindhoven (2017), Warsaw (2016), London (2015), and Nizza (2014).

The OWTNM 2018 encompasses 62 scientific contributions, including eight invited talks, distributed over eight oral and one poster session. The organization could benefit from the financial support of three companies and one institution, which will have posters on display in a separate section of the poster area. Adhering to a tradition of the OWTNM series, a topical collection (formerly a “special issue”) of the journal *Optical and Quantum Electronics* will be organized on the occasion of the workshop.

We are looking forward to an enjoyable, scientifically inspiring OWTNM 2018.

Dortmund, Hagen, and Paderborn, March 2018
The local steering committee

Organization

Local Steering Committee OWTNM 2018

- Claudia Hagemeyer
- Jens Förstner
- Andrej Hein
- Lena Ebers
- Samer Alhaddad
- Manfred Hammer
Paderborn University

- Stefan Helfert
FernUniversität Hagen

- Lukas Deinert
- Niclas Hildebrandt
- Hendrik Kleene
- Dirk Schulz
- Lukas Schulz
TU Dortmund University

OWTNM Technical Committee

- Arti Agrawal, City University of London, UK
- Trevor Benson, University of Nottingham, UK
- Jiří Čtyroký, Institute of Photonics and Electronics, Czech Academy of Sciences, Czech Republic
- Anne-Laure Fehrembach, Institut Fresnel, Marseille, France
- Manfred Hammer, Paderborn University, Germany
- Stefan Helfert, FernUniversität Hagen, Germany
- Bastiaan de Hon, Eindhoven University of Technology, The Netherlands
- Andrei Lavrinenko, Technical University of Denmark, Lyngby, Denmark
- Marian Marciniak National Institute of Telecommunications, Warsaw, Poland
- Andrea Melloni, Politecnico di Milano, Italy
- Ivan Richter, Czech Technical University, Prague, Czech Republic
- Dirk Schulz, TU Dortmund University, Germany
- Christoph Wächter, Fraunhofer IOF, Jena, Germany

Program

Workshop Schedule

Thursday, April 12, 2018

19:00 – 21:00	<i>Welcome reception & early registration</i>
---------------	---

Friday, April 13, 2018

08:00 – 16:00		<i>Registration</i>
08:55	Welcome address	
09:00 – 10:15	O-1: Functional devices	
	<i>Coffee break</i>	
10:45 – 12:00	O-2: Quantum optics / active devices	
	<i>Lunch</i>	
13:00 – 14:30	O-3: Numerical methods	
	<i>Coffee break</i>	
15:00 – 16:30	O-4: Waveguide theory	
	<i>Drinks</i>	
16:30 – 18:30	Poster session	
19:00	<i>Workshop dinner</i>	

Saturday, April 14, 2018

08:30 – 10:00		<i>Registration</i>
09:00 – 10:15	O-5: Plasmonics	
	<i>Coffee break</i>	
10:45 – 12:00	O-6: Nonlinear photonics	
	<i>Lunch</i>	
13:00 – 14:30	O-7: Biosensing and metamaterials	
	<i>Coffee break</i>	
15:00 – 16:15	O-8: Functional (nano-) photonics	
16:15	Closing remarks	

Friday 09:00 – 10:15, O-1: Functional devices

09:00	O-1.1	D.N. Chigrin (invited), <i>Multiphysics simulations in nanophotonics</i>	1
09:30	O-1.2	L. Ebers, M. Hammer, J. Förstner, <i>Slab waveguide steps with rounded corners at oblique incidence</i>	2
09:45	O-1.3	N. Dhingra, J.C. Song, G.J. Saxena, E.K. Sharma, B.M.A. Rahman, <i>Germanium Telluride Phase Change Material based 1×2 Electro-Optic Switch</i>	3
10:00	O-1.4	A.E. Kaplan, A. Parini, G. Bellanca, P. Bassi, S. Trillo, <i>A Compact Wavelength Router Dynamically Reconfigurable through Destructive Interference</i>	4

Friday 10:45 – 12:00, O-2: Quantum optics / active devices

10:45	O-2.1	J. Münzberg, A. Vetter, F. Beutel, W. Hartmann, S. Ferrari, W. Pernice, C. Rockstuhl (invited), <i>Design of integrated quantum optical single-photon detectors</i>	5
11:15	O-2.2	P.-I. Schneider, L. Zschiedrich, X. Garcia-Santiago, S. Burger, <i>Optimization of quantum optical devices with machine learning</i>	6
11:30	O-2.3	F. Spallek, A. Buchleitner, T. Wellens, <i>Upconversion in optimized photonic multilayer structures</i>	7
11:45	O-2.4	H. Lüder, M. Gerken, <i>FDTD modelling of nanostructured OLEDs: analysis of simulation parameters for accurate radiation patterns</i>	8

Friday 13:00 – 14:30, O-3: Numerical methods

13:00	O-3.1	N. Gregersen, J. R. de Lasson, L. H. Frandsen, O.S. Kim, O. Breinbjerg, F. Wang, O. Sigmund, A. Ivinskaya, A. Lavrinenko, P. Gutsche, S. Burger, T. Häyrynen, J. Mørk (invited), <i>Benchmarking state-of-the-art optical simulation methods for analyzing large nanophotonic structures</i>	9
13:30	O-3.2	G. Granet, <i>Multidomain spectral method for optical-waveguide analysis</i>	10
13:45	O-3.3	H. Kleene, D. Schulz, <i>An Assessment of Faber Polynomial Expansions for the Time Domain Solution of Maxwell's equations</i>	11
14:00	O-3.4	M.M.R. Elsayy, G. Renversez, <i>Vector solver for 2D highly nonlinear plasmonic waveguides: a rigorous analysis</i>	12
14:15	O-3.5	R. Kumar, A. Sharma, <i>Analysis of Absorption in the Absorbing Boundary Condition</i>	13

Friday 15:00 – 16:30, O-4: Waveguide theory

15:00	O-4.1	S. Phang, A. Vukovic, F. Fotsa-Ngaffo, G. Gradoni, S.C. Creagh, P.D. Sewell, T. Benson (invited), <i>Non-Hermitian Photonics from Parity-Time Symmetry to Pseudo-Hermitian Structures</i>	14
15:30	O-4.2	L. Cahill, <i>Field Solutions for Large Area Graded-Index Waveguides</i>	15
15:45	O-4.3	P. Kwiecien, I. Richter, V. Kuzmiak, J. Čtyroký, <i>Magneto-optic Rigorous Coupled Wave Analysis – numerical investigation of nonreciprocal waveguiding structures</i>	16
16:00	O-4.4	A.-L. Fehrembach, B. Gralak, A. Sentenac, <i>Vectorial semi-analytical model for Fano resonances in guided mode resonance gratings</i>	17
16:15	O-4.5	L. Yuan, Y.Y. Lu, <i>Bound States in the Continuum Surrounded by Ultra-strong Resonances</i>	18

Friday, 16:30 – 18:30: Poster session

P-01	D. Pereira-Martín, A. Sánchez-Postigo, A. Hadij-Elhouati, D.-X. Xu, P. Cheben, R. Halir, Í. Molina-Fernández, A. Ortega-Moñux, J.G. Wangüemert-Pérez, <i>Automatic design of high-performance fiber-chip surface grating couplers based on Floquet-Bloch mode analysis</i>	19
P-02	G. Demésey, G. Renversez, <i>Full-vector finite element 3D model for waveguide-based plasmonic sensors</i>	20
P-03	A.A. Shcherbakov, T. Kämpfe, Y. Jurlin, <i>Simulation of luminescence in periodically structured layers based on direct S-matrix calculation</i>	21
P-04	A.A. Shcherbakov, <i>Using spline interpolation for grating geometry description within the curvilinear coordinate Generalized Source Method</i>	22
P-05	T. Aso, T. Ishiguro, J. Yamauchi, H. Nakano, <i>Reduction in Bend Loss of a Si-wire Waveguide by Adjusting the Core Location</i>	23
P-06	J. Yamauchi, Y. Nakagawa, T. Tsuchiya, H. Nakano, <i>A Polarization Converter Consisting of a Bent Si-wire Waveguide</i>	24
P-07	J. Yamauchi, N. Takahashi, H. Ito, H. Nakano, <i>Polarization-dependent and -independent Absorbers with a Periodic Metal Grating</i>	25
P-08	J. Yamauchi, K. Shimada, R. Ando, H. Nakano, <i>Effectiveness of a Curvilinear Taper in Waveguide Applications</i>	26
P-09	J. Yamauchi, R. Nakada, H. Nakano, <i>Study of a Quarter-wave Plate Using an Array of Cross-shaped Apertures in a Metallic Plate</i>	27
P-10	J. Yamauchi, Y. Tanaka, S. Yoshino, H. Nakano, <i>Study of Perforated Metal Sheets Based on Square and Rectangular Lattices</i>	28
P-11	J. Yamauchi, T. Okawachi, D. Shimamura, H. Nakano, <i>Orthogonal Polarization Rotator for Arbitrary Incidence Plane of Polarization</i>	29
P-12	S.F. Helfert, J. Jahns, <i>Application of the Talbot-effect to the structured illumination of hollow waveguide arrays: numerical simulations</i>	30
P-13	V. Burdin, A. Bourdine, <i>A System of Nonlinear Characteristic Equations for Two-Mode Propagation in Step-Index Optical Fiber</i>	31
P-14	A. Bourdine, V. Burdin, <i>Simulation and Research of Few-Mode Optical Fiber DMD Degradation due to Geometry Deviation From Optimized Form</i>	32
P-15	A. Waqas, D. Melati, A. Melloni, <i>Polynomial chaos based stochastic augmented building block for process design kits</i>	33
P-16	S. Sunder, A. Sharma, <i>Evolution of Modes in Photonic Lanterns</i>	34
P-17	M. Hammer, L. Ebers, J. Förstner, <i>Oblique quasi-lossless excitation of a thin silicon slab waveguide</i>	35
P-18	P. Pareek, N. Malviya, V. Palodiya, <i>Steady State Analysis of SiGeSn/GeSn Interband MQWIP</i>	36
P-19	A. Abdrabou, Y.Y. Lu, <i>Families of Exceptional Points in Period Slabs</i>	37
P-20	M. Balasubrahmaniam, A. Nahata, S. Mujumdar, <i>Anderson Localization in 1D plasmonic terahertz waveguides</i>	38
P-21	C. Spenner, H. Kleene, P. Sarapukdee, K. Kallis, D. Schulz, <i>Analysis of SiO₂- and MgF₂-Based Surface Plasmon Resonance Sensors</i>	39
P-22	F. Binkowski, L. Zschiedrich, S. Burger, <i>Analysis of light-matter interaction of optical sources with dispersive nanoresonators via contour integration</i>	40
P-23	M.H. Muhammad, K.R. Mahmoud, M.F.O. Hameed, S.S.A. Obayya, <i>Optimization of Random Grating Thin Film Solar Cell</i>	41
P-24	A.H.K. Mahmoud, M.F.O. Hameed, M. Hussein, S.S.A. Obayya, <i>Highly efficient light trapping design for thin film solar cell</i>	42
P-25	Y. Abd El Hak, A.M.A. Said, S.S.A. Obayya, <i>Blocked Schur for Optical Discontinuity Analysis in Cylindrical Coordinates</i>	43
P-26	K.S.R. Atia, A.M. Heikal, S.S.A. Obayya, <i>Mass Redistributed Finite Element Time Domain Beam Propagation Method for Photonic Devices</i>	44
P-27	J.A.H. Odoeze, M.F.O. Hameed, H.M.H. Shalabyz, S.S.A. Obayya, <i>Novel Design of Photonic Crystal Fiber TE-Pass Polarizer</i>	45

Saturday 09:00 – 10:15, O-5: Plasmonics

09:00	O-5.1	A. Trügler (invited), <i>Plasmon and phonon polariton mapping in an electron microscope</i>	46
09:30	O-5.2	M. Burda, P. Kwiecien, I. Richter, <i>Nonlocal resonant behavior in plasmonic nanostructures: analytical and numerical approaches</i>	47
09:45	O-5.3	V. Myroshnychenko, N. Nishio, F.J. García de Abajo, J. Förstner, N. Yamamoto, <i>Nanoscale Imaging of Plasmon Modes of Metal Nanoparticles by Cathodoluminescence Spectroscopy</i>	48
10:00	O-5.4	T. Weiss, E.A. Muljarov, <i>On the mechanisms of plasmon-enhanced chiroptical response</i>	49

Saturday 10:45 – 12:00, O-6: Nonlinear Photonics

10:45	O-6.1	K. Busch (invited), <i>Atom-Surface Interaction: Theory and Computations</i>	50
11:15	O-6.2	W. Spiller, <i>The numerical investigation of colliding optical solitons as an all-optical-Gate using the Method of Lines (MoL)</i>	51
11:30	O-6.3	V. Jandieri, R. Khomeriki, D. Erni, W.C. Chew, <i>All-Optical Digital Amplification in Nonlinear Photonic Crystal Waveguides</i>	52
11:45	O-6.4	I. Allayarov, S. Upendar, M.A. Schmidt, T. Weiss, <i>A New Definition for the Kerr Nonlinearity Parameter</i>	53

Saturday 13:00 – 14:30, O-7: Biosensing and metamaterials

13:00	O-7.1	F. Michelotti (invited), <i>Theory and concepts for all-dielectric biosensing</i>	54
13:30	O-7.2	M.Y. Azab, M.F.O. Hameed, A.M. Nasr, S.S.A. Obayya, <i>Multifunctional Plasmonic Photonic Crystal Fiber Biosensor</i>	55
13:45	O-7.3	T. Repán, A. Novitsky, M. Willatzen, A. Lavrinenko, <i>Reversed phase propagation for hyperbolic surface waves</i>	56
14:00	O-7.4	S.A. Hack, J.J.W. van der Vegt, W.L. Vos, <i>“Cartesian” light: Unconventional propagation of light in a 3D crystal of bandgap cavities</i>	57
14:15	O-7.5	J. Čtyroký, P. Kwiecien, I. Richter, J.H. Schmid, J. Gonzalo Wangüemert-Pérez, Í. Molina-Fernández, A. Ortega-Moñux, P. Cheben, J. Litvik, M. Dado, <i>Design of Apodized and Chirped Bragg Gratings in Subwavelength Grating Metamaterial Waveguides</i>	58

Saturday 15:00 – 16:15, O-8: Functional (nano-) photonics

15:00	O-8.1	J. García de Abajo (invited), <i>Quantum Physics with Plasmons in Graphene and other Atomic-Scale Systems</i>	59
15:30	O-8.2	D.S. Kumar, S.C. Creagh, S. Sujecki, T.M. Benson, <i>Modelling capture of pump power in the core using deformed step index fibre</i>	60
15:45	O-8.3	F. Negredo, M. Blaicher, A. Nestic, P. Kraft, J. Ott, W. Döfler, C. Koos, C. Rockstuhl, <i>Efficient Optimization of the Trajectory of Photonic Wire Bonds</i>	61
16:00	O-8.4	M.V. Cojocari, A.A. Basharin, <i>Spatial separation of electric and magnetic field in toroidal metamaterial</i>	62

Papers

Multiphysics simulations in nanophotonics

Dmitry N. Chigrin^{1,2*}

¹ *I. Institute of Physics (IA), RWTH Aachen University, Aachen, Germany*

² *DWI - Leibniz Institute for Interactive Materials, Aachen, Germany*

* chigrin@physik.rwth-aachen.de

Novel optical and optoelectronic systems often rely on complex materials, where the complexity manifests itself in a nontrivial character of interactions among building elements leading to the emergence of novel physical properties. The interactions themselves typically take place at different time and length scales and involve physical phenomena of different nature. Theoretical description of such multi-scale and multiphysics phenomena requires development of appropriate theoretical and numerical methodologies. In this presentation we report on our recent developments of a multiphysics description of reconfigurable meta-surfaces incorporating phase-change materials as an active element.

Today it is possible to engineer the building blocks of artificial materials with feature sizes smaller than the wavelength of light in a largely arbitrary fashion adding a new degree of freedom in material engineering and allowing to create artificial materials with unusual electromagnetic properties rare or absent in nature [1], [2]. Achieving switchable and non-linear functionalities of such meta-materials leads to additional flexibility in designing active photonic devices [3]. Phase-change materials promise high flexibility in designing reconfigurable systems [4], [5]. In the infrared spectral range they offer a huge contrast in the refractive index between an amorphous and a crystalline phase [6]. The transition can be triggered thermally by annealing on a hot plate or by an electrical or an optical pulse. Using focused optical beam to alter optical properties of the phase-change material within an individual unit cell of a meta-surface enables an efficient post-production tuning and reconfigurability. Design of such reconfigurable meta-surfaces requires a careful consideration of multiphysical phenomena and involves self-consistent treatment of material, electromagnetic and thermal models. Here we discuss some aspects of their design and modelling. Kinetic phase transition model is self-consistently coupled to full wave electromagnetic and heat transfer models. Developed method is used to design meta-surface based tunable components. We demonstrate an importance of the multiphysical modelling and discuss deficiencies of the commonly used purely electromagnetic simulations approaches.

References

- [1] F. Capolino, Ed., *Theory and Phenomena of Metamaterials*, CRC Press, Boca Raton, 2009
- [2] F. Capolino, Ed., *Applications of Metamaterials*, CRC Press, Boca Raton, 2009
- [3] N. I. Zheludev and Y. S. Kivshar, "From metamaterials to metadevices," *Nature Materials*, vol. 11, no. 11, pp. 917–924, 2012.
- [4] A.-K. U. Michel, D. N. Chigrin, T. W. W. Maß, K. Schönauer, M. Salinga, M. Wuttig, and T. Taubner, "Using Low-Loss Phase-Change Materials for Mid-Infrared Antenna Resonance Tuning," *Nano Lett*, vol. 13, no. 8, pp. 3470–3475, 2013.
- [5] B. Gholipour, J. Zhang, K. F. MacDonald, D. W. Hewak, and N. I. Zheludev, "An All-Optical, Non-volatile, Bidirectional, Phase-Change Meta-Switch," *Adv Mater*, vol. 25, no. 22, pp. 3050–3054, 2013.
- [6] K. Shportko, S. Kremers, M. Woda, D. Lencer, J. Robertson, and M. Wuttig, "Resonant bonding in crystalline phase-change materials," *Nature Mater.*, vol. 7, no. 8, pp. 653–658, 2008.

Slab waveguide steps with rounded corners at oblique incidence

Lena Ebers *, Manfred Hammer, Jens Förstner

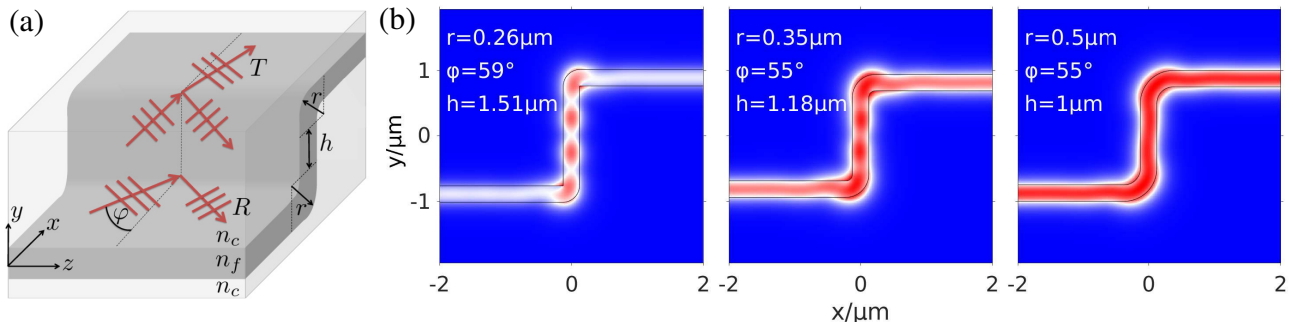
Theoretical Electrical Engineering, Paderborn University, Paderborn, Germany

* lena.ebers@uni-paderborn.de

Step structures in slab waveguides with rounded corners are investigated for incoming waves at oblique propagation angles. Numerical simulations predict full transmittance for increased curvature radii independent of the vertical height or incidence angle.

Power transmission across double-bend slab waveguide steps

In a context of 3-D silicon photonics, lossless transport of optical power between different levels is desirable. In this work slab waveguides at various heights connected by a third vertical slab with rounded corners (see Fig.(a)) are investigated for incoming waves at oblique incidence angles. This configuration can be seen as an extension of our previously presented concepts with sharp corners of [1]. With the help of the finite element software COMSOL Multiphysics the effective 2-D structures (infinitely expanded in $\pm z$ -direction) are analysed for different incidence angles φ , curvature radii r and step heights h . A variant of Snell's law applies to these structures and one defines critical angles beyond which radiation losses are fully suppressed. Additionally increasing the curvature radius also leads to quasi-lossless configurations for incidence angles below that critical angle. So for increasing curvature radii nearly full transmittance can be reached reasonably independent of the angle or height (see Fig.(b)).



(a) A double-bend step structure with refractive indices $n_c = 1.45$, $n_f = 3.4$ and thickness $d = 0.25\mu\text{m}$ at vacuum wavelength $\lambda = 1.55\mu\text{m}$ for oblique wave incidence. Step height h , curvature radius r and incidence angle φ are variable parameters. (b) Absolute electric field $|\mathbf{E}|$ for specific parameters with maximal transmittance.

Excitation through rib waveguides

Finally, also 3-D structures, i.e. configurations restricted in z -direction, were analysed for their transmittance properties. Rib waveguides are attached to the steps to excite a laterally confined plane wave. We assume wide rib widths and shallow etching to avoid spreading. Weighted superpositions of the former 2-D solutions are evaluated in MATLAB. For specific rib widths comparable transmittance values to the 2-D case are determined. For small curvature radii large widths are necessary to achieve comparable results, meanwhile by increasing the curvature radius narrow rib widths down to $10\mu\text{m}$ show acceptable results with high transmittance and might therefore be of practical interest for 3-D integrated optical circuits.

Reference

- [1] M. Hammer, A. Hildebrandt, and J. Förstner. Full resonant transmission of semi-guided planar waves through slab waveguide steps at oblique incidence. *J. of Lightwave Technology*, 34(3):997–1005, 2016.

Germanium Telluride Phase Change Material based 1×2 Electro-Optic Switch

Nikhil Dhingra^{1*}, Jun Chao Song², Geetika Jain Saxena³, Enakshi Khular Sharma¹, B M A Rahman²

¹ Department of Electronic Science, University of Delhi South Campus, Benito Juarez Road, New Delhi-110021, India

² Department of Electrical and Electronic Engineering, City, University of London, Northampton Square, London EC1V 0HB, UK

³ Department of Electronic, Maharaja Agrasen College, University of Delhi, Vasundhara Enclave, New Delhi-110096, India

* nikhildhingra2@gmail.com

We present the design of a compact 1×2 electro-optic switch using Germanium Telluride in Mach-Zehnder configuration at wavelength, $1.55 \mu\text{m}$. The high differential refractive index between the amorphous and crystalline phase was utilized to achieve a small device footprint with switching control area $0.5 \times 5.0 \mu\text{m}^2$.

The devices based on Silicon on insulator are very promising due to reduced chip footprint and low power consumption and their compatibility with microelectronic circuits based on CMOS technology [1]. The hybrid switches and modulators attracted a lot of attention in the last decade as the modulators and switches based on plasma dispersion effect require large length [2]. The hybrid switch using phase change materials which provides high differential refractive index in the two phases can mitigate the above-mentioned problems. The phase change material Germanium Telluride (GeTe) provides high differential refractive index between the amorphous and crystalline state. The losses in both the states are much lower than another phase change material GST. The schematic of the proposed 1×2 electro-optic switch in MZ configuration is shown in Fig. 1 along with the cross-sectional view of the control section. The voltage-controlled phase change of the GeTe layer can be achieved by the two ITO electrodes. Unlike other MZ switch design, the control section in this design forms a coupled structure consisting of Si NW with top ITO layer (wg_1) and an ITO-GeTe-ITO waveguide (wg_2). However, for $h_{GeTe} < 30 \text{ nm}$, the control section supports only one supermode in both amorphous and crystalline state.

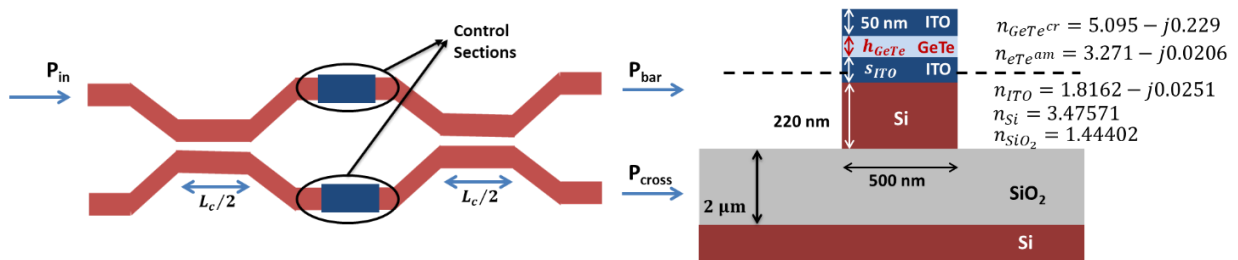


Figure 1(a) Schematic view of the MZI switch (b) Cross-sectional view of the control section

For cross-state, when both the arms are in amorphous state, an insertion loss of less than 1 dB can be achieved with almost complete power transmission to second waveguide. For bar state, when arm-1 is in amorphous state and arm-2 in crystalline state, the extinction ratio more than 10 dB can be achieved with 3 dB insertion loss. The switch promises a small device footprint with switching control area $0.5 \times 5.0 \mu\text{m}^2$.

References

- [1] G. T. Reed, G. Mashanovich, F. Y. Gardes, D. J. Thomson, *Silicon optical modulators*, Nature Photon. 4, 518-526 (2010).
- [2] Leuthold, J. et al., *Silicon-organic hybrid electro-optical devices*, IEEE J. Sel. Top. Quantum Electron. 19(6), 3401413 (2013).

A Compact Wavelength Router Dynamically Reconfigurable through Destructive Interference

Ali Emre Kaplan^{1*}, Alberto Parini¹, Gaetano Bellanca¹, Paolo Bassi², Stefano Trillo¹

¹Department of Engineering, University of Ferrara, Ferrara, Italy

²Department of Electrical, Electronic, and Information Engineering, University of Bologna, Bologna Italy

* aliemre.kaplan@unife.it

We investigate a novel compact 1×3 Wavelength-Selective Router based on two micro ring resonators. By exploiting a destructive interference between two counter-propagating waves, the routing paths allowed within the topology can be dynamically reconfigured.

Introduction

Emerging Silicon photonics technologies allow the fabrication of the complex on-chip devices for switching and filtering functionalities for WDM communication.

Fig.1 (a) and (b) shows the sketch and fabricated device, respectively, that can be operated in two alternative regimes. In the off-state (isolation), the two micro rings are tuned exactly on the same resonance comb. In this regime the signal coming from port 1 is equally (50:50) dropped by the rings toward the vertical bus. The signal dropped by the upper ring turns counter clockwise while the one dropped by the bottom ring turns clock wise. As a result, the two signals collide in the crossing region giving rise to a stationary standing wave. As a consequence, the strength of the receiving signals on the port 1 and port 2 reduce significantly, as shown in Fig. (d). On the contrary, when the device is in the on-state, the rings have different resonant wavelengths. Therefore, unlike the previous case, the destructive interference does not occur and the dropped signals arrive at both port 2 and port 4 as shown in Fig. 1(c). In this state, the device performs as a router.

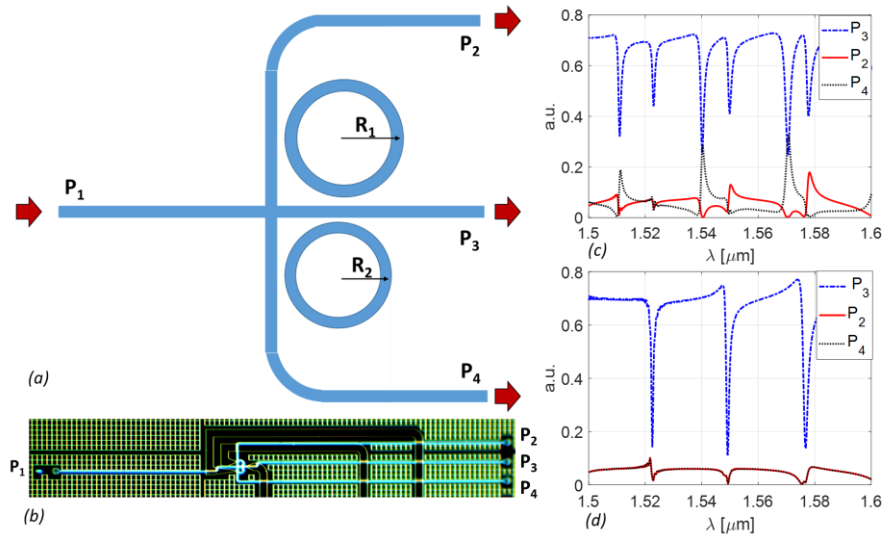


Figure 1: (a) Sketch of the proposed device, (b) fabrication in SOI platform, (c) and (d) are the transmission profiles of the FDTD simulations for the on and off states, respectively.

Results

Preliminary experimental results confirm the on and off states by the thermal tuning of the bottom ring. In this way, the proposed router can be controlled dynamically according to the desired states. The modeling and the complete experimental characterization will be presented and discussed.

Design of integrated quantum optical single-photon detectors

J. Münzberg¹, A. Vetter², F. Beutel^{3,4,5}, W. Hartmann^{3,4,5}, Simone Ferrari^{3,4,5}, W. Pernice^{3,4,5}, and C. Rockstuhl^{1,2*}

¹*Institute of Theoretical Solid State Physics, Karlsruhe Institute of Technology, Karlsruhe, Germany*

²*Institute of Nanotechnology, Karlsruhe Institute of Technology, Karlsruhe, Germany*

³*Institute of Physics, University of Münster, Münster, Germany*

⁴*CeNTech – Center for Nanotechnology, University of Münster, Münster, Germany*

⁵*Münster Nanofabrication Facility, University of Münster, Münster, Germany*

* carsten.rockstuhl@kit.edu

A key element of integrated photonic circuits is a highly efficient and ultra-fast single-photon detector. Here, we discuss suitable designs exploiting concepts of perfect absorbers and critical coupling that are implemented as photonic crystal based cavities. Experimental realizations demonstrate the liability of our concepts.

Overview

A single-photon detector with high efficiency and timing resolution is a key building block for quantum photonics [1]. For high bandwidth quantum communication, ultrafast detection is also needed. To achieve these ambitious goals in an integrated environment is even more important for a future generation of integrated quantum optical devices serving multiple applications, e.g. in the context of quantum metrology or quantum computation. We designed and realized extremely short superconducting nanowire detectors onto a silicon nanophotonic platform, which, thanks to their reduced kinetic inductance, can provide an extremely high detection rate [2]. To enhance their efficiency, these detectors were embedded into one- and two-dimensional photonic crystal cavities obtaining efficient and fast detectors with sub-ns recovery time. This contribution shall concentrate on the design of such detectors that can be guided by multiple physical principles. On the one hand (Fig. 1a), the concept of perfect absorption can be exploited. By feeding the optical waveguide into a Fabry-Perot cavity that consists of a perfect reflecting rear-mirror (so no transmission) and a partially reflecting front mirror that is designed to cause a destructive interference between the directly reflected light and the light that experiences multiple round trips in the cavity, complete dissipation takes place inside the cavity. This dissipation happens due to the desired absorption in the nanowire but also due to scattering losses at the junction. The junction in this initial design was necessary to give structural support to the superconducting nanowire. To mitigate this deficiency, we designed a further generation of devices that exploit the concept of critical coupling. The structures were integrated in a photonic crystal architecture (Fig. 1b), which strongly suppresses the occurrence of outcoupling losses. All designs are verified in their functionality by experiments. Results of characterized devices will be presented as well.

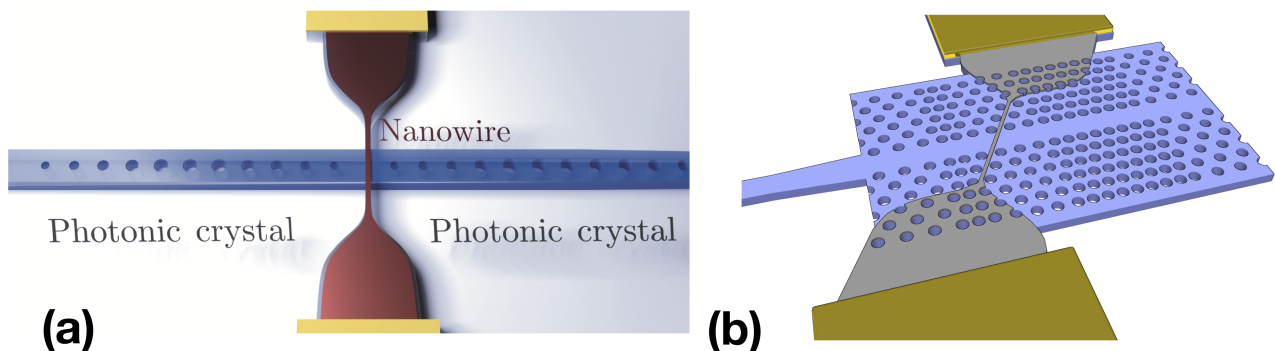


Figure 1: Two generations of integrated single-photon detectors. (a) A structure that exploits in its design concepts of a perfect absorber and (b) a structure that exploits in its design concepts of critical coupling.

References

- [1] J. L. O'Brien, *Optical Quantum Computing*, Science **Vol. 318** 1567, (2007)
- [2] A. Vetter, S. Ferrari, P. Rath, R. Alae, O. Kahl, V. Kovalyuk, S. Diewald, G. N. Goltsman, A. Korneev, C. Rockstuhl, and W. H. P. Pernice, *Cavity-Enhanced and Ultrafast Superconducting Single-Photon Detectors* Nano Letters **Vol. 16** 7085, (2016)

Optimization of quantum optical devices with machine learning

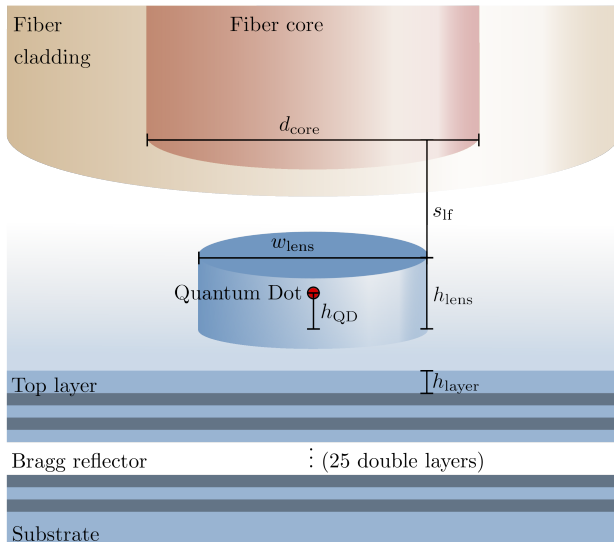
Philipp-Immanuel Schneider¹, Lin Zschiedrich¹, Xavier Garcia-Santiago¹, Sven Burger^{1,2}

¹ JCMwave GmbH, Berlin, Germany

² Zuse Institute Berlin, Germany

Single photon emitters (SPEs) are essential building blocks of future photonic and quantum optical devices. We apply and benchmark global optimization strategies to improve the quality of a specific device with respect to multiphoton emission, photon indistinguishability and out-coupling efficiency into an optical telecommunication fiber.

The surrounding solid-state structure of the emitting quantum dot (QD) has an important influence on the system's performance as it can enhance or suppress the rate of spontaneous emission (Purcell effect). Moreover, the efficiencies with which emitted photons are extracted into a specific direction or coupled into a waveguide depend strongly on the geometry of the surrounding structure [1]. To create optimized structures for specific purposes, numerical optimization based on the solutions of Maxwell's equations are an important tool.



The QD is embedded into a mesa structure made from gallium arsenide. An underlying Bragg multilayer structure reflects the light emitted by the QD back into the upper hemisphere. The light is coupled into an optical fiber above the QD consisting of a homogeneous fiber core and a homogeneous fiber cladding. The mesa structure is parametrized by four parameters, the width and height of the mesa, the elevation of the QD within the mesa, and the thickness of the GaAs layer above the Bragg reflector.

In the presentation we benchmark various classical and machine learning approaches for the optimization of a specific single-photon emitter at a vacuum wavelength of $\lambda = 1,300$ nm as shown above (c.f. [2]).

We acknowledge funding from the Senate of Berlin (IBB, PROFIT grant agreement No 10160385, FI-SEQUR), co-financed by the European Fund for Regional Development (EFRE), and funding from the European Unions Horizon 2020 research and innovation programme under the Marie Skłodowska-Curie grant agreement No 675745 (MSCA-ITN-EID NOLOSS).

References

- [1] W.L. Barnes, G. Björk, J.M. Gérard, P. Jonsson, J.A.E. Wasey, P.T. Worthing, and V. Zwiller. Solid-state single photon sources: light collection strategies. *Eur. Phys. J. D*, 18(2):197–210, feb 2002.
- [2] M. Gschrey, A. Thoma, et al. Highly indistinguishable photons from deterministic quantum-dot microlenses utilizing three-dimensional in situ electron-beam lithography. *Nat. Communications*, 6:7662, 2015.

Upconversion in optimized photonic multilayer structures

Fabian Spallek¹, Andreas Buchleitner, Thomas Wellens

Physikalisches Institut, Albert-Ludwigs-Universität, Freiburg, Germany

Leistungszentrum Nachhaltigkeit Freiburg, Albert-Ludwigs-Universität, Freiburg, Germany

¹ fabian.spallek@physik.uni-freiburg.de

We consider dielectric multilayer structures with embedded upconverter material to improve silicon solar cells. The multilayer nano-structures are optimized for upconversion efficiency, which in turn, results from the enhanced local irradiance and the modified local density of photonic states.

Using upconversion to improve silicon solar cells

Upconversion materials, which convert two low-energy photons into one photon with higher energy, combined with photonic structures, open promising possibilities to improve the efficiency of silicon solar cells by utilising the full range rather than only a fraction of the solar spectrum. Quantum yield and the luminescence enhancement, which quantify the overall efficiency of the embedded upconverter material, are determined by the interplay of energy transfer processes, local irradiance and local density of (photonic) states - all of which can be influenced by photonic dielectric nanostructures [1].

Field intensity enhancement and tailoring the local density of photonic states

By tuning the thickness of each individual layer in a multi-layered photonic structure, we show that it is possible to trap incident photons of a given wavelength inside this structure, and thus considerably increase the local irradiance in those layers which contain the upconverter material [2]. We compare the achievable enhancement of the local irradiance, as well as its robustness under manufacturing errors, as obtained for the resulting optimal geometries to thus far experimentally implemented Bragg structures [1].

Furthermore we derive the local density of states from macroscopic QED [3], for arbitrary finite multi-layered dielectric structures. This allows for an additional optimization of the structure, such as to enhance desired, or to suppress unwanted spontaneous emission processes from distinct excited energy levels of the upconverter material.

Determining the combined influence of the local density of states and the local irradiance enhancement within a rate equation model, we also make predictions for the achievable upconversion luminescence and quantum yield of optimised structures as compared to the above mentioned Bragg structures.

References

- [1] C. L. M. Hofmann, B. Herter, S. Fischer, J. Gutmann, J. C. Goldschmidt, *Upconversion in a Bragg structure: photonic effects of a modified local density of states and irradiance on luminescence and upconversion quantum yield*, Opt. Express 24, 14895-14914 (2016)
- [2] F. Spallek, A. Buchleitner, T. Wellens, *Optimal trapping of monochromatic light in designed photonic multilayer structures*, J. Phys. B: At. Mol. Opt. Phys. 50, 214005 (2017)
- [3] H. T. Dung, L. Knoll, D.-G. Welsch, *Intermolecular energy transfer in the presence of dispersing and absorbing media*, Phys. Rev. A 65, 043813 (2002)

FDTD modelling of nanostructured OLEDs: analysis of simulation parameters for accurate radiation patterns

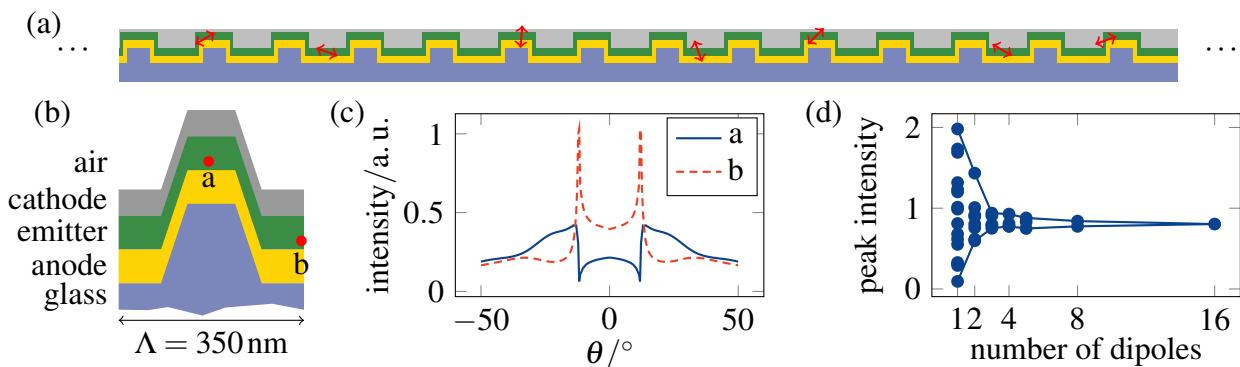
Hannes Lüder¹, Martina Gerken¹

¹ *Chair for Integrated Systems and Photonics, Faculty of Engineering, Kiel University, Germany*
{halu, mge}@tf.uni-kiel.de

The radiation pattern of OLEDs with integrated nanostructures is calculated by superposition of dipoles at different positions. It is demonstrated that the dipole position relative to the nanostructure significantly influences the radiation pattern and that at least four dipoles are necessary to approximate a continuous emission layer.

Nanostructures in organic light-emitting diodes (OLEDs) provide the possibility to tailor the OLEDs' radiation pattern [1]. This can be used to control the main outcoupling direction, which is of particular interest for compact optical sensors. Depending on the specific OLED design, the grating induced resonance effects result in increased or decreased outcoupling [2]. Therefore, it is necessary to accurately simulate emission layers in the vicinity of nanostructures to obtain the desired radiation pattern. In an OLED, the emitters are incoherent and randomly distributed in the active layer (see figure (a)). The emission may be calculated using an inverse approach [3]. Here, we simulate directly the radiation patterns for multiple dipole positions using the FDTD method (commercial software FDTD Solutions by Lumerical Inc.) and investigate how many dipole positions are necessary to approximate the behavior of a continuous emission layer.

Figure (b) depicts examples of two possible dipole positions relative to the grating structure. Figure (c) shows the corresponding radiation patterns, which differ significantly. Varying the number of emitter positions, it is observed that at least four independent dipoles placed at points without high symmetry should be simulated and the results superimposed to obtain a reliable approximation for a continuous layer, as shown in figure (d). Additionally, simulation domain size, grid and wavelength resolution and the treatment of metal interfaces is discussed for FDTD simulations of OLED structures.



(a) Part of the simulated 2D structure (simplified view). Multiple random dipole positions are indicated. (b) Detailed schematic of a nanostructured OLED with two possible emitter positions. (c) TE radiation patterns for these emitter positions ($\lambda = 460 \text{ nm}$). (d) Peak intensities of the resonant outcoupling peaks for the cumulated results for different numbers of dipoles randomly but approximately evenly distributed in one grating period.

References

- [1] U. Geyer et. al., J. Appl. Phys., 104(9), 093111, 2008.
- [2] J. Hauss et. al., Opt. Express, 19(S4):A851–A858, 2011.
- [3] S. Zhang et. al., Synthetic Metals, 205:127–133, 2015.

Benchmarking state-of-the-art optical simulation methods for analyzing large nanophotonic structures

Niels Gregersen^{1*}, Jakob Rosenkrantz de Lasson¹, Lars Hagedorn Frandsen¹, Oleksiy S. Kim²,
Olav Breinbjerg², Fengwen Wang³, Ole Sigmund³, Aliaksandra Ivinskaya⁴, Andrei Lavrinenko¹,
Philipp Gutsche⁵, Sven Burger⁵, Teppo Häyrynen¹ and Jesper Mørk¹

¹ DTU Fotonik, Department of Photonics Engineering, Technical University of Denmark

² DTU Elektro, Department of Electrical Engineering, Technical University of Denmark

³ DTU Mekanik, Department of Mechanical Engineering, Technical University of Denmark

⁴ ITMO University, St. Petersburg, Russia

⁵ Zuse Institute Berlin, Germany

* ngre@fotonik.dtu.dk

Five computational methods are benchmarked by computing quality factors and resonance wavelengths in photonic crystal membrane L5 and L9 line defect cavities. Careful convergence studies reveal that some methods are more suitable than others for analyzing these cavities.

Geometry under study

The photonic crystal (PhC) membrane represents a platform for planar integration of components, where cavities and waveguides may play a key role in realizing compact optical components. A finite-length defect waveguide forms an L_n cavity, where n denotes the length of the cavity. Such L_n cavities support spectrally discrete optical modes, and the fundamental cavity mode profile of an L9 cavity is shown in Fig. 1. Light may be confined to such an L_n cavity for extended periods, as quantified by the quality (Q) factor. The Q factor thus represents a key parameter in the design of a PhC membrane cavity.

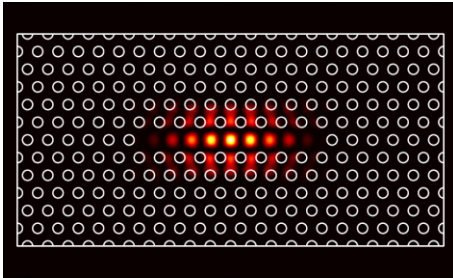


Fig. 1: Optical field $|E_y|^2$ profile for the L9 cavity mode.

Table 1: Calculated Q factors and resonance wavelengths λ .

	FDTD	FDFD	FEM	SIE	FMM
λ^{L5} (nm)	1568	1572	1571	1572	1567
λ^{L9} (nm)	1574	1580	1578	1579	1570
Q^{L5}	1670	1725	1705	1707	1700
Q^{L9}	104,000	108,000	105,000	104,000	60,000

Methods and results

The combination of the large size of the PhC L_n cavity and the full 3D nature of the geometry makes the calculation of the cavity Q factor an extremely demanding numerical challenge. In this work, we focus on two structures, a low-Q L5 cavity and a high-Q L9 cavity. We employ five different computational methods, the finite-difference time-domain (FDTD) technique, the finite-difference frequency-domain (FDFD) technique, the finite-element method (FEM), the surface integral equation (SIE) approach and the Fourier modal method (FMM), to compute the cavity Q factor and the resonance wavelength for both structures. For each method, the relevant computational parameters are systematically varied to quantify the computational errors. The final results summarized in Table 1 show that the resonance wavelengths agree fairly well for the two geometries among the five methods. On the other hand, significant deviations are observed for the Q factor. Our study highlights the importance of careful convergence checks and systematic estimation of the computational error, both of which are generally missing in the literature.

Multidomain spectral method for optical-waveguide analysis.

G erard Granet

¹ *Universit e Clermont Auvergne, CNRS, Institut Pascal, F-63000 CLERMONT-FERRAND, FRANCE*
gerard.granet@uca.fr

A multi-domain spectral method for modal analysis of optical-waveguides is developed. The waveguide is decomposed into homogeneous sub-domains which correspond also to the support of the basis functions used for numerical computation. In this way, exact boundary conditions may be imposed at the boundaries of the structure

Introduction

The accurate calculation of full-vectorial modes of optical waveguides is a mandatory step for the engineering of many photonic devices. Among rigorous methods, the finite difference frequency domain modal method and the Fourier modal method are both popular. As known, the major difficulty of any numerical modal method is how to handle the interface conditions at the index discontinuities. In regards to the Fourier modal method (FMM), many stages of improvements have been proposed: the so-called Fourier factorization rules, adaptive spatial resolution (ASR) and the use of symmetries. Nevertheless, it still converges slowly for structures with permittivity function with negative real part while such structures are of common use in modern optics and plasmonics.

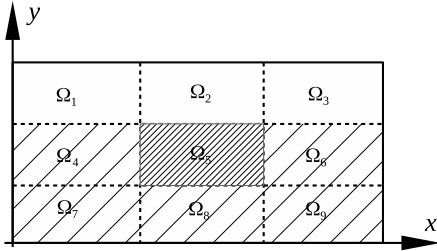


Figure 1: The figure to the left is an example of a buried channel waveguide. The computational domain is composed of the juxtaposition of nine homogeneous sub-domains. The channel waveguide is sub-domain Ω_5

Short description of the method

In order to enforce rigorously the boundary conditions which determine the accuracy of the eigen-solutions, we expand the field on a tensorial basis whose elements are defined on domains Ω_j , $j = 1, 2, \dots, 9$.

$$\psi^{(j)}(x, y, z) = \sum_{mnq} \psi_{mn,q}^{(j)} P_m(x) P_n(y) \exp(-i\gamma_q z)$$

where P_m and P_n are Legendre polynomials for example. Thanks to the above expansion, it is possible to derive an algebraic eigenvalue problem which incorporates in an exact manner the boundary conditions at interfaces between domains Ω_j . The above approach was previously used in [1], [2] for 1D grating problems. The method is successfully validated by comparison with previously published data and with our own implementation of ASR-FMM.

References

- [1] R.H.Morf, *Exponentially convergent and numerically efficient solution of Maxwell's equations for lamellar gratings*, J. Opt. Am. A, **12**, pp. 1043-1056, 1995.
- [2] M.H. Randriamihaja, G. Granet, K. Edee, K. Raniriharinosy, *Polynomial modal analysis of lamellar diffraction gratings in conical mounting*, J. Opt. Soc. Am. A., **33**, pp.1679-1686, 2016.

An Assessment of Faber Polynomial Expansions for the Time Domain Solution of Maxwell's equations

Hendrik Kleene¹, Dirk Schulz¹,

¹ *Chair for High Frequency Technology, TU Dortmund University, Dortmund, Germany*
hendrik.kleene@tu-dortmund.de

We investigate the numerical time domain solution of Maxwell's equations on the basis of Faber polynomial expansions. They allow the application of large time steps while approximating the time domain propagator in a very accurate manner. We demonstrate the capabilities of the inclusion of several material models.

Summary of the Approach

The numerical time domain solution of Maxwell's equations offers several beneficial features for the analysis of photonic devices. A feasible method for this purpose is the well know FDTD method. Unfortunately, this method is limited by the choice of small time steps due to the CFL limit, which couples the maximum time step in the simulation with the spatial discretization width. This leads to large computational costs especially when fine featured devices are analyzed. Therefore, we investigate methods allowing larger time steps. A promising approach is the application of Faber polynomial expansions to the time domain propagator [1]. They have comparable convergence properties as the Chebyshev method, but allow the consideration of absorbing materials and absorbing boundary conditions like perfectly matched layers (PML).

To illustrate the inclusion of additional material models, the system is extended by a first order Drude model. This is done using additional differential equations (ADE's). Of course, other models can be included in the same manner. With this, we rewrite Maxwell's equations as follows:

$$\frac{\partial \vec{\Psi}(\vec{r}, t)}{\partial t} = \mathcal{H} \cdot \vec{\Psi}(\vec{r}, t); \quad \mathcal{H} = \begin{bmatrix} 0 & \frac{1}{\epsilon_{\infty}(\vec{r})} \nabla \times & -1/\epsilon_{\infty}(\vec{r}) \\ -\frac{1}{\mu(\vec{r})} \nabla \times & 0 & 0 \\ \epsilon_0 \omega_D^2(\vec{r}) & 0 & -\gamma_D(\vec{r}) \end{bmatrix}; \quad \vec{\Psi}(\vec{r}, t) = \begin{bmatrix} \vec{E}(\vec{r}, t) \\ \vec{H}(\vec{r}, t) \\ \vec{i}(\vec{r}, t) \end{bmatrix} \quad (1)$$

For the spatial discretization of (1) we employ finite differences using a staggered grid. The formal solution is given by $\vec{\Psi}(t + \Delta t) = \exp(\Delta t \cdot \mathcal{H}) \cdot \vec{\Psi}(t)$. Now, we apply the Faber polynomial expansion to the matrix exponential. The expansion of the matrix exponential takes place in the complex eigenvalue plane of \mathcal{H} and depends on the shape of the spectrum. The Faber polynomial expansion allows to fit the convergence region of the expansion tightly to the spectrum of the matrix \mathcal{H} . This allows an optimization of the time stepping scheme to the current simulation model, but also requires some preliminary knowledge about the eigenvalues spectrum of \mathcal{H} . The resulting approximation can be evaluated using a recurrence relation requiring the storage of only three vectors of the size of $\vec{\Psi}(t)$. This feature allows an explicit formulation of the time stepping scheme and, furthermore, results in low memory requirements, even if large steps are applied.

Due to these features and the possibility of the direct inclusion of additional material models, the application of Faber polynomials is an interesting option for highly accurate electromagnetic time domain simulations.

References

- [1] P. Novati, *Solving linear initial value problems by Faber polynomials*, Numer. Linear Algebr. with Appl., no 3, vol 10, pp 247-270, 2003.

Vector solver for 2D highly nonlinear plasmonic waveguides: a rigorous analysis

Mahmoud M. R. Elsayy, Gilles Renversez*

Aix–Marseille Univ, CNRS, Centrale Marseille, Institut Fresnel, 13013 Marseille, France

* gilles.renversez@fresnel.fr

We study stationary solutions propagating in 2D cross-section highly nonlinear plasmonic waveguides using an accurate vector nonlinear solver. We show the importance of our solver in quantifying directly the third-order nonlinear Kerr-effect rather than relying on the linear properties which are commonly used in the literature.

Recently nonlinear plasmonic slot waveguides (NPSWs) have drawn attention due to the reinforcement of the nonlinear effects they offer [1, 2]. Nevertheless, accurate modelling tools for realistic 2D cross section waveguides are still lacking due to the difficulties to take into account the nonlinearity. Consequently, most of the nonlinear studies rely only on the waveguide linear properties [3, 4].

We use our vector nonlinear solver to study the stationary solutions in 2D cross-section waveguides with a Kerr nonlinear core. Our solver is a 2D generalization of the 1D fixed power algorithm we developed within the finite element method [2]. Fig. 1(a) illustrates the 2D NPSW under investigation (we use hydrogenated amorphous silicon as nonlinear material [2]). In Fig. 1(b), we study the $\Re e(n_{eff})$ for the nonlinear fundamental symmetric mode for different height values as a function of the input power (color curves) and compare the results with the one obtained from the 1D model (black curve). We show that for small h values, even in the low power regime, 1D studies do not provide accurate results compared to 2D ones. Moreover, for $h \gg \lambda = 1.55 \mu\text{m}$, the results obtained from 2D model in the nonlinear regime is different from the 1D case, even if they are similar in the low power regime.

Second, in Fig. 1(c), we move to nanoscale NPSW with h and $d_{core} \ll \lambda$. in which we show

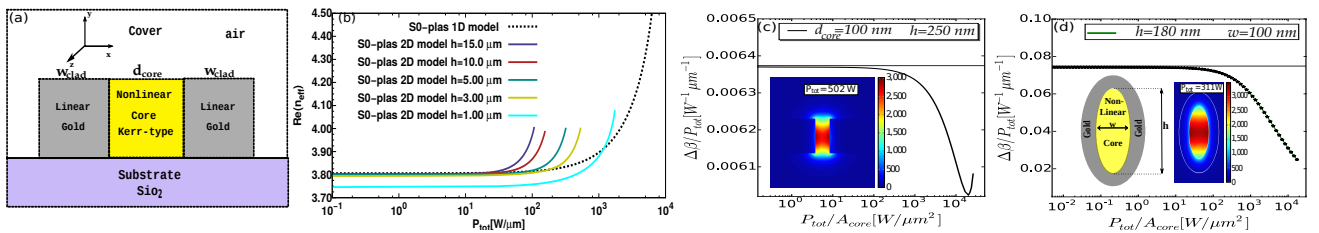


Fig. 1. (a): The cross-section of the studied symmetric NPSW. (b) $\Re e(n_{eff})$ for NPSW with $d_{core} = 400 \text{ nm}$ for different h as a function of P_{tot}/h , the dashed black curve represents the results from the 1D model. (c): the results obtained for $h = 250 \text{ nm}$, with $d_{core} = 100 \text{ nm}$. (d): the results for nonlinear plasmonic nanoshell [4].

again the importance of our 2D nonlinear solver by studying the link between the nonlinear parameter γ_{nl} [3] based on the linear effective mode area and the change of the nonlinear propagation constant $\Re e(\Delta\beta)/P_{tot}$ induced by the power P_{tot} . As it can be seen, at low power the conventional way of computing γ_{nl} based on the linear properties (horizontal line) fits with $\Re e(\Delta\beta)/P_{tot}$. However, at high power it fails to predict the exact behaviour. To justify this point, we consider a nonlinear plasmonic nanoshell (Fig. 1(d)), once again, the conventional way of computing γ_{nl} shown by the horizontal line fails to predict the behaviour at high powers. This means that it is required to have a rigorous nonlinear solver in order to quantify correctly the nonlinear characteristics rather than relying only on their linear properties. Our solver can also treat highly nonlinear anisotropic configurations, where the formula used in the literature to compute γ_{nl} is not valid anymore [3, 4].

References

- [1] M. Kauranen and A. V. Zayats, Nature Photon. **6**, 737 (2012).
- [2] M. M. R. Elsayy and G. Renversez, Journal of Optics **19**, 075001 (2017).
- [3] C. Koos, L. Jacome, C. Poulton, J. Leuthold, and W. Freude, Opt. Express **15**, 5976 (2007).
- [4] M. M. Hossain, M. D. Turner, and M. Gu, Opt. Express **19**, 23800 (2011).

Analysis of Absorption in the Absorbing Boundary Condition

Ramesh Kumar^{*}, Anurag Sharma[#]

Department of Physics, Indian Institute of Technology, New Delhi – 110 016, India

^{}rameshphnt@gmail.com, [#]asharma@physics.iitd.ac.in*

We have used the mode expansion method of propagation to analyze the action of the absorption layer in an absorbing boundary condition implemented. Our findings include that the actual modes of the absorbing layer have insignificant role in the absorption of a propagating beam.

Summary

The perfectly matched layer (PML) has been commonly used for suppression of reflections from the numerical boundaries for the last two decades. Recently it has been shown that the PML fails in the structures where refractive index is not an analytic function, for example in the termination of the photonic crystal structures, and also for the cases where waveguide is entering in the absorbing layer [1,2]. This has renewed interest in the absorbing boundary condition. We have shown that the gradual absorbing boundary condition (gABC) works nearly as well as the PML [3]. In this paper, we present an analysis of the absorption of the ABC layer in terms of the modes. The modes and the effective indices of the numerical domain are obtained using the collocation method. The termination using absorbing layer results the discretization of the infinite continuum of the modes into the modes of the absorbing layer and the propagating modes. The propagation is carried out in terms of these modes. The modal propagation technique allows the suppression of the selected modes to examine their importance. As a test case we consider the propagation of a tilted Gaussian beam. By selective suppression of modes, we have found that the suppression of the modes of the absorbing layer have no effect on the propagation and the absorption at the boundary. Further work is in progress more results will be presented at the workshop.

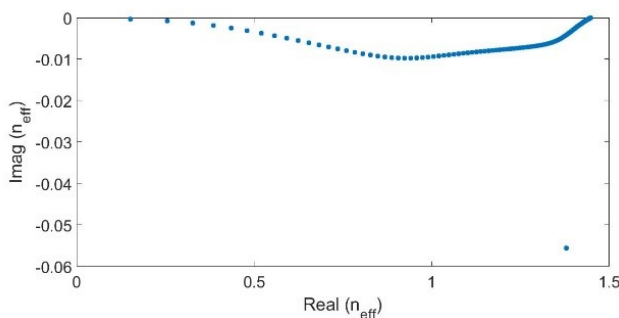


Fig.1 Real and Imaginary part of the effective indices.

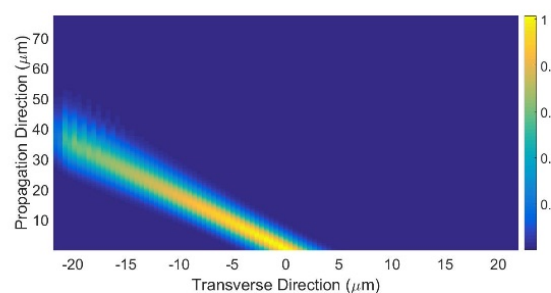


Fig.2 Propagation of a Gaussian beam with suppression of the ABC modes.

References

1. Ardavan F. Oskooi, Lei Zhang, Yehuda Avniel, and Steven G. Johnson, "The failure of perfectly matched layers, and towards their redemption by adiabatic absorbers," *Opt. Express* **16**, 11376-11392 (2008).
2. Po-Ru Loh, Ardavan.F. Oskooi, Mihai Ibanescu, Maksim Skorobogatiy, Steven G. Johnson, "Fundamental relation between phase and group velocity, and application to the failure of perfectly matched layers in backward-wave structures", *Phys. Rev. E* **79**, 065601-065604 (2009).
3. Ramesh Kumar and Anurag Sharma, "Gradual absorbing boundary condition for beam propagation methods," *Photonics West 2018*, paper# 10526-84 (2018).

Non-Hermitian Photonics from Parity-Time Symmetry to Pseudo-Hermitian Structures

Sendy Phang¹, Ana Vukovic², Fernanda Fotsa-Ngaffo³, Gabriele Gradoni¹, Stephen C. Creagh¹, Phillip D. Sewell¹, Trevor Benson²

¹ School of Mathematical Sciences, University of Nottingham, Nottingham, UK

² George Green Institute for Electromagnetics Research, University of Nottingham, Nottingham, UK

³ Department of Physics, Faculty of Science, University of Buea, P.O. Box 63, Buea, Cameroon
sendy.phang@nottingham.ac.uk

Loss, an inherent property of matter, has been considered harmful in the development of photonic devices. Adding gain element to compensate the loss, however, may lead to an unstable operation of such device. In 1998, Bender and Boettcher [1] shows that under judicious configuration, known as Parity and Time (PT) symmetry, the Hamiltonian of such structure have a stable operation in the PT-symmetry regime, but there exists an exceptional point at which the PT-symmetry broken which leads to an unstable operation. Subsequently, different structures have been studied both theoretically and experimentally in recent years, including gratings, lattices, waveguides, plasmonics and resonant cavities. Interesting properties including loss-induced invisibility, simultaneous lasing and coherent perfect absorption, asymmetric beam scattering and laser generation by reversing the effect of loss at threshold have been discovered [2, 3].

In this contribution, we will review the progress in the study of non-Hermitian structures, from the strictly idealised PT-symmetric structures to the recent less-strict Pseudo-Hermitian structures in photonics. These structures include, (linear and non-linear) PT-Bragg grating, PT-chain resonators, time-modulated gain/loss resonators and pseudo-Hermitian trimers structures (see Fig. 1).

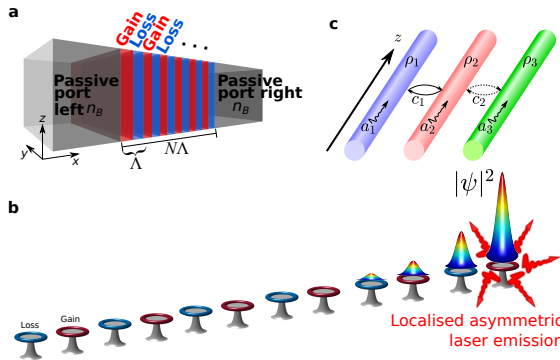


Figure 1. Non-Hermitian structures: (a) PT-Bragg Gratings; (b) PT-chain resonators; and (c) Pseudo-Hermitian Trimer

S.P. acknowledge support from the European Commission through the Horizon 2020 FET project NEMF21, grant no. 664828.

References

- [1] Carl M Bender, Stefan Boettcher, and Peter N Meisinger. PT-symmetric quantum mechanics. *Journal of Mathematical Physics*, 40(5):2201–2229, 1999.
- [2] S Phang, TM Benson, H Susanto, SC Creagh, G Gradoni, PD Sewell, and A Vukovic. Theory and numerical modelling of parity-time symmetric structures in photonics: Introduction and grating structures in one dimension. In *Recent Trends in Computational Photonics*, pages 161–205. Springer, 2017.
- [3] S Phang, A Vukovic, G Gradoni, PD Sewell, TM Benson, and SC Creagh. Theory and numerical modelling of parity-time symmetric structures in photonics: Boundary integral equation for coupled microresonator structures. In *Recent Trends in Computational Photonics*, pages 207–233. Springer, 2017.

Field Solutions for Large Area Graded-Index Waveguides

Laurence Cahill

Department of Engineering, La Trobe University, Melbourne, Australia

l.cahill@latrobe.edu.au

This paper examines exact and approximate analytical field solutions for graded-index planar and rectangular waveguides. Previous results for such waveguides were largely limited to single or few-moded structures. In this study, we concentrate on large area waveguides that propagate large numbers of modes.

There has been renewed interest in multimode graded index waveguides for use in high speed interconnects [1]. Polymer waveguides having a large cross-sectional area (typically 30 to 60 μm^2) ease alignment tolerances and can be easily integrated in board-level interconnects. It is the purpose of this paper to examine approximate analytical field solutions for a variety of index profiles and to present new results for higher order modal solutions.

Although, numerical solutions are usually the method of choice for determining the fields of graded-index rectangular waveguides, there is some value in pursuing suitable approximate analytical solutions, where that is possible, for independent checking of computer simulations, for gaining insight into the behavior of the guiding structure, as well as highlighting the importance of certain parameters.

Early analyses of graded-index planar waveguides yielded field solutions for a number of different index profiles such as linear, Gaussian, power-law, and hyperbolic. Some of these early results were based on previous solutions of Schrodinger's equation in the fields of quantum mechanics and quantum chemistry. Analytical solutions for the fields of graded-index planar structures could often be incorporated in three-dimensional analyses to produce approximate solutions for rectangular waveguides by means of the effective index method or by separation of variables where the permittivity was separable.

However, nearly all of these early solutions were limited to at most a few modes. For example, solving the Gaussian profile planar waveguide by means of the variational principle, yields only a bound on the modal solution. It will be shown that not only does this bound become increasingly inaccurate for higher order modes, it becomes increasingly difficult to compute the relevant eigenvalues. Similarly, whilst there are known TE and TM solutions for the uncladded sech-squared profile, it will be shown that there is no similar straightforward TM solution for the cladded case. In addition, some new analytical solutions are presented in this paper and some new results for high order modal solutions will be given,

In summary, this paper examines techniques for deriving approximate analytical solutions for the fields of large-area graded-index rectangular waveguides. The results of this study should find application in high-speed multimode optical interconnects.

References

- [1] J. Chen, N. Bamiedakis, P. P. Vasil'ev, T. J. Edwards, C. T. A. Brown, R. V. Penty and I. H. White, *High Bandwidth and Large Coupling Tolerance Graded-Index Multimode Polymer Waveguides for On-Board High-Speed Optical Interconnects*, J. Lightwave Technol., Vol. 34, No. 12, June 15, 2016.

Magneto-optic Rigorous Coupled Wave Analysis – numerical investigation of nonreciprocal waveguiding structures

P. Kwiecien¹, I. Richter^{1*}, V. Kuzmiak,² J. Čtyroký²

¹ Czech Technical University in Prague, Faculty of Nuclear Sciences and Physical Engineering, Department of Physical Electronics, Břehová 7, 11519 Prague 1, Czech Republic

² CAS Institute of Photonics and Electronics, Chaberská 57, 182 51 Praha 8, Czech Republic

* ivan.richter@fjfi.cvut.cz

Based on magneto-optic Fourier modal method (MOaRCWA) simulations, both in 2D in 3D, we have studied the magnetoplasmons in plasmonic nanostructures, such as InSb within the THz spectral region.

Introduction

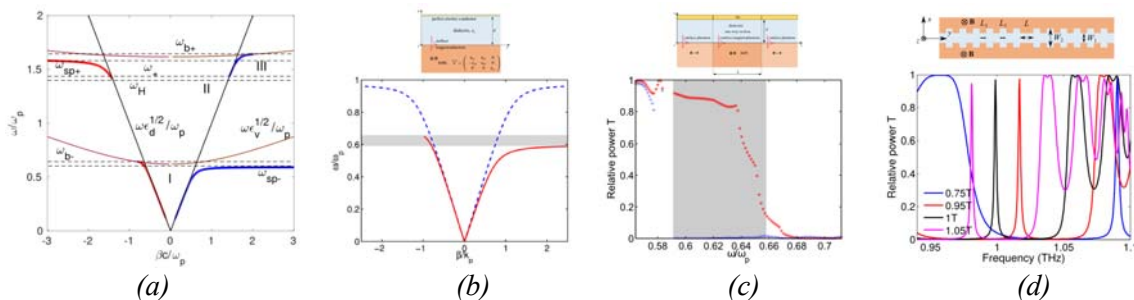
One of only few possibilities how to impose nonreciprocity in guiding subwavelength structures is to apply an external magnetic field (mainly in the Voigt configuration). In such a case, one-way (nonreciprocal) propagation of SP is not only possible but may bring many interesting phenomena in connection with magnetoplasmons (MSP).

Results – MOaRCWA simulations

We have developed an efficient 2D numerical technique based on MO aperiodic rigorous coupled wave analysis – MOaRCWA [1]. In our in-house tool, the artificial periodicity is imposed within a periodic 1D RCWA method, in the form of the complex transformation and / or uniaxial perfectly matched layers. We have combined the MOaRCWA simulations with (quasi)analytical predictions in order to study MSP performance of plasmonic nanostructures with highly-dispersive polaritonic InSb material, in the presence of external magnetic field. Here, Voigt MO effect can be used to impose nonreciprocity (one-way propagation) bringing new interesting phenomena in connection with MSP.

As an example, Figs.(a)-(c) show one of these structures studied, InSb-based THz waveguides. We have shown that the one-way bandwidth can be controlled by an external magnetic field and by the permittivity and thickness of the dielectric guiding layer. Based on such analysis of simple guiding structures, we have proceeded with modeling of several more complex magneto-optical InSb microstructures in THz range (see Fig.(d)). Finally, recently, we have worked on the extension of our MOaRCWA numerical tool to fully 3D case;

Acknowledgements: This work was financially supported by the Czech Science Foundation (project 16-00329S).



(a) Dispersion curves of surface MSP at InSb/air interface (without losses), (b) InSb/dielectric/metal structure and its dispersion diagram (dashed curves – without magnetic field, solid curves – with magnetic field $B = 1$ T), (c) InSb/dielectric/metal structure with the excitation and detection sections (without magnetic field), relative spectral transmittance T of the forward and backward propagating waves, (d) THz with MO Bragg grating - relative spectral transmittance T for different external magnetic fields.

- [1] P. Kwiecien, I. Richter, V. Kuzmiak, J. Čtyroký, "Nonreciprocal waveguiding structures for THz region based on InSb," JOSA A 34 (6), 892 (2017).

Vectorial semi-analytical model for Fano resonances in guided mode resonance gratings

Anne-Laure Fehrembach, Boris Gralak, Anne Sentenac

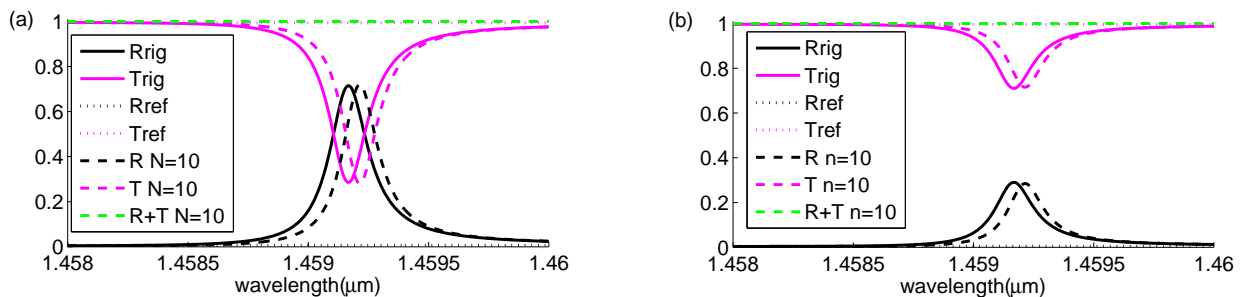
Aix-Marseille Univ, CNRS, Centrale Marseille, Institut Fresnel, Marseille, France
anne-laure.fehrembach@fresnel.fr

We present a semi-analytical self-consistent model, based on the Green's function formalism, to calculate the field diffracted by resonant periodic sub-wavelength structures. We obtain an intuitive expression of the reflectivity and transmittivity matrices in terms of coupling integrals between the eigenmodes and with radiating modes. These expressions are used to derive a physical analysis in configurations where the effect of the incident polarization is not trivial. We provide numerical validations of our model.

The starting point of the method is the Helmholtz's equation. The grating is considered as a perturbation on a reference planar structure, which supports guided modes. The Green's tensor solution of the Helmholtz's equation for the planar reference structure is introduced to obtain a set of rigorous integral equations for the field diffracted by the structure in each diffraction order. The singular part of the Green's tensor is used to express the permittivity of the reference structure, and its regular part is expanded over the eigenmodes of the structure [1].

Thanks to simplifying hypothesis, the set of rigorous integral equations is transformed into a set of approached linear equations, involving the coupling integrals between the eigenmodes and with radiating modes. Its resolution leads to an approached expression of the field diffracted in each order of the structure, from which we deduce the reflectivity (resp. transmittivity) matrix of the structure. It is expressed as the sum of the reflectivity (resp. transmittivity) matrix of the reference structure and the matrices due to the coupling in and out of the modes. Our model is close to the one presented in [2], the main novelty being that it solves the full vectorial diffraction problem.

Fig. 1 provides a validation of the method by comparison with rigorous calculation. An eigenmode is excited through the first diffraction order of a 1D grating illuminated under conical incidence (e.g. plane of incidence neither parallel nor perpendicular to the grating grooves). The resonance appears both for the s and p polarizations, and requires a vectorial model to be represented properly.



Approached model (R, T) and rigorous calculation (R_{rig}, T_{rig}) - reflectivity and transmittivity spectrum for a guided mode resonance grating under conical incidence, (a) s polarization, (b) p polarization.

References

- [1] P.M. Morse, P.M. Feshbach, *Methods of theoretical physics*, Ed. G.P. Harnwell, McGraw-Hill, 1953.
- [2] I. Evenor, E. Grinvald, F. Lenz, S. Levit *Analysis of light scattering off photonic crystal slabs in terms of Feshbach resonances*, Eur. Phys. J. D., 2012, 66, 231-239 .

Bound States in the Continuum Surrounded by Ultra-strong Resonances

Lijun Yuan¹, Ya Yan Lu²

¹ College of Mathematics and Statistics, Chongqing Technology and Business University, China

² Department of Mathematics, City University of Hong Kong, Hong Kong

mayylu@cityu.edu.hk

On periodic structures, a bound state in the continuum (BIC) is always surrounded by a family of resonant modes with Q -factors tending to infinity. The Q -factors typically blow up quadratically, which could limit the applications. We identify a condition on the BIC, such that the Q -factors has a fourth power blowup.

BICs and resonances

We consider 2D structures which are invariant in z , periodic in y with period L , bounded in the x direction, and surrounded by air. The dielectric function ϵ satisfies $\epsilon(x, y + L) = \epsilon(x, y)$ for all (x, y) , and $\epsilon(x, y) = 1$ for $|x| > D$. The structure may have guided and resonant modes which can be written as $\phi(x, y)e^{i\beta y}$ where ϕ is periodic in y with period L and β is the Bloch wavenumber. A guided mode has a real β and a real angular frequency ω , and $\phi \rightarrow 0$ as $x \rightarrow \pm\infty$. A resonant mode has a real β and a complex ω , and ϕ satisfies outgoing radiation conditions as $x \rightarrow \pm\infty$.

Most guided modes exist below the light line, i.e., $k_0 < |\beta|$, where k_0 is the free space wavenumber. BICs on periodic structures are special guided modes above the light line, i.e., $k_0 > |\beta|$ [1]. For a given structure, BICs can only exist as isolated points in the $\beta\omega$ plane. If there is a BIC ϕ_* with frequency ω_* and Bloch wavenumber β_* , then there must be a family of resonant modes for all β near β_* [2]. The complex frequency ω of this family of resonant modes depends on β . As $\beta \rightarrow \beta_*$, we have $\text{Re}(\omega) \rightarrow \omega_*$, $\text{Im}(\omega) \rightarrow 0$, and the Q -factor $Q = -0.5\text{Re}(\omega)/\text{Im}(\omega) \rightarrow \infty$. Therefore, a BIC can also be regarded as a special resonant mode with an infinite Q -factor. Typically, $Q \sim (\beta - \beta_*)^{-2}$ for β near β_* . We present a general condition for BICs to have $Q \sim (\beta - \beta_*)^{-4}$.

Condition for ultra-strong resonances

Using a perturbation theory, we show that if a BIC $\{\phi_*, \omega_*, \beta_*\}$ satisfies

$$\int \bar{\varphi}_l G d\mathbf{r} = \int \bar{\varphi}_r G d\mathbf{r} = 0, \quad (1)$$

then $Q \sim (\beta - \beta_*)^{-4}$. In the above, G is related to ϕ_* , $\partial_y \phi_*$, β_* , ω_* and ϵ , and it can be explicitly written down; φ_l and φ_r are diffraction solutions (for the same ω_* and β_*) for incident plane waves given in the left ($x < -D$) and right ($x > D$) media, respectively; and the integrals are evaluated in one period of the structure given by $|y| < L/2$ and $-\infty < x < \infty$. The condition can be further simplified if the structure and the BIC have symmetries. As numerical examples, we calculate BICs satisfying Eq. (1) for a periodic array of circular cylinders, and study the dependence of these special BICs on the radius and dielectric constant of the cylinders.

References

- [1] L. Yuan and Y. Y. Lu, *Bound states in the continuum on periodic structures: perturbation theory and robustness*, Optics Letters **42**(21), 4490-4493 (2017).
- [2] L. Yuan and Y. Y. Lu, *Strong resonances on periodic arrays of cylinders and optical bistability with weak incident waves*, Physical Review A **95**, 023834 (2017).

Automatic design of high-performance fiber-chip surface grating couplers based on Floquet-Bloch mode analysis

D. Pereira-Martín^{1*}, A. Sánchez-Postigo¹, A. Hadij-Elhouati¹, D.-X. Xu², P. Cheben², R. Halir¹, I. Molina-Fernández¹, A. Ortega-Moñux¹, J. G. Wangüemert-Pérez¹

¹ Universidad de Málaga, Dpto. de Ingeniería Comunicaciones, ETSI Telecomunicación, Málaga, Spain

² National Research Council Canada, Ottawa, Canada

* dpm@ic.uma.es

We propose a new strategy to automatically design highly efficient fiber-chip surface grating couplers. High performance designs are achieved with a substantially reduced computational cost by combining Floquet-Bloch mode analysis with a multi-objective optimization technique (genetic algorithms).

Introduction

Surface grating couplers are nanophotonic structures commonly used in integrated optics for fiber-chip coupling, allowing wafer-scale testing and robust misalignment tolerances. Surface grating couplers are generally designed by re-simulating the entire structure in each step of the optimization process. However, this procedure implies high computational cost, particularly when aiming for high performance which may require optimization of multiple structural parameters.

Methodology and results

We divide the whole structure in two quasi-decoupled electromagnetic problems that can be efficiently solved by analyzing the Floquet-Bloch mode for a single period of the grating with our 2D Fourier expansion tool [1]. Specifically, we first optimize the coupling efficiency (CE) of the periodic structure and then we find the input adaptation section that minimizes back reflections. This way, our technique dramatically reduces the computation time. The proposed technique can be used with any constrained multi-objective optimization procedure, such as genetic algorithms or particle swarm optimization (here the former is applied, see Fig. 1.a). The proposed algorithm is tested by optimizing the grating geometry reported in [2] (see Fig. 1.b), which exhibits a high coupling efficiency. After only 4 hours of computation time, a device with similar peak coupling efficiency and bandwidth as that reported in [2] is obtained.

Conclusions

Our results demonstrate that the proposed optimization procedure can yield devices with state-of-the-art performance automatically, with a minimum designer interaction.

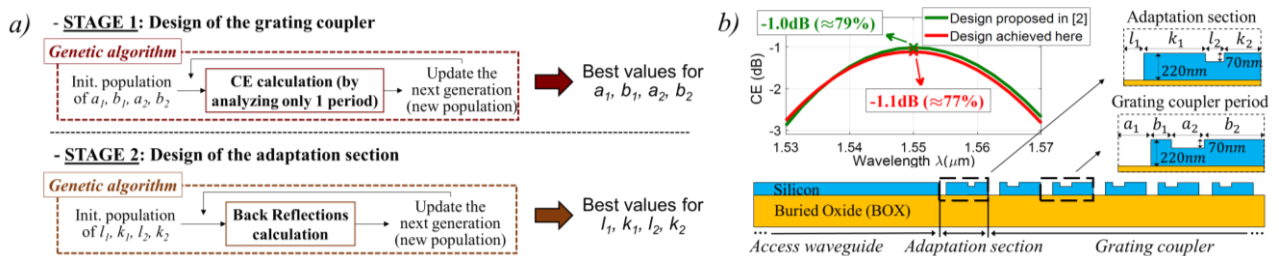


Fig. 1: (a) Automatic design strategy for highly efficient grating couplers and (b) Application example.

References

- [1] Zavargo-Peche, L., et al. *Progress Electromagn. Res.* 123, 447 (2012).
- [2] Alonso-Ramos, C., et al. *Opt. Lett.* 39, 5351 (2014).

Full-vector finite element 3D model for waveguide-based plasmonic sensors

Guillaume Demésy, Gilles Renversez,*

Aix-Marseille Univ, CNRS, Centrale Marseille, Institut Fresnel, 13013 Marseille, France

* gilles.renversez@fresnel.fr guillaume.demesy@fresnel.fr

This study aims at designing an efficient plasmonic waveguide for infrared sensing. The device configuration is fully integrated and based on a ridge waveguide upon which metallic scattering nano-objects ensure the coupling between the guided modes and superstrate of the device. Full vector 3D modelling based on the finite element method is used to optimize the device parameters taking into account the mode used as excitation.

This study aims at designing an efficient plasmonic waveguide for infrared sensing [1, 2]. The device configuration is fully integrated and based on a ridge waveguide upon which metallic scattering nano-objects will ensure the coupling between the guided modes and superstrate of the device. Chalcogenide glasses are chosen for the main layers due to their high transparencies for infrared wavelengths [3]. Ultimately, the metallic scatterers are planned to be functionalized in order to react to the targeted chemical species. As a result, the guidance properties of the full structure are modified ensuring the sensor function. In order to model the response of the 3D guiding structure, we adopt a diffracted field formulation consisting of two sequential steps, the output of first step being the input of the second one. First, we determine the guided leaky modes for a fixed frequency (corresponding to a wavelength of 7.7 microns because we are looking for a response in the infrared range) of the unperturbed 2D waveguide (i.e. without the plasmonic nanostructures). This is a ridge waveguide made of chalcogenide layers on a silicium substrate, assumed to be invariant along its propagation axis. We use usual vector FEM method with the Galerkin approach to solve the associated eigenvalue problem [4]. In this step, we use edge elements for the transverse field and nodal element for the longitudinal one. This first step provides both the mode field profile and the associated propagation constants. Second, these guided modes (eventually only the fundamental one) are used as an incident field for the full 3D problem (i.e. with the metallic nanostructures). The electromagnetic problem to solve for this second step is then a scattering problem [5, 6]. It is finally possible to define an energy balance (transmission and reflexion into the ridge guide, absorption taking place into the plasmonic rods, radiation losses) allowing to characterize the efficiency of the device as a plasmonic sensor. We use our 3D vector finite element method with edge elements on tetrahedrons to solve the problem [4]. Our method allows to compute all the needed energy-related quantities to investigate quantitatively the behaviour of the full structure including the impact of the metal nanoparticles located on the top of the waveguide and to take into account the way it is excited by the selected propagating mode. We will present a study of the influence of the nano-particle parameters on the output field as well as a study of more complex nano-structuration on top of the ridge waveguide consisting of arrays of metallic particles.

References

- [1] A. Gutierrez-Arroyo, E. Baudet, L. Bodiou, J. Lemaitre, I. Hardy, F. Fajjan, B. Bureau, V. Nazabal, and J. Charrier, *Opt. Express* **24**, 23,109–23,117 (2016).
- [2] E. Baudet, A. Gutierrez-Arroyo, P. Němec, L. Bodiou, J. Lemaitre, O. D. Sagazan, H. Lhermitte, E. Rinnert, K. Michel, B. Bureau, J. Charrier, and V. Nazabal, *Opt. Mater. Express* **6**, 2616–2627 (2016).
- [3] V. Nazabal, F. Charpentier, J.-L. Adam, P. Nemeč, H. Lhermite, M.-L. Brandily-Anne, J. Charrier, J.-P. Guin, and A. Moreac, *Int. J. Appl. Ceram. Technol.* **8**, 990–1000 (2011).
- [4] F. Zolla, G. Renversez, A. Nicolet, B. Kuhlmeij, S. Guenneau, D. Felbacq, A. Argyros, and S. Leon-Saval, *Foundations of Photonic Crystal Fibres, 2nd ed.* (Imperial College Press, London, 2012).
- [5] G. Demésy, F. Zolla, A. Nicolet, M. Commandré, and C. Fossati, *Opt. Express* **15**, 18,089–18,102 (2007).
- [6] G. Demésy, F. Zolla, A. Nicolet, and M. Commandré, *J. Opt. Soc. Am. A* **27**, 878–889 (2010).

Simulation of luminescence in periodically structured layers based on direct S-matrix calculation

Alexey A. Shcherbakov¹, Thomas Kämpfe², Yves Jourlin³,

¹ *Laboratory of Nanooptics and Plasmonics, Moscow Institute of Physics and Technology, Dolgoprudny, Russia*

² *University of Lyon, UJM-Saint-Etienne, CNRS, Institut d'Optique Graduate School, Laboratoire Hubert Curien UMR 5516, F-42023 Saint-Etienne, France*
alex.shcherbakov@phystech.edu

We address the problem of rigorous electromagnetic simulation of periodically patterned light-emitting layers of luminescent materials. To cope with the problem we make use of analytical components for arbitrary grating S-matrices in the Fourier domain. This result is shown to directly contribute to a method for simulation of luminescence radiation pattern based on the S-matrix propagation algorithm and plane wave decomposition of the dipole field.

Simulation of patterned light-emitting structures

Being introduced into light-emitting diodes and other luminescent structures periodical patterning is known to be capable to dramatically modify performance of such devices. When the patterning has wavelength scale features an efficient rigorous simulation method is required for optimization of light-emitting structures. Additionally, in case of patterned dielectric or semiconductor heterostructures a rigorous electromagnetic simulation method can help to distinguish between macroscopic and microscopic effects.

Previously there were proposed several approaches to solve the described problem, and a method of [1] based on the Differential Method from the grating diffraction theory seems to be among the most suitable techniques. Here we develop an alternative approach, which simplifies the mentioned one in terms of formulation and computing efforts, and benefits from a previously developed direct S-matrix calculation method [2]. The latter comprises analytically derived components of S-matrices in the Fourier space for arbitrary 1D and crossed gratings, and naturally incorporates calculation of self-consistent fields from internal dipole sources.

Acknowledgement

Alexey A. Shcherbakov acknowledges support by Russian Science Foundation (project 17-79-20345).

References

- [1] H. Rigneault, F. Lemarchand, and A. Sentenac, "Dipole radiation into grating structures," *J. Opt. Soc. Am. A*, **17**, 1048–1058 (2000).
- [2] A. A. Shcherbakov, Yu. V. Stebunov, D. F. Baidin, T. Kämpfe, and Y. Jourlin, "Direct S-matrix calculation for diffractive structures and metasurfaces," arXiv:1712.08361 [physics.optics] (2018).

Using spline interpolation for grating geometry description within the curvilinear coordinate Generalized Source Method

Alexey A. Shcherbakov¹

¹ *Laboratory of Nanooptics and Plasmonics, Moscow Institute of Physics and Technology, Dolgoprudny, Russia*
alex.shcherbakov@phystech.edu

The Generalized Source Method with curvilinear coordinate transformations was demonstrated to efficiently solve grating diffraction problems with metal-dielectric structures. In the preceding work its application was limited to sinusoidal profiles only. Here we release this restriction by developing a general approach comprising grating geometry definition by spline interpolation.

Simulation of metasurfaces using curvilinear coordinate transformations

Currently different kinds of metasurfaces made of both metals and dielectrics attract a lot of attention. Despite existence of numerous approaches and corresponding software one may still face challenges while analysing complex realistic metal-dielectric crossed periodic structures, which is necessary, for example, for estimation of impact of fabrication defects on device performance.

To extend the class of rigorously numerically solvable metal-dielectric metasurface structures the Generalized Source Method in the curvilinear coordinate formulation (GSMCC) [1, 2] is further developed here. Briefly the method benefits from the introduction of local curvilinear metric in a grating region so as to straighten a grating corrugation interface to a plane. The idea is analogous to the one used in the C-method in the grating diffraction theory, however the requirement of translational invariance of curvilinear coordinates is released, which makes efficient and rigorous simulation of complex multilayer structures possible.

Previously the GSMCC was formulated in detail only for sinusoidal profiles, which substantially limited its applicability. In this work we demonstrate how the method can be applied for periodic metasurface structures which interfaces are described by 1D and 2D spline interpolation. This considerably extends the method usefulness for practical applications, as well as paves a way towards an efficient simulation of realistic complex metasurface structures.

Acknowledgement

The work was supported by Russian Science Foundation (project 17-79-20345).

References

- [1] A. A. Shcherbakov, and A. V. Tishchenko, "Efficient curvilinear coordinate method for grating diffraction simulation," *Opt. Express*, **21**, 25236-25247 (2013).
- [2] A. A. Shcherbakov, and A. V. Tishchenko, "Generalized source method in curvilinear coordinates for 2D grating diffraction simulation," *J. Quantitative Spectrosc. Radiat. Transf.*, **187**, 76-96 (2017).

Reduction in Bend Loss of a Si-wire Waveguide by Adjusting the Core Location

T. Aso, T. Ishiguro, J. Yamauchi, H. Nakano
 Faculty of Science and Engineering, Hosei University, Tokyo, Japan
takehiro.ishiguro.9h@stu.hosei.ac.jp

A buried bent Si-wire waveguide is analyzed by the recently developed cylindrical Yee-mesh-based imaginary-distance BPM. It is found that only the adjustment of a core location enables us to reduce the pure bend loss (PBL) and the polarization dependent loss (PDL) over a wide spectral range from 1.3 to 1.65 μm .

Summary

To reduce the bend loss, various techniques have been developed [1]. Recently, we have proposed a new simple technique, in which the core is slightly buried from the air/cladding interface [2]. However, in Ref. [2], we have treated a weakly guiding waveguide and only pointed out the possibilities in a strongly guiding waveguide. In this work, we study a bent Si-wire waveguide buried in a silica cladding. The analysis is carried out using the cylindrical YM-BPM with an enhanced amplification factor [3]. Fig. 1 shows the configuration with a square Si-core of $w = 0.32 \mu\text{m}$. The bending radius R_c is fixed to be $2.0 \mu\text{m}$ and the loss of a 90° bend is investigated. The distance between the core and the air region is designated as d_{air} . Preliminary calculation shows that a reduced PBL for both quasi-TE and quasi-TM modes is achieved for $d_{\text{air}} = 0.15 \mu\text{m}$. We, therefore, examine the structure with $d_{\text{air}} = 0.15 \mu\text{m}$. The wavelength characteristics of the PBL and PDL are, respectively, presented in Figs. 2(a) and (b), in which the results obtained for $d_{\text{air}} = \infty$ and $d_{\text{air}} = 0$ are also shown for comparison. Although the PBL tends to increase as the wavelength becomes longer, the slightly buried core significantly reduces the PBL for both modes. Fig. 2(b) indicates that the PDL also tends to increase as the wavelength is increased. However, the proposed structure reduces the PDL over a wide spectral range from 1.3 to 1.65 μm . In other words, the PBL can be suppressed regardless of polarization with realizing a subsequent reduced PDL.

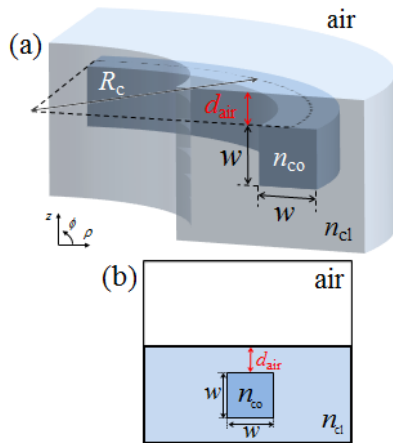


Fig.1. Configuration. (a) Overview.
 (b) Cross-section view.

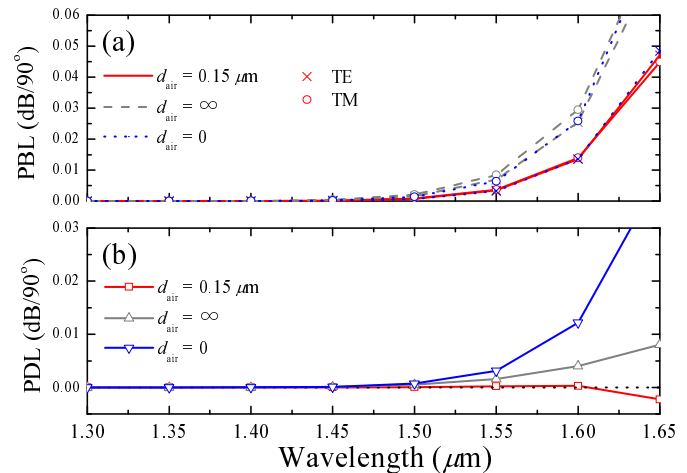


Fig.2 Wavelength characteristics. (a)PBL. (b)PDL.

References

- [1] B. Howley *et al.*, "Experimental evaluation of curved polymer waveguides with air trenches and offsets," *J. Appl. Phys.*, vol. 100, 023114, May 2006.
- [2] Y. Nito *et al.*, "Reduction in bend losses of a buried waveguide on a silicon substrate by adjusting the core location," *J. Lightw. Technol.*, vol. 34, no. 4, pp. 1344-1349, Feb. 2016.
- [3] T. Aso *et al.*, "Development of an imaginary-distance cylindrical YM-BPM with an enhanced amplification factor," *Int. Symp. Microw. Opt. Technol.*, TA3-4, June 2017.

A Polarization Converter Consisting of a Bent Si-wire Waveguide

J. Yamauchi, Y. Nakagawa, T. Tsuchiya, H. Nakano
 Faculty of Science and Engineering, Hosei University, Japan
yuto.nakagawa.8p@stu.hosei.ac.jp

The cylindrical Yee-mesh-based BPM with an enhanced amplification factor and the FDTD method are applied to the analysis of a polarization converter with a bent waveguide. The conversion length and insertion loss are reduced, compared with a converter consisting of a straight waveguide.

Summary

An asymmetric waveguide, such as an L-shaped one [1], efficiently yields a polarization conversion property. Recently, some attempts to use a bent waveguide were made in a polarization conversion section, since the conversion length can be reduced [2]. In this work, we treat the bent Si-wire waveguide on the silica substrate shown in Fig. 1. We first consider the effect of the aspect ratio (h_{co}/w_{co}) on the polarization crosstalk to investigate a desirable configuration. Fig. 2 shows the polarization crosstalk of a 90° bend as a function of core aspect ratio, when the eigenmode of a straight waveguide is illuminated. It is found that a rectangular core with h_{co}/w_{co} being slightly less than 1.0 is liable to generate the polarization coupling, compared with a square one. Based on this fact, we design a conversion section with parameters, such as $w_{co} = 0.4 \mu\text{m}$, $h_{co} = 0.22 \mu\text{m}$, $w_d = 0.2 \mu\text{m}$, and $h_d = 0.16 \mu\text{m}$. The eigenmode analysis based on the Yee-mesh-based BPM [3] provides a reduced conversion length L_c from $3 \mu\text{m}$ to $2.85 \mu\text{m}$ when a bending radius of $R_c = 2 \mu\text{m}$ is introduced. The effectiveness of using a bent waveguide lies in the fact that the transition loss at the junction between the input (output) waveguide and the conversion section is reduced, since the loaded part remains to be small in comparison with a straight counterpart. The reduction in the insertion loss becomes significant particularly at longer wavelengths, as shown in Fig. 3. As a result, an extinction ratio of more than 15 dB is achieved with an insertion loss of less than 3 dB over a wavelength range of 1.5 to $1.6 \mu\text{m}$.

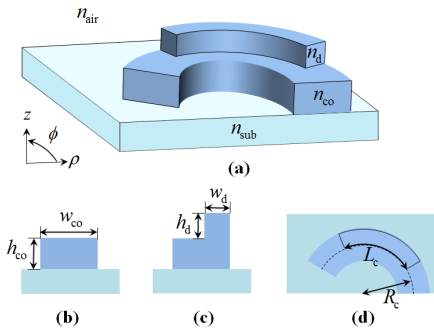


Fig. 1. Configuration. (a) Perspective view. (b) Input section. (c) Converter. (d) Top view.

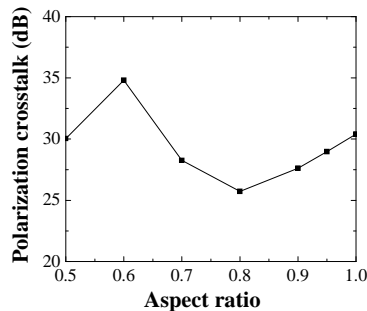


Fig. 2. Polarization crosstalk of a 90° bend as a function of core aspect ratio.

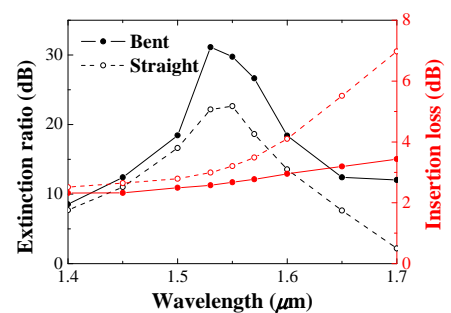


Fig. 3. Extinction ratio and insertion loss as a function of wavelength.

References

- [1] Y. Wakabayashi *et al.*, "Short waveguide polarization converter operating over a wide wavelength range," *J. Lightw. Technol.*, vol. 31, no. 10, pp. 1544-1550, May 2013.
- [2] T. Cao *et al.*, "Ultra-compact and fabrication-tolerant polarization rotator based on a bend asymmetric-slab waveguide," *Appl. Opt.*, vol. 52, no. 5, pp. 990-996, Feb. 2013.
- [3] T. Aso *et al.*, "Development of an imaginary-distance cylindrical YM-BPM with an enhanced amplification factor," *Int. Symp. Microw. Opt. Technol.*, TA3-4, Seoul, June 2017.

Polarization-dependent and -independent Absorbers with a Periodic Metal Grating

J. Yamauchi, N. Takahashi, H. Ito, H. Nakano
 Faculty of Science and Engineering, Hosei University, Japan
naoki.takahashi.2g@stu.hosei.ac.jp

A planar layered structure whose top layer is patterned using a periodic metal grating is analyzed using the FDTD method. An Ag-stripe grating leads to polarization selectivity, i.e., only the TM wave is absorbed. The use of a square Fe-patch realizes ultra wideband absorption of more than 93% regardless of polarization.

Summary

A planar absorber composed of metal-dielectric film pairs has been proposed [1][2]. The top layer is often patterned as metallic gratings to enhance the absorption. In this work, we design a polarization-dependent and -independent absorbers using the unit-cell configuration shown in Fig. 1. The dispersion properties of metals (n_m) are determined by the Drude-Lorentz model [3], and the dielectric substrate is chosen to be SiO₂ ($n_s = 1.52$). We first consider a polarization-selective absorber with Ag-stripe gratings in visible wavelengths. The configuration parameters are set to be $t_m = 50$ nm, $t_p = 40$ nm, $\Lambda = 400$ nm, $w_{p1} = 100$ nm, and $t_{s1} = t_{s2} = 170$ nm. To obtain a stripe configuration, w_{p2} is taken to be Λ . A plane wave is normally incident towards the $+z$ direction. The absorption spectrum is depicted in Fig. 2. The structure is found to absorb the TM wave, while reflecting the TE wave. It is interesting to note that the absorption for the TM wave has two peaks, so that an absorption of more than 80% is retained over a wavelength range of 520 to 540 nm. We next realize an ultra-broadband absorber independent of polarization. Although Ref. [4] suggested the effectiveness of Fe-stripes in terms of impedance matching, no attempt has been made to achieve polarization independency. The parameters are redesigned as $t_m = 10$ nm, $t_p = 95$ nm, $\Lambda = 300$ nm, $t_{s1} = 145$ nm, and $t_{s2} = 30$ nm. To obtain the same response regardless of polarization, a square patch ($w_{p1} = w_{p2}$) is employed. Fig. 3 shows the absorption spectrum, in which the data without patches ($w_{p1} = w_{p2} = 0.0\Lambda$) and for a flat metal sheet (1.0Λ) are also included. It should be noted that the square patch with $w_{p1} = w_{p2} = 0.7\Lambda$ contributes to the improvement at shorter wavelengths. It is worth mentioning that the absorption exceeding 93% is achieved over a wide wavelength range of 500 to 1600 nm with the use of square patches.

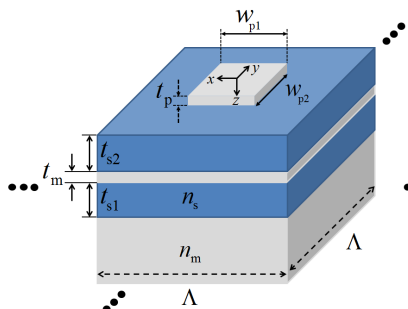


Fig. 1. Configuration of a unit cell.

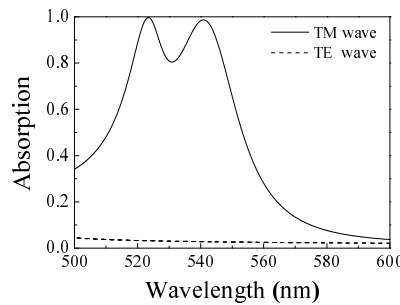


Fig. 2. Polarization-selective properties.

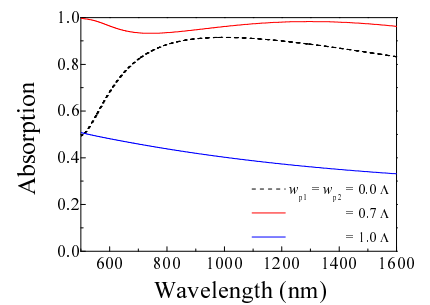


Fig. 3. Polarization-independent properties.

References

- [1] Y. Cui *et al.*, "Plasmonic and metamaterial structures as electromagnetic absorbers," *Laser Photon. Rev.*, vol. 8, no. 4, pp. 496-520, 2014.
- [2] Y. K. Zhong *et al.*, "Polarization-selective ultra-broadband super absorber," *Opt. Express*, vol. 25, no. 4, pp. A124-A133, 2017.
- [3] E. D. Palik, *Handbook of Optical Constants of Solids*, Academic Press, New York, 1985.
- [4] D. Wu *et al.*, "Numerical study of an ultra-broadband near-perfect solar absorber in the visible and near-infrared region," *Opt. Lett.*, vol. 42, no. 3, pp. 450-453, 2017.

Effectiveness of a Curvilinear Taper in Waveguide Applications

J. Yamauchi, K. Shimada, R. Ando, and H. Nakano
 Faculty of Science and Engineering, Hosei University, Japan
keigo.shimada.4i@stu.hosei.ac.jp

A curvilinear taper is applied to a spot size converter in a lightwave circuit and a rod antenna at microwave frequencies. A rectangular Si-core improves the spot size conversion for both TE and TM waves, even for a horizontally tapered core. The curvilinear taper contributes to a high directivity, compared with a linear taper.

Summary

A tapered waveguide is widely used in transforming an input mode field to a field with a different size [1]. The radiation caused by the mode transformation should be minimized to enhance the conversion efficiency. We first consider the spot size converter proposed in Ref. [1]. The configuration is shown in Fig. 1, which intends the mode conversion from a Si-wire waveguide to a SiO₂ waveguide. In Ref. [1], a square Si-core is used together with a linear taper in the horizontal direction. This, however, results in a long conversion length as well as unbalanced conversion between the TE and TM modes. To solve this problem, we introduce a rectangular Si-core and the curvilinear taper expressed as $w_{co}(z) = w_i - (w_i - w_o)(z/l)^{(1/r)}$ [2], where l is the taper length and r is the parameter controlling the taper profile ($r = 1$ corresponds to the conventional linear taper). Special attention is paid to the local taper angle between the waveguide axis and the tangent to the core-cladding interface, since the taper angle is closely related to radiation [3]. Preliminary calculation shows that the square Si-core yields a large difference in allowable taper angles in both TE and TM modes as long as the taper is introduced in one direction. Also, use of a rectangular core brings the allowable taper angles closer to each other. Fig. 2 shows the guided-mode power as a function of wavelength, in which w_i and w_o are fixed to be $0.3 \mu\text{m}$ and $0.04 \mu\text{m}$, respectively. In Fig. 2(a) we find the effectiveness of the rectangular core for the TM mode. The performance is further improved for $r = 1.5$, as shown in Fig. 2(b). The curvilinear taper also serves to enhance the directivity of the cylindrical rod antenna shown in the inset of Fig. 3. The dielectric rod is fed by a metallic waveguide (WCI-120). The rod with a length of 23.9λ and a relative permittivity of 2.0 is tapered from the inside of a launching horn. The rod diameter at the free end is reduced to half that of the initial one. It is found that a gain increase of more than 2.5 dB is obtained when n is changed from 1 to 5 at an operating frequency of 11 GHz.

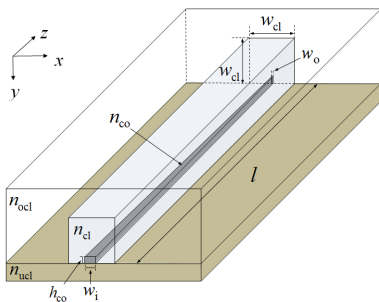


Fig. 1. Configuration of a spot size converter.

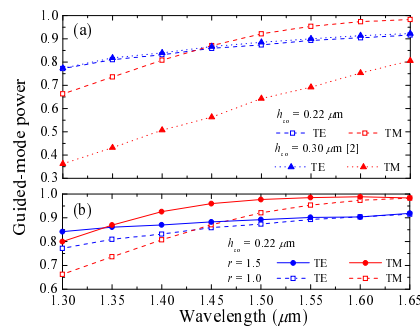


Fig. 2. Wavelength properties.

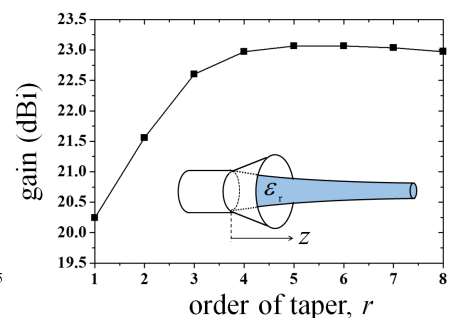


Fig. 3. Gain of a dielectric rod antenna.

References

- [1] T. Tsuchizawa *et al.*, "Microphotonic devices based on silicon microfabrication technology," *IEEE J. Sel. Topics Quantum Electron.*, vol. 11, no. 1, pp. 232-240, 2005.
- [2] T. Ando *et al.*, "Linearly and curvilinearly tapered cylindrical-dielectric-rod antennas," *IEEE Trans. Ant. Propag.*, vol. 53, no. 9, pp. 2827-2833, 2005.
- [3] F. Ladouceur and J. D. Love, *Silica-based Buried Channel Waveguides and Devices*, Chapman & Hall, London, 1996.

Study of a Quarter-wave Plate Using an Array of Cross-shaped Apertures in a Metallic Plate

J. Yamauchi, R. Nakada, H. Nakano

Faculty of Science and Engineering, Hosei University, Tokyo, Japan
ryota.nakada.2c@stu.hosei.ac.jp

The wavelength responses of a metallic quarter-wave plate are evaluated by the FDTD method with the periodic boundary condition. The polarization conversion behaviors exhibit two peaks of the ellipticity as a function of wavelength. Widening the widths of cross slots leads to a transmittance of almost 70%.

Summary

Various plasmonic wave plates have been proposed using a periodic structure. A quarter-wave plate based on a thin Ag film [1] can be realized by tuning the length of a cross-shaped aperture. However, the transmittance of the previous quarter-wave plate is at best 40%. This is mainly due to the fact that the aperture ratio (slot area to total plate area) remains to be as low as 10%. In this work, special emphasis is placed on the effect of the width of the cross-shaped aperture on the transmittance, paying attention to the ellipticity. The analysis is carried out using the FDTD method with the periodic boundary condition. The structure to be studied is shown Fig. 1. The optical constants of Ag are taken from Ref. [2], and the plate is assumed to be surrounded in free space. The periodicity Λ is $0.6 \mu\text{m}$ and the Ag film thickness t is $0.21 \mu\text{m}$. The width of the cross slot w is varied, while the lengths of the horizontal and vertical slots being fixed to be $l_x = 0.345 \mu\text{m}$ and $l_y = 0.30 \mu\text{m}$, respectively. A linearly polarized plane wave, with its polarization orientation of $\phi_{\text{in}} = 45^\circ$, is normally incident towards the $+z$ direction from the air region. Fig. 2 shows the transmittance as a function of w . Since a nearly circular polarization of less than 3 dB is obtained at two wavelengths, two data designated as λ_S and λ_L are plotted. Note that open symbols mean insufficient ellipticity. It is found that the transmittance achieves above 50% at both wavelengths by choosing $w = 0.165 \mu\text{m}$ or more. The maximum transmittance approaches approximately 70%. The E_x field distributions observed at the output of the structure at resonant wavelengths of $0.67 \mu\text{m}$ and $0.66 \mu\text{m}$ are depicted in Figs. 3(a) and (b), respectively. Fig. 3(a), corresponding to narrow slots, indicates that the field predominantly exists in the slot along the y direction. In addition, the field is particularly localized at the inner edges. On the other hand, for the wide slot shown in Fig. 3(b), the field is distributed along not only in the slot along the y direction but also in the x direction, with slight peaks being retained at the inner edges. When the slot width is further increased to $w = 0.3 \mu\text{m}$, the cross-shaped aperture becomes a rectangular one, resulting in the field significantly localized at both sides along the y direction.

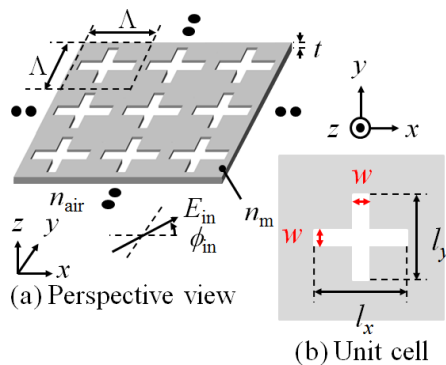


Fig.1. Configuration.

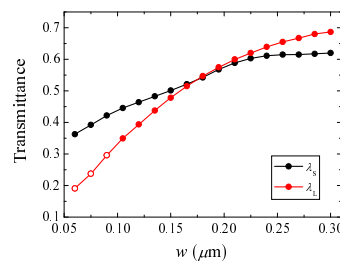


Fig.2. Transmittance.

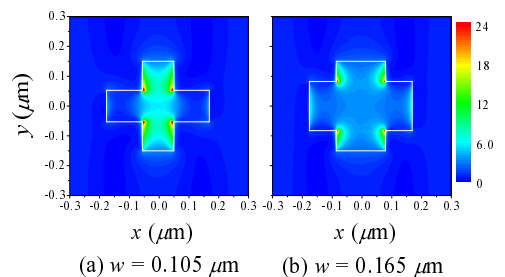


Fig.3. E_x field distributions.

References

- [1] A. Roberts and L. Lin, "Plasmonic quarter-wave plate," *Opt. Lett.*, vol. 37, no. 11, pp. 1820-1822, June 2012.
- [2] R. B. Johnson and R. W. Christy, "Optical constants of the novel metals," *Phys. Rev. B.*, vol. 6, no. 12, pp. 4370-4379, Dec. 1972.

Study of Perforated Metal Sheets Based on Square and Rectangular Lattices

J. Yamauchi, Y. Tanaka, S. Yoshino, H. Nakano
 Faculty of Science and Engineering, Hosei University, Japan
yuki.tanaka.3a@stu.hosei.ac.jp

Polarization conversion properties of an array of rectangular apertures in a metal sheet are investigated using square and rectangular lattices. The FDTD analysis shows that the difference in the lattice type affects the generation of evanescent waves at the input and output interfaces, causing different ellipticities.

Summary

A sub-wavelength hole array has received much attention since the discovery of an extraordinary transmission by Ebbesen *et al.* [1]. Recently, we proposed a polarization converter consisting of a metal sheet with an array of rectangular apertures based on a square lattice [2]. The proposed structure can operate at not only lightwaves but also microwaves. Meanwhile, a similar configuration has also been independently developed by Helfert *et al.* [3], in which a rectangular lattice is employed. They succeeded in developing a polarization converter and explained the operation mechanism using the guided modes of a metallic hollow waveguide. In this article, the characteristics of the converter obtained for the square lattice are compared with those for the rectangular lattice. Fig. 1 shows the overall configuration and the unit cell. The metal sheet consisting of Ag is periodically perforated. The periodicity is determined by Λ_x and Λ_y , where Λ_x is fixed to be $0.92 \mu\text{m}$. Other configuration parameters are taken to be $l_x = 0.88 \mu\text{m}$, $l_y = 0.60 \mu\text{m}$, and $t = 0.36 \mu\text{m}$. A linearly polarized plane wave with its polarization orientation of $\phi = 45^\circ$ is normally incident towards $+z$ direction so as to excite two orthogonal modes with almost the same amplitude. The transmittance and the ellipticity versus wavelength are shown in Figs. 2(a) and (b), respectively. It is found that a circularly polarized wave is obtained for the square lattice over a wavelength range of 0.97 to $1.2 \mu\text{m}$, while retaining a fairly large transmittance of more than 70%. In contrast, the result for the rectangular lattice with $\Lambda_y = 0.7 \mu\text{m}$ yields elliptical polarization. The difference of the behavior may be explained in terms of the decomposition of the propagating wave in the aperture. Figs. 3 (a) and (b), respectively, show the E_x - and E_y -field distributions for the square lattice, plotted in the direction of the z axis. The fields are decomposed at a wavelength of $1.1 \mu\text{m}$. We first subtract the traveling wave (denoted as Once), and then subtract the reflected wave (Twice). Appreciable evanescent waves can be found for the E_y field at the input and output interfaces. Further calculation, however, shows that there are slight evanescent waves for the rectangular lattice. Since the existence of the evanescent waves affects the phase relation between the E_x - and E_y -fields, the different polarization properties are observed.

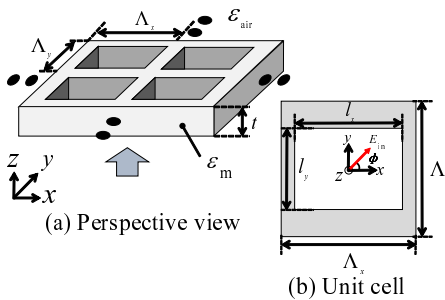


Fig. 1. Configuration.

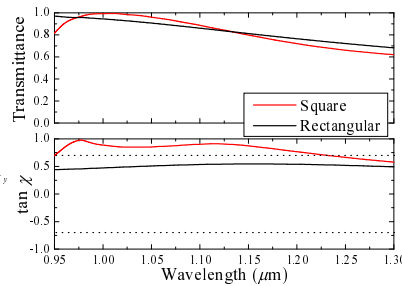


Fig. 2. Transmittance and ellipticity.

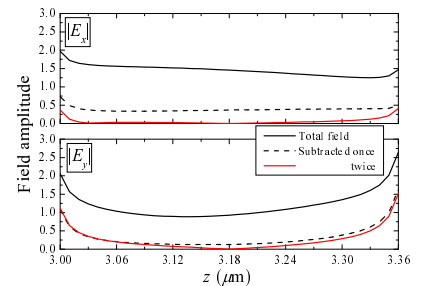


Fig. 3. Decomposition of the field distributions.

References

- [1] T. W. Ebbesen *et al.*, "Extraordinary optical transmission through sub-wavelength hole arrays," *Nature*, vol. 391, no. 12, pp. 667-669, 1988.
- [2] J. Yamauchi *et al.*, *Patent Pending*, P2014-174956, Aug. 2014.
- [3] S. E. Helfert *et al.*, "Hollow waveguides as a polarization converting elements: A theoretical study," *J. Eur. Opt. Soc.-Rapid*, vol. 10, 15006, 2015.

Orthogonal Polarization Rotator for Arbitrary Incidence Plane of Polarization

J. Yamauchi, T. Okawachi, D. Shimamura, H. Nakano
 Faculty of Science and Engineering, Hosei University, Tokyo, Japan
takumi.okawachi.4g@stu.hosei.ac.jp

A polarization rotator consisting of a 45°-skew stack of a dielectric plate is analyzed by the FDTD method with the periodic boundary condition. The polarization rotation by 90° is achieved for arbitrary incident linear polarization. A transmittance of more than 82% is obtained over a wavelength range of 1.25 μm to 1.66 μm.

Summary

Controlling the polarization state of light is of importance in modern optics. Various polarization rotators have been proposed and discussed, including a triangular or rectangular hole array in a dielectric plate [1],[2]. Although these plates act as an efficient polarization rotator over a wide wavelength range, the operation is limited to a specific incidence plane of polarization. To eliminate this limitation, some attempts have been made to realize a rotator independent of the incidence plane of polarization [3],[4]. However, some drawbacks still exist such as a narrow wavelength operation and a low transmittance because of the use of a lossy metallic plate. In this work, we propose a polarization rotator independent of incidence plane of polarization using parallel dielectric plates. Two rotators are stacked in a 45°-skew arrangement, as shown in Fig. 1. Each rotator is composed of silicon and silica materials, whose refractive indexes are $n_H = 3.5$ and $n_L = 1.5$, respectively. The periodicity is set to be $\Lambda = 0.3 \mu\text{m}$, and the filling factor is defined as $f = w_H/\Lambda$. The eigenmode analysis [2] shows that the shortest conversion length is obtained for $f = 0.5$, so that the plate thickness t is taken to be $1.0 \mu\text{m}$. In order to improve the transmission, anti-reflection layers made of silica are set at the input and output interfaces. Fig. 2 shows the transmittance, polarization rotation angle $\Delta\phi$ and ellipticity as a function of wavelength for various incidence planes of polarization. A wave with $|\tan \chi| < 0.3$ may be regarded as linear polarization. It is found that the rotator achieves polarization rotation by 90° over a wide wavelength range of 1.25 μm to 1.66 μm regardless of the incidence plane of linear polarization. A high transmittance of more than 82% is obtained in the same wavelength range. Further calculation shows that the rotator operates successfully even for an obliquely incident wave.

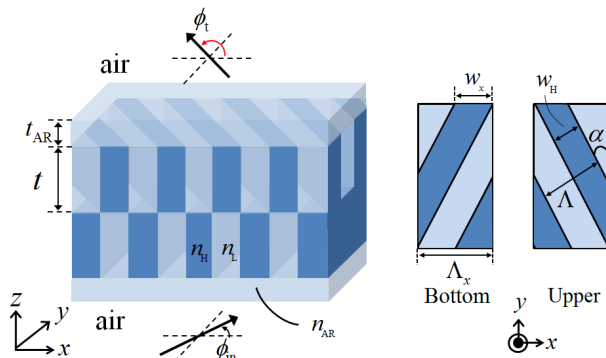
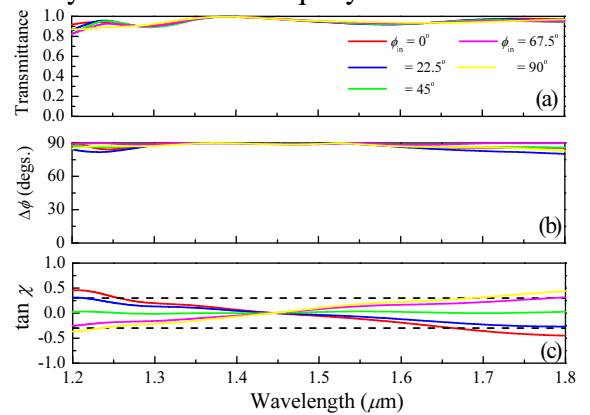


Fig.1. Configuration.



(a) Transmittance (b) $\Delta\phi$ (c) Ellipticity
 Fig.2 Wavelength characteristics.

References

- [1] J. Yamauchi *et al.*, "Quarter-wave plates consisting of subwavelength triangular hole arrays," *Integ. Photon. Research Silicon Nanophoton*, JT3A.22, San Diego, Ca., Jul. 2014.
- [2] T. Aso *et al.*, "An imaginary-distance YM-BPM with an enhanced amplification factor for the analysis of a periodic structure," *IEEE Int. Conf. on Computational Electromagnetics*, pp. 289-290, Mar. 2017.
- [3] B. Bai *et al.*, "Optical activity in planar chiral metamaterials: Theoretical study," *Phys. Rev. A*, vol. 76, 023811, Aug. 2007.
- [4] M. Iwanaga *et al.*, "Subwavelength orthogonal polarization rotator," *Opt. Lett.*, vol. 3, no. 2, pp. 109-111, Jan. 2010.

Application of the Talbot-effect to the structured illumination of hollow waveguide arrays: numerical simulations

S. F. Helfert, J. Jahns

FernUniversität in Hagen, Chair of Micro- and Nanophotonics, 58084 Hagen, Germany
stefan.helfert@fernuni-hagen.de

It is shown that structured illumination of a metallic hollow waveguide array can be achieved by applying the Talbot-effect. In this way the transmission can be improved up to 50% compared to a uniform illumination.

Introduction

Recently it was shown theoretically and experimentally that structured metallic films can be used as polarization converters [1] [2]. The principle of the polarization conversion can be easily understood with the theory of hollow waveguides. Therefore, the structures are named hollow waveguide array (HWA). The fabrication process requires quite large metallic regions in the cross-section. As consequence a uniform illumination results in high reflections due to the light that hits the metal walls. In this presentation, we show how the transmission efficiency can be improved by applying the Talbot self-imaging effect.

Structured illumination of hollow waveguide arrays

The principle of the beam shaping with the Talbot-effect is presented in Fig. 1a. A dielectric grating is illuminated with a uniform plane wave. As can be seen, a cosine shaped field occurs behind the grating with very small values in the metallic area. For optimization, numerical simulations were performed where the fill factor f and the height h_G of the grating were varied [3]. Various points in the parameter space were found that lead to high transmissions and further issues like sensitivity or issues with the fabrication can be considered for a practical realization of the device. A comparison of the electric field distribution with and without grating is shown in Fig. 1b,c. In case of a uniform illumination the reflections are clearly recognizable. On the other hand, the grating leads to a focusing of the field into the air region of the HWA. As consequence, the transmission increases from 67% (uniform illumination) to 97% for the structured illumination.

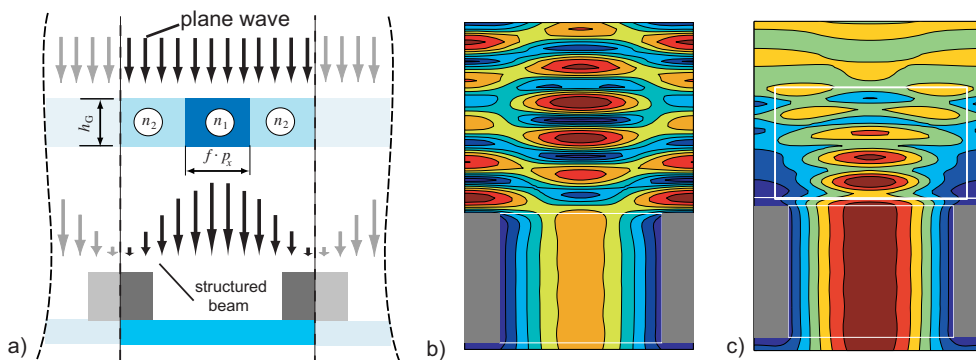


Fig. 1. Illumination of an HWA, a dielectric grating is used to structure the shape of the beam a) principle; b) electric field distribution without grating. i.e., for a uniform illumination of the HWA; c) electric field distribution when a grating is introduced, the focusing is recognizable

References

- [1] S. F. Helfert, A. Edelmann, and J. Jahns, *J. Europ. Opt. Soc.: Rap. Publ.* **10**, 15006 (2015).
- [2] S. F. Helfert, T. Seiler, J. Jahns, J. Becker, P. Jakobs, A. Bacher, *Opt. Quant. El.* **49**, 313, (2017)
- [3] S. Helfert, J. Jahns in *Proc. EOS Topical Meet. on Diffr. opt. 2017 (DO2017)*, Joensuu, Finland 55-56.

A System of Nonlinear Characteristic Equations for Two-Mode Propagation in Step-Index Optical Fiber

Vladimir Burdin^{1*}, Anton Bourdine¹

¹ Povolzhskiy State University of Telecommunication and Informatics, Department of Telecommunication lines, Samara, Russia

* burdin@psati.ru

A system of nonlinear characteristic equations for a two-mode propagation in a step-index optical fiber with a Kerr nonlinearity is presented. Estimates of the spectral characteristics of the radii of the spot of the mode LP₀₁ and LP₁₁ are presented. Spectral characteristics was considered depending on the optical power in the optical fiber and optical power distribution between modes.

The progress of femtosecond lasers stimulated interest in studies of the dependence of the mode parameters of fibers on nonlinearity. The proposed paper presents a system of nonlinear characteristic equations for a two-mode propagation in a step-index optical fiber with a Kerr nonlinearity. This system of equations was obtained by the method of Gauss approximation [1]. For LP₀₁ and LP₁₁ modes the dependences of the equivalent radii of the mode spot on the wavelength and the power of the optical radiation in the fiber and the power distribution between the modes were calculated. It were obtained as a result of calculations based on the solution of this system. It is shown that the propagation conditions of two modes LP₀₁ and LP₁₁ are performed in a limited wavelength range.

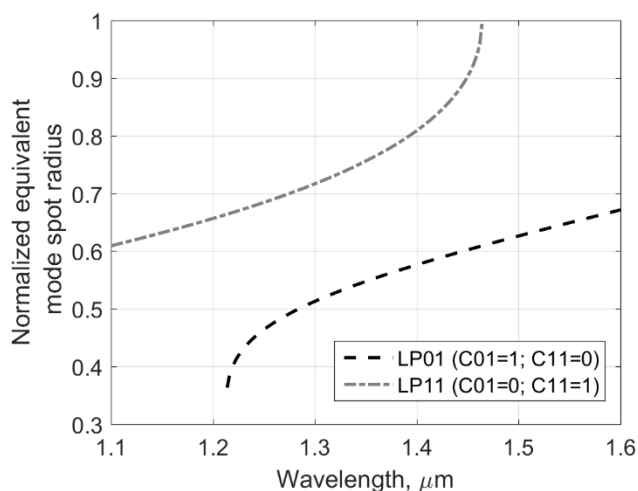


Fig.1 Spectral characteristic of mode spot radius.

And with an increase in optical power the boundaries of this range shift to the long waves. The short waves limit is due to the self-focusing effect of the fundamental mode. The long waves limit is due to the cutoff of the LP₁₁ mode. As an example, Fig. 1 shows the spectral characteristics of the equivalent radius of the mode spot for the LP₀₁ and LP₁₁ modes in the optical fiber of the SMF28 type. This curves was obtained for an optical power in the lightguide of 5 MW for the two limiting cases of power distribution between the modes. All solutions for other power distributions are located between the this limit curves shown in the graph.

Acknowledgment

The reported study was funded by RFBR according to the research project No. 16-37-60015 mol_a_dk

References

- [1] Snyder A., Love J. Optical waveguide theory/ US: Springer, 1983. – 738 p.

Simulation and Research of Few-Mode Optical Fiber DMD Degradation due to Geometry Deviation From Optimized Form

Anton Bourdine^{1,2*}, Vladimir Burdin¹

¹Povolzhskiy State University of Telecommunications and Informatics (PSUTI), Samara, Russia

²"OptoFiber Lab" LLC, Skolkovo Innovation Center, Moscow, Russia

* bourdine@yandex.ru

This work reports results of simulation and research of few-mode optical fiber (FMF) differential mode delay (DMD) spectral curve degradation due to real FMF non-circularity and local refractive index fluctuations and variation from optimized refractive index profile form. We considered 16-mode FMFs with core diameter 42 μm enough to suppress non-linearity and mode effective area more 140 μm^2 with earlier on synthesized graded refractive index profile providing DMD reducing less 120 ps/km all over "C"-band down to 40 ps/km and less at $\lambda=1550$ nm region [1]. FMF core ellipticity as well as refractive index profile local distortions and deviations from optimal form were simulated and set by reports of real commercially available laser-optimized multimode optical fibers (LOMFs) of TIA/ISO Cat. OM2+/OM3 refractive index profile measurements performed by lab optical fiber analyzer kit [2].

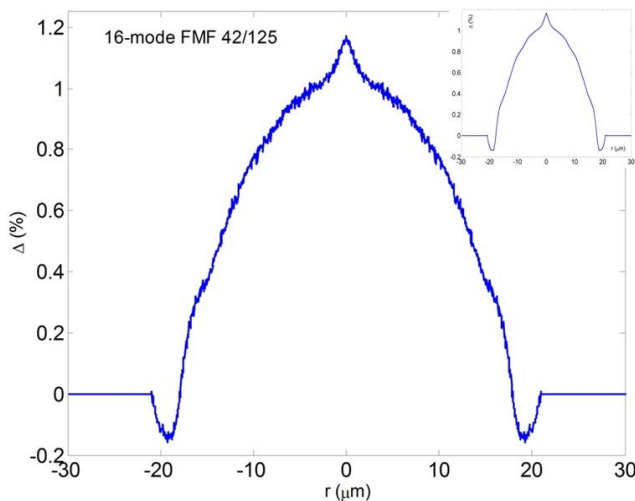


Fig. 1. Optimized refractive index profile for FMF 42/125 with overlapped strong distortions

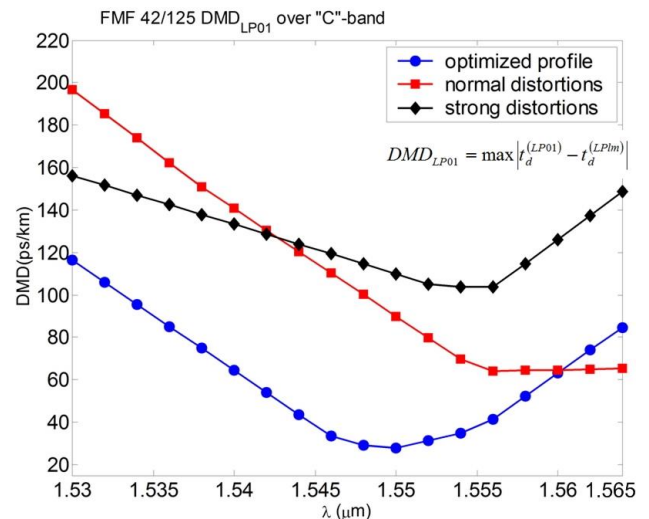


Fig. 2. Spectral $DMD_{LP01}(\lambda)$ curves over "C"-band for FMF 42/125 with optimized refractive index profile and overlapped normal and strong distortions

Acknowledgements

The reported study was funded by RFBR according to the research project No. 16-37-60015 mol_a_dk

References

- [1] V.A. Andreev et al. *Design of Low DMD Few-Mode Optical Fibers with Extremely Enlarged Core Diameter Providing Nonlinearity Suppression for Operating over "C"-Band Central Region*, Proc. of SPIE, vol. 10342, P. 1034207-1 – 1034207-8 (2016).
- [2] A.V. Bourdine et al. *Investigation of defects of refractive index profile of silica graded-index multimode fibers*, Proc. of SPIE, vol. 7992, P. 799206-1 – 799206-8 (2011).

Polynomial chaos based stochastic augmented building block for process design kits

Abi Waqas^{1*}, Daniele Melati², Andrea Melloni¹

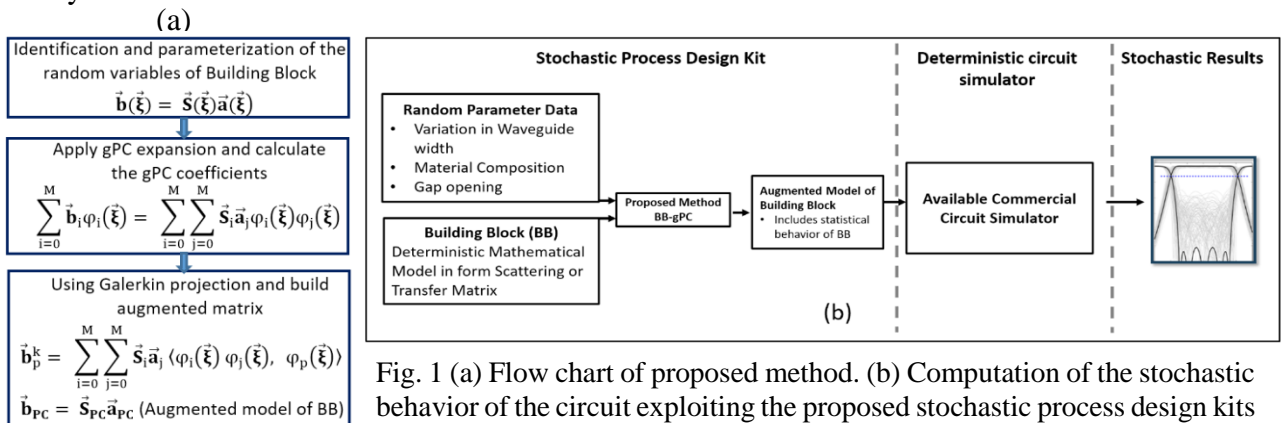
¹Dipartimento di Elettronica, Informazione e Bioingegneria, Politecnico di Milano, Italy; ²Department of Telecommunication Engineering, Mehran University of Engineering and Technology, Pakistan; ²National Research Council Canada, Ontario K1A 0R6, Canada;

* abi.waqas@polimi.it

Fabrication tolerances can significantly degrade the performance of photonic circuits. It is essential to include these stochastic uncertainties in the design phase. This paper presents a method to build a novel class of stochastic process design kits for the efficient variability analysis of photonic circuits.

Stochastic augmented building block

Process Design Kits (PDKs) have recently emerged in photonics as a powerful tool for the analysis and design of complex circuits and as useful framework for the in-depth exploitation of the potentiality of photonic for the large-scale integration of complex circuits. A PDK contains foundry specific technology information and provides a library of the offered building blocks incorporating all the information related to a particular device generally in the form of a scattering matrix [1]. In this scenario, a major issue is represented by fabrication tolerances, which can be particularly detrimental in large and complex circuits. Statistical variations in the fabrication processes of a device affects the entire circuit performance [2]. The possibility to include information on the expected variability in each building block and the availability of efficient computational strategies to predict the statistical behavior of the final circuit are hence of primary importance. Monte Carlo is the mainstream approach to acquire statistical properties of the circuit but requires a prohibitively very large number of samples. Alternative to Monte Carlo, the generalised polynomial chaos (gPC) has recently been proposed for the variability analysis of photonic devices which requires relatively small number of samples. Both Monte Carlo and gPC approaches are circuit-specific and has to be repeated each time the circuit parameters or its layout changes. In this work, we propose a method [see Fig. 1(a)] in which we exploit a gPC approach to realize a completely novel class of device models to be used within photonic PDKs. Stochastic collocation and stochastic Galerkin methods are combined to build augmented macro-models of each building block, directly embedding stochastic information. The augmented BB models are circuit independent and is calculated once and replace the original deterministic macro-model of the BBs in the PDK [see Fig. 1(b)]. These stochastic models inherently convey stochastic information, which allows performing statistical analyses without any repeated simulation end enables an unprecedented simulation efficiency compared to classical gPC implementations. The new matrices can hence be combined according to the building blocks connections to derive with a single run of the deterministic circuit simulator the stochastic behavior of any circuit.



[1] Melati., et al. "Waveguide-based technique for wafer-level measurement of phase and group effective refractive indices." JLT (2016)

[2] A. Waqas., et al., "Sensitivity Analysis and Uncertainty Mitigation of Photonic Integrated Circuits". JLT (2017).

Evolution of Modes in Photonic Lanterns

Sugeet Sunder^{*}, Anurag Sharma[#]

Department of Physics, Indian Institute of Technology Delhi, New Delhi – 110 016 India

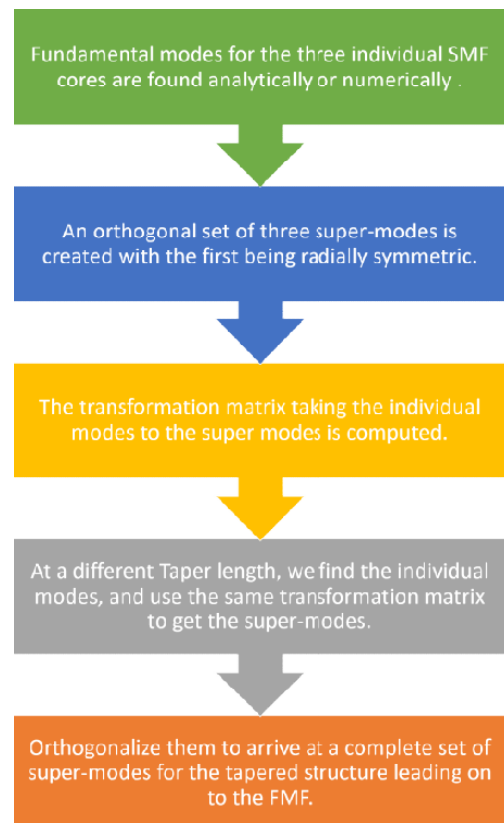
** sugeet.research@gmail.com, # asharma@physics.iitd.ac.in*

Photonic Lanterns are being used as spatial multiplexers in Space-division Multiplexing. We have analyzed the evolution of modes from the single mode regime to the few-mode regime under adiabatic tapering of SMFs into a single FMF multicore fiber. We present some initial results towards development of an algorithm describing the transformation.

Summary

Moving towards all-fiber communication technology and to keep up with the increasing bandwidth demands, few mode fibers (FMFs) are being considered. Photonic Lanterns have emerged as very promising devices to be used as Spatial and Modal multiplexers. These devices are fan-in devices having SMFs on one end, adiabatically tapered to a multi-core end, which then leads on to an FMF. We have investigated the evolution of modes of the structure along the taper. Adiabatic taper ensures that the mode retains its characteristics. We then are able to relate the individual modes at the single mode regime to the super modes at the multi-mode regime.

Three Single mode fibers were considered to be adiabatically tapered to $1/5^{\text{th}}$ its size into a three-core fiber, with a ‘V-value’ such that it supports 3 modes. The modes of individual fibers were calculated at a taper ratio of $1/2$. Assuming that the first super-mode of the structure at this taper made as a linear combination of these individual modes resembles a radially symmetric Gaussian, we calculated the overlap with an appropriate Gaussian function. Using the overlap coefficients we made three super-modes of the structure and used the Gram-Schmidt Scheme to orthogonalize them. This resulted in a transformation matrix leading from individual modes to the super-modes. We assert that this transformation matrix preserves itself along the taper. We then calculated the individual modes at a taper of $1/5$, used this matrix to get the supermodes, orthogonalised them, which were then compared to the super-modes of the structure. We obtained very high overlap between the two sets of super-modes. This shows that using this procedure we can obtain the supermodes in terms of individual local modes at any point along the taper. This can be used to obtain the field evolution along the photonic lantern.



The algorithm in a flow chart

References

- [1] Leon-Saval, Sergio G. *et al.* "Photonic lanterns: a study of light propagation in multimode to single-mode converters." *Optics Express* **18**, 8430-8439 (2010).
- [2] Fontaine, Nicolas K. *et al.* "Geometric requirements for photonic lanterns in space division multiplexing." *Optics express* **20**, 27123-27132 (2012).

Oblique quasi-lossless excitation of a thin silicon slab waveguide

Manfred Hammer*, Lena Ebers, Jens Förstner

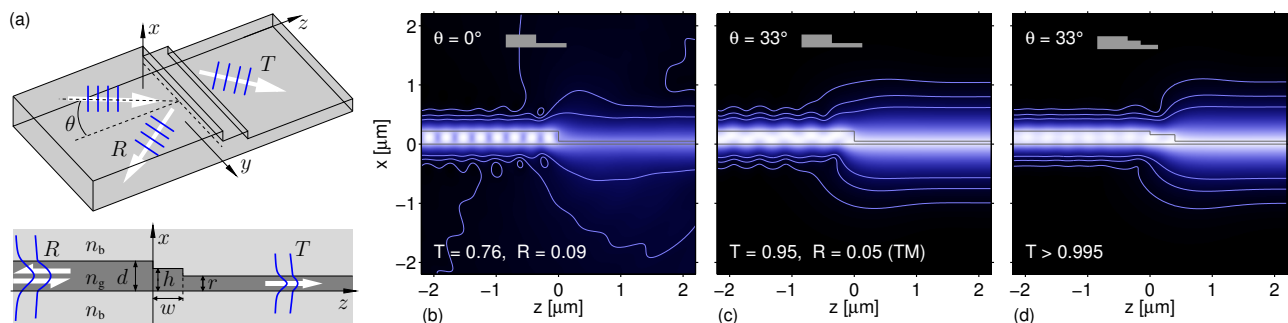
Theoretical Electrical Engineering, Paderborn University, Paderborn, Germany

* manfred.hammer@uni-paderborn.de

Radiation losses at a junction of high-contrast Si/SiO₂-slabs can be avoided, if, for semi-guided waves, the angle of incidence is raised beyond a critical angle. By introducing an additional segment of intermediate thickness, reflections can be suppressed; our simulations predict near-full transmittance for the “coated” interface.

Interfacing slab waveguides of different thickness

In a traditional 2-D setting, guided waves traversing an abrupt interface between different slab waveguides typically generate more or less pronounced reflections and scattering losses. High-contrast silicon slabs are considered, as introduced in part (a) of the figure. The field (b) relates to the standard setting, with normal incidence of the guided TE wave. Applying a semi-analytical vectorial mode expansion solver [1] for the effective 2-D problems, we now investigate what happens when the waves come in at oblique angles. Arguments based on a variant of Snell’s law, adapted to the present case of polarized semi-guided waves, predict critical angles of incidence, beyond which all scattering losses are suppressed. In that regime (c), the transmittance is already raised to about 95%. The waves, however, are still partly reflected, mainly into the backwards TM mode. The waves, however, are still partly reflected, mainly into the backwards TM mode.



Artists impression and cross section view (a) of the waveguide interface. Single-mode Si/SiO₂-waveguides of thicknesses $d = 0.22 \mu\text{m}$ and $r = 0.05 \mu\text{m}$ are considered, with refractive indices $n_g = 3.45$ and $n_b = 1.45$, at a wavelength of $1.55 \mu\text{m}$. Transmittances T and reflectances R are given for semi-guided TE excitation at angle θ . Results for abrupt interfaces at normal (b) and oblique incidence (c), and for a “coated” interface (d), with a segment of height $h = 0.16 \mu\text{m}$ and width $w = 0.4 \mu\text{m}$, are shown. The plots relate to the absolute magnetic field $|H|$ in the x - z cross section plane, with contours at 2%, 5%, and 10% of the maximum levels.

A guided-wave-variant of an anti-reflection coating

Motivated by the traditional technique of reflection suppression, we introduce a short waveguide segment of intermediate thickness at the former interface. Optimization of the transmittance through varying the height and width of that segment leads to configuration (d) with a guided-wave TE-to-TE transmittance above 99.5%. Rigorous finite-element simulations (COMSOL) confirm these findings.

Reference

- [1] M. Hammer. Oblique incidence of semi-guided waves on rectangular slab waveguide discontinuities: A vectorial QUEP solver. *Optics Communications*, 338:447–456, 2015.

Steady State Analysis of SiGeSn/GeSn Interband MQWIP

Prakash Pareek^{1*}, Nishit Malviya^{2,3}, Vikram Palodiya⁴

¹ Dept. of Electronics and Communication Engineering, Vaagdevi College of Engineering, Warangal, India

² Dept. Of Electronics Engg., Indian Institute of Technology (ISM) Dhanbad, India

³ City, University of London, London, England

⁴ Dept. of ECE, Sphoorty Engineering Colege, Hyderabad, India

[*ppareek1@gmail.com](mailto:ppareek1@gmail.com)

Steady state analysis of SiGeSn/GeSn interband multiple quantum well infrared photodetector (MQWIP) is carried out in this work. Responsivity is calculated by solving rate equation at considering inter-well carrier transport.

Introduction and Formulation

In recent times, Sn doped Ge alloy emerges as one of the potential path to realize midinfrared optical interconnects as well as low cost integrated detectors [1]. In present work, GeSn/SiGeSn MQWIP is investigated at steady state considering inter-well carrier charge interaction. Schematic structure of Si_{0.09}Ge_{0.8}Sn_{0.11}/Ge_{0.83}Sn_{0.17} MQWIP, considered in our analysis, is shown in Fig. 1(a). It is formed by M number of alternate layers of compressively strained GeSn well and tensile strained SiGeSn barriers, on a strain relaxed GeSn buffer. In this analysis, we have followed the technique by Ryzhii [2] but with necessary modification suitable for interband transition. Responsivity is calculated by solving rate equation in each well of MQWIP considering interaction of charge carriers of each well.

Result

Variation of peak responsivity is plotted as a function of M (number of wells) but for different bias voltages and is shown in Fig. 1(b). It can be seen from the figure that with increasing bias, responsivity increases. As applied bias increases, effective barrier height of quantum well reduces which causes more escape of carriers, and hence photocurrent increases. However, as number of well increases further, saturation in responsivity is observed due to exponential decay of incident light. Increment of responsivity with number of wells also indicate that the proposed device is viable to be used as monolithic detector.

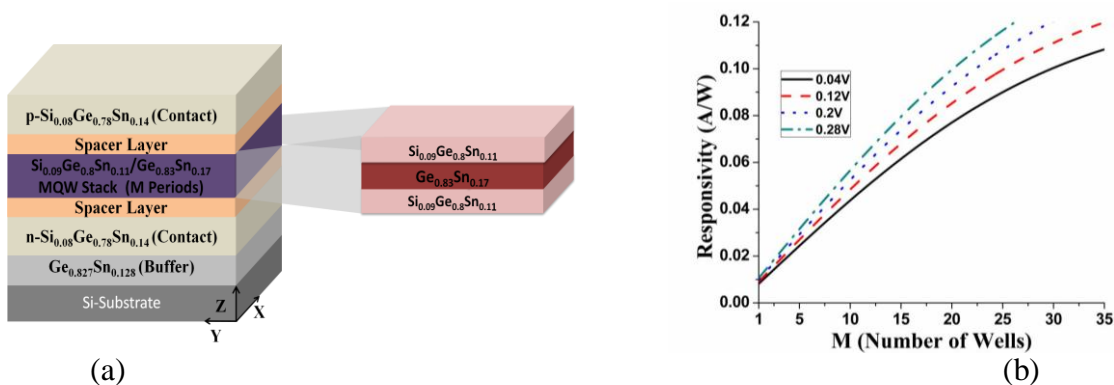


Fig. 1: (a) Schematic of SiGeSn/GeSn MQWIP ; (b) Variation of responsivity as function of M

References

- [1] J. Kouvetakis, et. al., *Tin based group IV semiconductors: new platforms for opto and micro electronics and silicon*, Annual Review of Material Research, vol. 36, pp. 497-554, 2006.
- [2] V Ryzhii , *Characteristics of quantum well infrared photodetectors*, Journal of Applied Physics, vol. 81, pp.6442-6448, 1997.

Families of Exceptional Points in Period Slabs

Amgad Abdrabou , Ya Yan Lu

Department of Mathematics, City University of Hong Kong, Hong Kong
mabdrabou2-c@my.cityu.edu.hk

Exceptional points (EPs) for resonant states, where both the eigenvalues and eigenfunctions coalesce, are studied for a dielectric slab with periodic gaps. A theory on the formation EPs at the lightline is developed in the limit of zero gap width.

Mathematical Formulations

For the periodic slab shown in Fig. 1, and the E-polarization, the electric field component $u = E_x$, satisfies the two dimensional (2D) Helmholtz equation, $\nabla^2 u + k^2 \varepsilon(y, z)u = 0$, where $k = \omega/c$ is the free-space wavenumber, ω is the angular frequency, and c is the speed of light in vacuum. A Bloch mode solution takes the form, $u(y, z) = \phi(y, z) e^{i\beta y}$, where β is a real Bloch wavenumber satisfying $|\beta| \leq \pi/d$, and $\phi(y, z)$ is d -periodic in y .

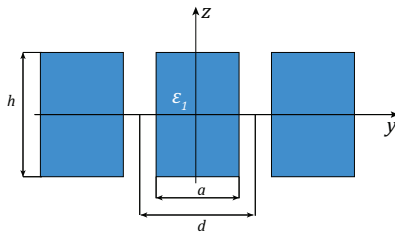


Fig. 1.: A 1D-periodic slab.

We seek resonant mode solutions to the Helmholtz equation. These are solutions with complex ω , that satisfy outgoing radiation conditions as $z \rightarrow \pm\infty$. We consider a situation where some a and h selections lead to accidental degeneracies in the resonant states, known as EPs. An EP is characterized as a degeneracy of two complex frequencies with their eigenfunction coalescing together [1].

Numerical Results

An efficient numerical scheme is developed to continuously follow EPs in the parameter space. The curves in Fig. 2 represent parameters where EPs exist for $\varepsilon_1 = 15.42$, where $\mathcal{D}(a) := [h^*, \beta^*, \text{Re}(k^*), \text{Im}(k^*)]$ represents an EP solution. These curves originate at the lightline from $a = d$ (zero gap) and can be classified as $\mathcal{D}^{(m,n)}(d)$. The integers, m and n are related to the “degeneracies” that occur when the uniform slab is regarded as a periodic structure. For example, the (h^*/d) -component of $\mathcal{D}^{(2,1)}(d)$ has the value 1.713719, that is in excellent agreement with that obtained via $\lim_{a \rightarrow d} \mathcal{D}^{(2,1)}(a)$ using our numerical scheme, as shown in Fig. 2 .

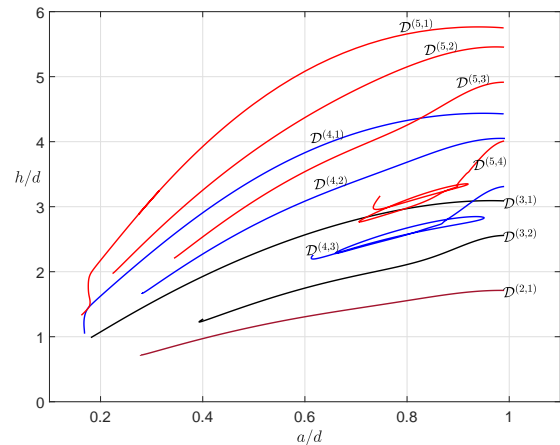


Fig. 2.: The EPs parameter curves for $\varepsilon_1 = 15.42$.

References

- [1] B. Zhen, C. W. Hsu, Y. Igarashi, L. Lu, I. Kaminer, A. Pick, S-L. Chua, J. D. Joannopoulos, M. Soljačić, *Spawning rings of exceptional points out of Dirac cones*, Nature **525**, 354–358 (2015).

Anderson Localization in 1D plasmonic terahertz waveguides

M. Balasubrahmaniyam¹, Ajay Nahata² and Sushil Mujumdar¹

¹*Tata Institute for Fundamental Research, Mumbai, India*

²*Department of Electrical and Computer Engineering, University of Utah, Salt Lake City, Utah 84112, USA*

balasubrahmaniyam.m@tifr.res.in

Using a finite-element technique, we numerically investigate a one-dimensional coupled resonator waveguide, realized by periodically arranging identical sub-wavelength resonators at terahertz frequencies. Anderson localization of terahertz plasmons is observed when randomness is added to the array. The numerical study elaborates the disorder dependence of the inverse participation ratio and the modal loss.

Anderson localization is a phenomenon that arises due to interference of waves in random multiply scattering media and leads to the arrest of diffusion. An explicit signature of localization is the exponentially decaying tail of the wavefunctions induced by disorder. However, the observation of an exponential decaying tail is often considered ambiguous in such systems as the intrinsic losses in the system also lead to exponentially decaying intensity profiles. Therefore, a systematic study of deliberately dissipative localizing systems is in order.

In this work, we address this issue using a 1D periodic-on-average random system (PARS) with losses. This numerical work follows up on and augments earlier experimental results on such a system.[1] A 1D array of subwavelength holes in a stainless steel sheet is studied at THz frequencies. The array acts as a coupled resonator waveguide wherein terahertz energy is transported via propagating plasmons whose dispersion is determined by the array parameters. When disorder is introduced in the waveguide, the plasmons undergo Anderson localization. We compute the dispersion of the periodic array, and observe the localization of plasmons under disorder. To measure the dissipation in the modes, we use finite element method based eigenmode analysis and separately quantify the loss lengths and localization lengths.[2] Close to the Bragg frequency, the system possesses modes with localization length two orders of magnitude smaller than the loss length.

We further analyze the interplay between loss and localization under stronger disorder inaccessible in the experiments, i.e when the system departs from the periodic-on-average regime. We find that the rate at which the inverse participation ratio increases with disorder is slowed down at higher disorder. Simultaneously, the rate of reduction of the modal loss also slows down at strong disorder.

References

- [1] Shashank Pandey, Barun Gupta, Sushil Mujumdar & Ajay Nahata, "Direct Observation of Anderson Localization in Plasmonic Terahertz Devices," *Light: Science and Applications (Nature)*, **6**, 16232 (2017).
- [2] M. Balasubrahmaniyam, Ajay Nahata & Sushil Mujumdar, "Anderson localization in a plasmonic coupled-resonator array at terahertz frequencies", (Under Review).

Analysis of SiO_2 - and MgF_2 -Based Surface Plasmon Resonance Sensors

Christian Spenner¹, Hendrik Kleene¹, Pongsak Sarapukdee², Klaus Kallis², Dirk Schulz¹,

¹ Chair for High Frequency Technology, TU Dortmund University, Dortmund, Germany

² Micro- and Nanoelectronics Devices Group, TU Dortmund University, Dortmund, Germany
christian.spenner@tu-dortmund.de

MgF_2 - and SiO_2 -based grating coupled surface plasmon resonance sensors are investigated, in which the analyt is placed at the back side of the grating. Different configurations to increase the sensitivity and the reflected intensity at the plasmonic resonance are studied and compared.

Introduction

Sensors utilizing MgF_2 - and SiO_2 -based claddings (Fig.1a) [1] are numerically investigated with respect to sensitivity and to reflected intensity. Especially, the excitation of long range modes is essential for a highly sensitive detection of analytes. For this purpose the permittivity of both materials above and below a metal should be similar. Because of the fact that the permittivity of the analyt is different from the permittivity above the grating a matching layer is needed. These requirements result in a layer structure shown in Fig. 1a) including the layer characterizing the analyt, the matching layer and the cladding layer either using MgF_2 or SiO_2 . For the investigation of the influence of the matching layer onto reflectivity and sensitivity, a conventional FDTD-method is applied. Periodic boundary conditions are applied and a total field scattering approach is utilized to extract the reflections properly. For the modelling of the material parameters a common Drude model is applied.

Results

For the analyt we apply a permittivity related to water-based solutions. Investigations show, that an increase of the matching layer d leads to a higher coupling efficiency but lower sensitivity, so that a compromise has to be found. Due to the lower reflected intensity at the plasmonic resonance, MgF_2 allows a better compromise concerning the matching layer thickness d . As an example, this can be demonstrated by Fig.1b depicting the reflectivities dependent on the incident angle θ for $d = 20 \text{ nm}$. Sensitivities of 24 deg/RIU and 30 deg/RIU are obtained for a MgF_2 - and SiO_2 cladding.

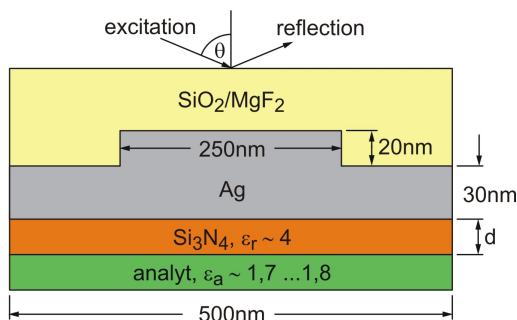


Fig.1a: Schematic of the grating period

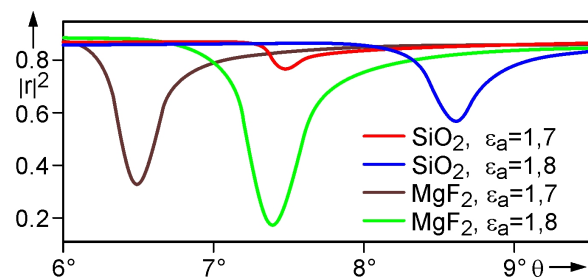


Fig.1b: Reflected intensity dependent on θ

References

- [1] S. Pi, X. Zeng, N. Zhang, D. Ji, B. Chen, H. Song, A. Cheney, Y. Xy, S. Jiang, D. Sun, Y. Song, Q. Gan, *Dielectric-Grating-Coupled Surface Plasmon Resonance From the Back Side of the Metal Film for Ultra-sensitive Sensing*, IEEE Photonics Journal 8 (2016), Nr. 1.

Analysis of light-matter interaction of optical sources with dispersive nanoresonators via contour integration

Felix Binkowski¹, Lin Zschiedrich², Sven Burger^{1,2}

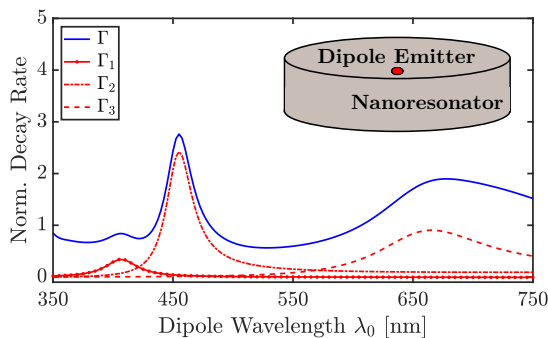
¹ Zuse Institute Berlin, Takustraße 7, 14195 Berlin, Germany

² JCMwave GmbH, Bolivarallee 22, 14050 Berlin, Germany
binkowki@zib.de

We present theory and a numerical method for the investigation of optical sources interacting with open and dispersive nanoresonators. Based on contour integration in the complex frequency-plane, we compute quantities describing the emitter-nanoresonator coupling yielding, in particular, mode specific normalized decay rates.

For the design of nanoantennas with novel functionalities [1], a modal picture of the resonating structure is essential. A reasonable approach is to use the underlying resonant states, so-called quasinormal modes (QNMs), as projectors for an expansion of the electromagnetic field. For this approach, orthogonality relations of the QNMs are required. Studying nanooptical resonators, where material dispersion has to be taken into account, the development of such relations can be a challenging task [2, 3]. In [4], we derived a theory which is not based on orthogonality relations of the QNMs. The resulting projectors, so-called Riesz projectors, were used for an expansion of the electromagnetic field. Furthermore, we developed and implemented a complete numerical method which only relies on contour integration in the complex frequency-plane by solving time-harmonic scattering problems. The method was applied to an exemplary nanostructure.

Here, we review this method and present an application to a nanoresonator hosting a dipole emitter (position \mathbf{r}_0 , radiating at ω_0 , dipole moment \mathbf{p}). Of special interest for this problem setup is the modal normalized decay rate $\Gamma_m(\omega_0) = -(1/2)\text{Re}(\mathbf{E}_m(\mathbf{r}_0, \omega_0) \cdot \mathbf{p}) / \Gamma_b$ where $\mathbf{E}_m(\mathbf{r}, \omega_0)$ is the Riesz projection for the m -th eigenfrequency and Γ_b is the decay rate of the emitter in the hosting bulk material [4]. We compute Γ_m -spectra for a relevant frequency range, see figure below.



Nanoresonator hosting a dipole emitter. The dipole emits at frequency $\omega_0 = 2\pi c/\lambda_0$. Normalized decay rate: Γ (quasiexact solution from solving time-harmonic Maxwell's equations with a dipole source term). Modal normalized decay rates: Γ_m (Riesz projections corresponding to physical eigenfrequencies).

We acknowledge support by the Einstein Foundation Berlin through ECMath within subproject OT9.

References

- [1] A. I. Kuznetsov, A. E. Miroshnichenko, M. L. Brongersma, Y. S. Kivshar, B. Luk'yanchuk, *Optically resonant dielectric nanostructures*, Science 354, aag2473 (2016).
- [2] C. Sauvan, J. P. Hugonin, I. S. Maksymov, P. Lalanne, *Theory of the Spontaneous Optical Emission of Nanosize Photonic and Plasmon Resonators*, Phys. Rev. Lett. 110, 237401 (2013).
- [3] W. Yan, R. Faggiani, P. Lalanne, *Rigorous modal analysis of plasmonic nanoresonators*, arXiv:1711.05011v1 [physics.optics].
- [4] L. Zschiedrich, F. Binkowski, N. Nikolay, O. Benson, G. Kewes, S. Burger, *in preparation*.

Optimization of Random Grating Thin Film Solar Cell

Muhammad H. Muhammad¹, Korany R. Mahmoud^{1,2}, Mohamed Farhat O. Hameed^{1,3},
S. S. A. Obayya¹

¹Centre for Photonics and Smart Materials, Zewail City of Science and Technology, October Gardens, 6th of October City, Giza, Egypt. (Email: sobayya@zewailcity.edu.eg)

²Electronics and Communication Engineering Dept., Faculty of Engineering, Helwan University, Cairo, Egypt.

³Nanotechnology Engineering Program, University of Science and Technology, Zewail City of Science and Technology, October Gardens, 6th of October City, Giza, Egypt. (Email: mfarahat@zewailcity.edu.eg)

A novel design of thin film solar cell (TF-SC) with non-uniform grating distribution is reported and studied. The non-uniform grating positions and geometrical parameters of the proposed design are optimized using modified hybrid gravitational search algorithm and particle swarm optimization (GSA-PSO). Further, the absorption enhancement in the active layer is reported using 3D finite difference time domain (FDTD) method. The numerical results show that the non-uniform grating offers better light absorption than the periodic grating distribution by increasing the optical path length of the incident light through the active layer. Therefore, the suggested SC achieves a broadband absorption with an enhancement of 67.5% over the conventional TF-SC. Additionally, the effect of the active layer material on the performance of the reported SC is studied. The hydrogenated amorphous silicon (a-Si:H) based design shows high ultimate efficiency of 38.73% and short circuit current density (J_{SC}) of 34.69 mA/cm². The modified GSA-PSO algorithm shows also high potential for the design and optimization of solar cells.

Numerical Results

Figure 1 shows the absorption spectra of a-Si:H TF-SC, periodic grating SC and the proposed random grating design optimized by GSA-PSO and modified GSA-PSO. It may be seen from this figure that the conventional grating SC has low absorption at short and long wavelengths. Further, the periodic grating SC has larger absorption than the conventional TF-SC. Moreover, the absorption of the optimized design by the MGSA-PSO is superior to that of the periodic grating SC and the optimized SC by the GSA-PSO. This is due to the multiple reflections of the light between the gratings (each slit or groove acts as a light source). Furthermore, the grating design will absorb the reflected light from the substrate. Therefore, the optical path length inside the active layer and hence a large absorption improvement is achieved relative to the TF-SC

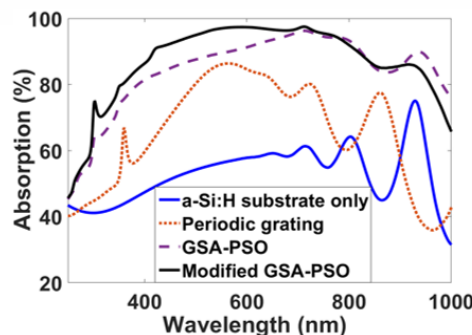


Fig.1 Absorption spectra of TF-SC, periodic grating SC and the optimized designs by the GSA-PSO and MGSA-PSO.

Highly efficient light trapping design for thin film solar cell

Amr Hisham K. Mahmoud¹, Mohamed F. O. Hameed^{1,2}, Mohamed Hussein¹, S. S. A. Obayya^{1*,2}

¹Centre for Photonics and Smart Materials, Zewail City of Science and Technology, October Gardens, 6th of October City, Giza, Egypt. (Email: sobayya@zewailcity.edu.eg)

²Faculty of Engineering, Mansoura University, Mansoura, Egypt.

In this paper, a novel design of modified nanopyramid structure solar cell (SC) is investigated and examined. The finite difference time domain (FDTD) is utilized for computing the optical characteristics of the suggested design. The ultimate efficiency, short circuit current density J_{sc} and power conversion efficiency are used as a figure of merit to measure the optoelectronic performance of the reported design. The modified nanopyramid has an upper tapered nanopyramid placed on lower rectangle part. The geometrical parameters of the modified nanopyramid are adjusted to maximize the optical ultimate efficiency. The reported structure provides an optical ultimate efficiency of 40.93% and J_{sc} of 33.49 mA/cm² respectively, with an improvement of 28.3% over conventional nanopyramid design.

Design and Numerical Results

Figure 1(a) shows a schematic diagram of the modified nanopyramid unit cell. The suggested design consists of a nanopyramid of height $h_p=1200$ nm with base length $B_p=700$ nm. The nanopyramid is placed over nano-rectangle section with height $h_r=400$ nm and width $W_r=1000$ nm. Further, a substrate and Ag back reflector with thicknesses of 2000 nm and 400 nm, respectively are used to increase the optical path length and hence the ultimate efficiency of the proposed design. Two flat monitors M_1 and M_2 are used to calculate the reflection, transmission and hence the absorption through the active layer as shown in Fig.1 (a). Figure 1 (b) shows the absorption spectra of the nanopyramid and the modified nanopyramid designs. It may be seen from this figure that the reported design has higher absorption than the conventional nanopyramid. The ultimate efficiency and short circuit current density for the studied designs are shown in Fig. 2(c). The modified nanopyramid shows an ultimate efficiency of 39.6% which is greater than 31.9% of the conventional pyramid.

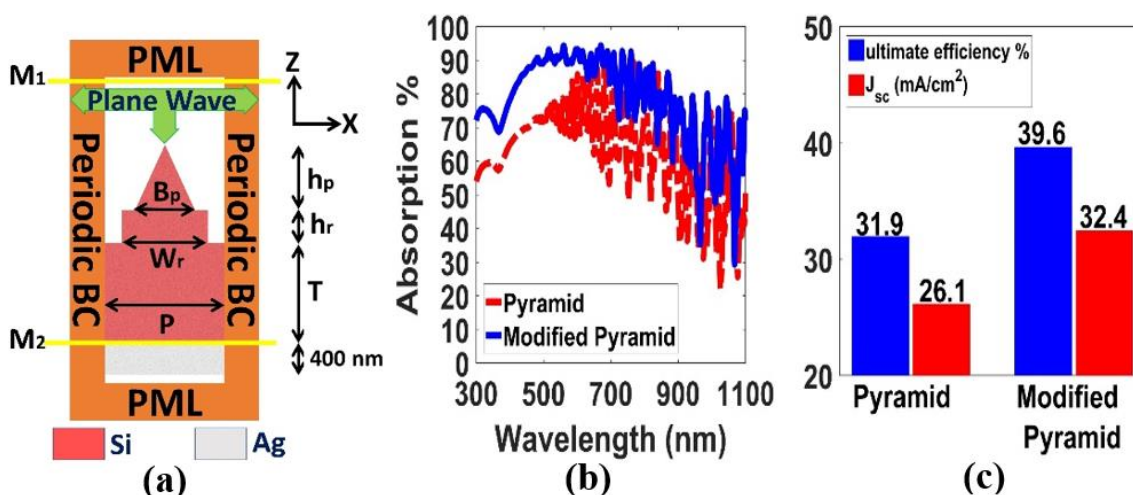


Fig.1 (a) schematic diagram of the proposed modified nanopyramid unit cell, (b) absorption spectra and (c) ultimate efficiency and short circuit current density for the proposed design, and conventional nanopyramid SC.

Blocked Schur for Optical Discontinuity Analysis in Cylindrical Coordinates

Yasmeen Abd El Hak¹, Afaf M. A. Said¹, S. S. A. Obayya^{1*}

¹ Center for Photonics and Smart Materials (CPSM), Zewail City of Science and Technology, Giza, 12578 Egypt. * sobayya@zewailcity.edu.eg

We developed the new method based on Blocked Schur algorithm [1] for the analysis of optical discontinuities in cylindrical coordinates [2] keeping the computational resources minimum and avoiding the probable instability problem of iterative methods such as Taylor expansion.

Analysis and Results

To introduce the validation and the importance of the suggested method, the 2-D structure of the optical-fiber-facet shown in Fig. 2 in [2] is characterized by solving Helmholtz wave equation. First, we divided the transverse direction into a number of first-order linear elements using the standard Galerkin's finite element procedure in cylindrical coordinates [2]. Then, the problem of scattering of the scalar LP₀₁ mode from the uncoated fiber facet will be considered. The LP₀₁ mode is excited at the input of the fiber facet at 1550 nm wavelength. Then, the continuity of transverse electric and magnetic fields conditions are applied at the discontinuity section to calculate the transmission and reflection. As a result, the square root operators $\sqrt{[A]_i}$ of the characteristic matrices $[A]_i$ representing the waveguides i are required to solve the linear equations produced by the continuity conditions. The iterative methods like Taylor and Padé approximations [2] are frequently used in photonic devices analysis to calculate these square root operators; however, they may suffer from numerical instability while dealing with challenging high-index-contrast structures [2]. Therefore, we adopt here Blocked Schur algorithm which is more efficient while dealing with the evanescent and even non-physical modes [1]. Because Schur decomposition $[A] = [Q][T][Q^*]$ represents all the eigenvalues of the characteristic matrix $[A]$ in the diagonal of the triangular matrix $[T]$. Fig. 1 shows the reflection and the power stability as a function of the core radius of the fiber. Although the presented Blocked Schur method and the third order of Taylor expansion [2], $n=3$, using a branch-cut angle = 10° , shows excellent stability and a great agreement with the FSRM results reported in [2], the Taylor expansion starting from the fourth order, $n=4$, fails. Higher orders than $n=4$ have been also calculated with different branch-cut angles; however, the results are still unstable.

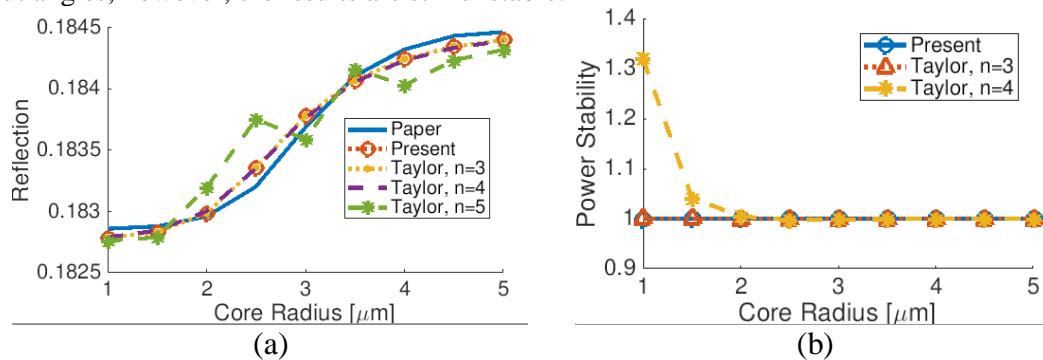


Fig. 1. (a) Reflection of LP₀₁ mode as a function of the core radius of the uncoated optical fiber, terminated by Air, (b) and its power stability.

References

- [1] Said, Afaf MA, A. M. Heikal, Nihal FF Areed, and S. S. A. Obayya. "Why Do Field-Based Methods Fail to Model Plasmonics?." *IEEE Photonics Journal* 8, no. 5 (2016): 1-13.
- [2] Obayya, S. S. A. "Scalar finite-element analysis of optical-fiber facets." *Journal of lightwave technology* 24, no. 5 (2006): 2115.

Mass Redistributed Finite Element Time Domain Beam Propagation Method for Photonic Devices

Khaled S. R. Atia¹, Ahmed M. Heikal^{1,2}, and S. S. A. Obayya^{1,2}

¹Centre for Photonics and Smart Materials, Zewail City of Science and Technology, October Gardens, 6th of October City, Giza, Egypt. (Email: sobayya@zewailcity.edu.eg)

²Faculty of Engineering, Mansoura University, Mansoura, Egypt, Mansoura, 35516, Egypt

This paper introduces a novel improved finite element method (FEM) for time domain analysis of photonic devices. The balance between the FEM mass matrix and stiffness matrix is responsible for the dispersion error introduced by the method. By redistributing the mass in the mass matrix, a tuned balance between the mass matrix and the stiffness matrix is obtained.

Formulation

In order to redistribute the mass matrix, a tuning parameter t is introduced to express the location of Gauss points. Therefore, the mass matrix can be written in parameter t as

$$[M] = \frac{A_e}{3} \begin{bmatrix} t^2 + \frac{(1-t)^2}{2} & t(1-t) + \frac{(1-t)^2}{4} & t(1-t) + \frac{(1-t)^2}{4} \\ t(1-t) + \frac{(1-t)^2}{4} & t^2 + \frac{(1-t)^2}{2} & t(1-t) + \frac{(1-t)^2}{4} \\ t(1-t) + \frac{(1-t)^2}{4} & t(1-t) + \frac{(1-t)^2}{4} & t^2 + \frac{(1-t)^2}{2} \end{bmatrix} \quad (1)$$

where A_e is the area of the element. It is found after equating the discretized wave equation under these assumptions to the analytical solution that the optimum value of t is 0.8604. Then, the propagation in time is accomplished by Padé approximation to treat wide band optical pulses.

Numerical Results

The numerical dispersion of the proposed modification is calculated by measuring the pulse speed V inside the single mode slab waveguide shown in Fig. 1(a). The time step size and the wavelength are fixed to 1 fs and 1.5 μm , respectively. Figure 1(b) shows absolute error of the pulse speed introduced by the proposed method compared with the conventional FEM. The error is computed with respect to the analytical speed $V_a = 0.083643 \mu\text{m}/\text{fs}$. The structure is simulated for 200 fs.

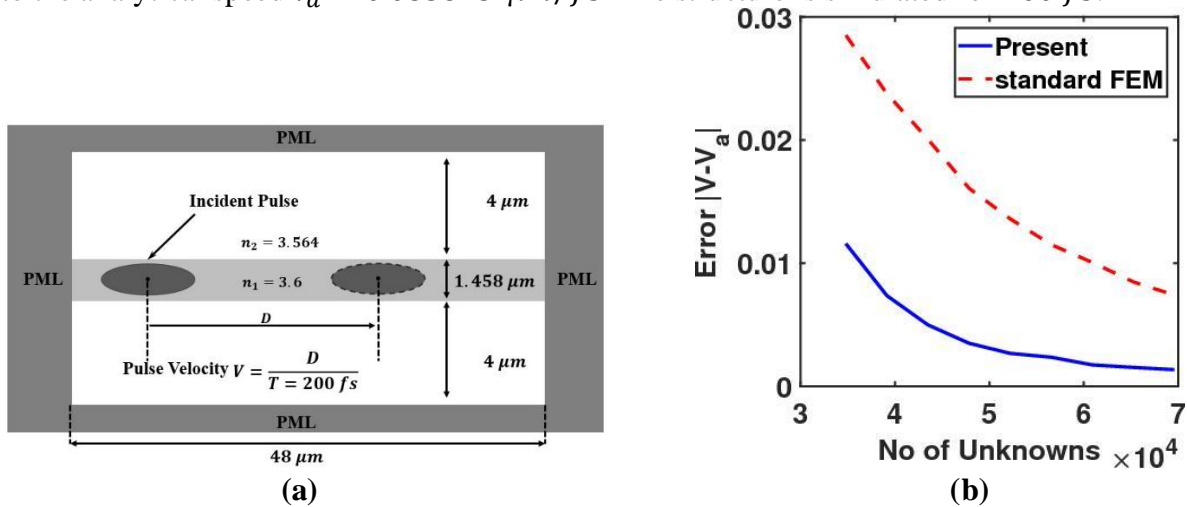


Fig.1 (a) Schematic diagram of a single mode slab waveguide (b) Absolute error of the pulse speed computed using the proposed mass redistribution technique (solid blue line) compared with the standard FEM (dashed red line).

Novel Design of Photonic Crystal Fiber TE-Pass Polarizer

Jidefor A. H. Odoeze^{1,2,3}, Mohamed Farhat O. Hameed^{3,4}, Hossam M. H. Shalabyz², Salah S.A. Obayya^{3,4}

¹ Department of Electronic Engineering, University of Nigeria, Nsukka 410001, Nigeria.

² Egypt-Japan University of Science and Technology (E-JUST), Alexandria 21934, Egypt.

³ Zewail City of Science and Technology, October Gardens, 6th of October City, Giza, Egypt.
(Email: sobayya@zewailcity.edu.eg, mfarahat@zewailcity.edu.eg)

⁴ Faculty of Engineering, Mansoura University, Egypt, Mansoura, 35516, Egypt.

A novel design of transverse electric (TE) pass polarizer based on Si-core photonic crystal fiber (SC-PCF) is reported and studied using full vectorial finite element method. The proposed PCF has a SiO₂ cladding background and is selectively filled with gold nanorods. In addition, an elliptical Si-core is used to increase the birefringence between the two polarizing modes. Therefore, the surface plasmon modes around the gold nanorods are highly coupled with the quasi-transverse magnetic (TM) core modes while no coupling occurs with the quasi-TE core mode. Therefore, high and low confinement losses occur for the quasi TM and quasi TE core modes, respectively. Accordingly, a TE-pass polarizer is realized with an insertion loss (IL) of -0.000108 dB. Additionally, a good extinction ratio (ER) of -13.18 dB is obtained at a short device length of $29 \mu\text{m}$.

Design and Numerical Results

Figure 1(a) shows the cross-section of the suggested device design. The device leverages on the low-loss and strong mode confinement nature of photonic crystal fiber and the lossy nature of plasmonic mode around the gold nanorods to achieve an ultra-low loss TE-pass polarizer. Figure 1 (b) illustrates the variation of IL and ER with the device length. It may be seen from this figure that the proposed TE-pass polarizer has a very low IL and a good extinction ratio. Figure 1(c) shows the propagation of the quasi-TE and quasi-TM mode through the suggested device at wavelength of $1.55 \mu\text{m}$. It is evident from this figure that quasi-TE core mode passes through the suggested design with negligible loss, whereas quasi-TM core mode is attenuated greatly.

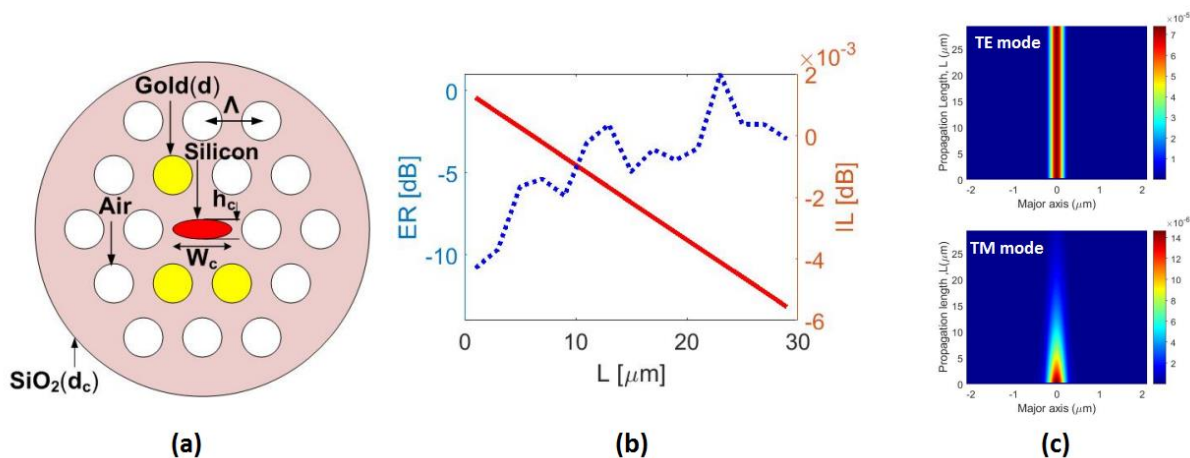


Fig.1(a) Cross-section of the proposed PCF, (b) variation of IL and ER with the device length (L) and (c) light propagation of the two polarized modes through the suggested device

Plasmon and phonon polariton mapping in an electron microscope

Andreas Trügler

Institute of Physics, University of Graz, Universitätsplatz 5, Graz 8010, Austria
andreas.truegler@uni-graz.at

In this talk I will report on our recent studies of phonon polariton modes in single nanocubes [1,2] and the reconstruction of 3D plasmonic fields in terms of plasmon tomography [3].

Electron energy loss spectroscopy (EELS) and microscopy allow probing of evanescent fields of particle plasmons with nanometer resolution. In EELS swift electrons pass by or through a metallic nanoparticle and lose a tiny fraction of their kinetic energy by exciting particle plasmons. By spectrally analyzing the energy loss and raster-scanning the electron beam over the specimen one can map the plasmon polariton nearfields with sub-eV and nanometer resolution. By a similar token, EELS with extremely high energy resolution of about 10 meV allows investigating nanoscale phonon polariton properties [1], which have recently received tremendous attention in the context of phononics and nearfield heat transport at the nanoscale.

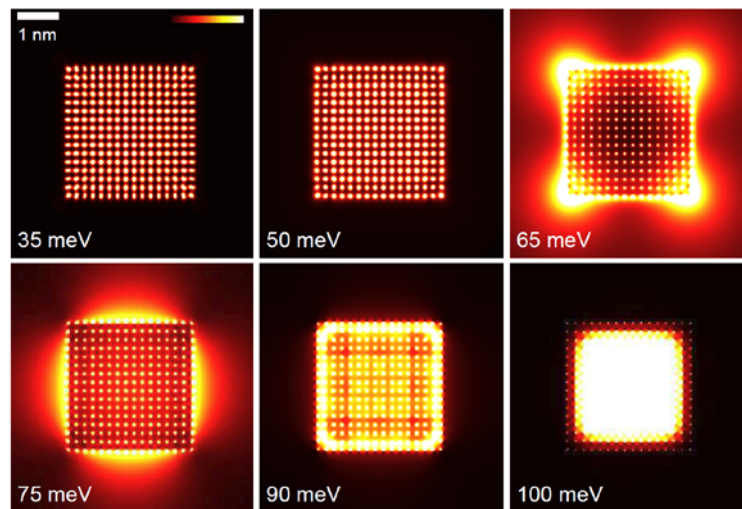


Figure. EELS maps for a molecular MgO cube and for selected phonon loss energies.

I will comment on the excitation of phonon polaritons in terms of complex eigenmodes and introduce our molecular and lattice dynamics simulations for such ionic systems that go beyond the usual local dielectric description of nanostructures [2]. I will also discuss our recent efforts to correlate experimental and simulated EELS maps of coupled nanostructures [3]. This work paves the way for detailed investigations of the enhanced fields of realistic and complex plasmonic nanostructures. When additionally using a series of rotated EELS maps, it becomes possible to reconstruct the full 3D photonic environment of the nanoparticles in terms of plasmon tomography. In the later parts of my talk I will also give a short overview about the possibilities of EELS for nonlocal dielectric approaches [4].

References

- [1] M. J. Lagos, A. Trügler, U. Hohenester, P. Batson, *Nature* **543**, 533 (2017)
- [2] U. Hohenester, A. Trügler, P. E. Batson, and M. J. Lagos, *submitted* (2018)
- [3] A. Hörl, G. Haberfehlner, A. Trügler, et al., *Nature Communications* **8**, 37 (2017)
- [4] A. Trügler, U. Hohenester, and F. J. García de Abajo, *IJMP B* **31**, 1740007 (2017)

Nonlocal resonant behavior in plasmonic nanostructures: analytical and numerical approaches

M. Burda, P. Kwiecien, I. Richter*

¹ CTU in Prague, Faculty of Nuclear Sciences and Physical Engineering, Prague, Czech Republic

* ivan.richter@fffi.cvut.cz

In this contribution, our recent results of both analytical and numerical approaches incorporating nonlocal behavior of plasmonic nanostructures based on the hydrodynamical model with generalized damping.

Introduction

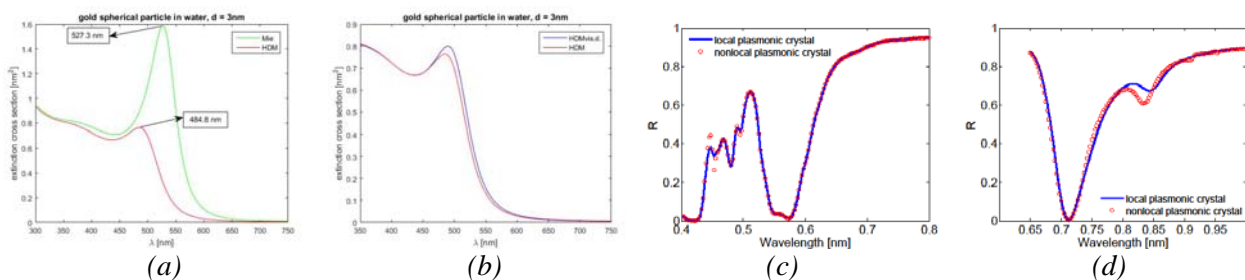
The most common approach in standard nanoplasmonics for the analysis of the resonant behavior of light interaction with these nanostructures has been the application of the local-response approximation, using – depending on the structure complexity and relation between a characteristic dimension and the interacting wavelength – either (quasi)analytic or numerical approaches. Recently, however, as the characteristic dimensions of such structures have scaled down, it has turned out that more complex models based on the nonlocal response are required for explaining novel effects (new resonances, blue spectral shifts, etc.).

Hydrodynamic nonlocal model with viscose damping

We have concentrated on understanding the interaction and developing a simple model based on the linearized hydrodynamic (HD) model, generalizing the standard Abajo's nonlocal model, incorporating both radiative, viscose damping, and Landau damping, being applicable to spherical nanoparticles. Using this generalized model, we have systematically studied the nonlocal responses of gold and silver nanoparticles, in dielectric surrounding media (such as air or water).

Numerical modelling of SWG-based Bragg filter designs

In parallel, as an alternative (and more general) approach, based on our previous rich experience with Fourier modal methods, we have considered and developed the extension of the rigorous coupled wave analysis (RCWA) technique capable of treating nonlocal response numerically, for more general structures.



Example of application of analytical model - comparison of extinction cross sections of gold spherical particle (3 nm in diameter) in water: (a) Mie / HD model, (b) HD / HD model with viscose damping. Example of application of numerical implementation of HD model in RCWA (2D hole array in gold film with thickness (c) 250 nm, and (d) 100 nm).

References

- [1] M. Burda, P. Kwiecien, J. Fiala, I. Richter, Nonlocal resonances in nanoplasmonics: analysis and simulations, oral talk, paper [10227-24], SPIE O+O 2017 (April 2017, Prague, Czech Republic).
- [2] M. Burda, P. Kwiecien, I. Richter, Generalized nonlocal hydrodynamical model with viscose and radiative damping, *to be submitted*.

Nanoscale Imaging of Plasmon Modes of Metal Nanoparticles by Cathodoluminescence Spectroscopy

Viktor Myroshnychenko¹, Natsuki Nishio², F. Javier García de Abajo³, Jens Förstner¹, Naoki Yamamoto²

¹ *Theoretical Electrical Engineering, Paderborn University, Paderborn, Germany*

² *Physics Department, Tokyo Institute of Technology, Tokyo, Japan*

³ *ICFO-Institut de Ciències Fotoniques, The Barcelona Institute of Science and Technology, Castelldefels (Barcelona), Spain*

viktor.myroshnychenko@uni-paderborn.de

Localized plasmon modes of the gold nanoprisms and nanoprism pairs are investigated using cathodoluminescence (CL) spectroscopy. We demonstrate that combination of the angle- and polarization-resolved CL provides a powerful technique with ability to detect and image degenerate, weakly radiative, masked, and dark modes.

Introduction

Localized surface plasmon (SP) resonances of metal nanoparticles have been deeply studied due to their significant role in a wide range of applications. Experimental access to the electromagnetic field distribution associated with SPs is of crucial importance. In recent years an electron-based cathodoluminescence spectroscopy has attracted significant attention because it offers a rich source of information about the physics of SP modes and high spatial resolution [1, 2].

In this work, we use electron-beam lithography to pattern high quality gold triangular nanoprisms and nanoprism pairs on SiO₂ layer. The optical properties of these nanostructures are investigated using angle- and polarization-resolved CL performed in a scanning transmission electron microscope equipped with a parabolic mirror and combined with a light detection system [3]. To interpret the experimental results, numerical simulations are conducted using the retarded boundary-element method.

Results

By exciting nanostructures with an electron beam, we measured spectral features and spatially resolved maps of SPs in the far-field with nanometer spatial resolution. By resolving polarization of the light emission, we can access information on symmetry of multipolar plasmon modes and explore their degeneracy. Moreover, the combined angle- and polarization-resolved detection capabilities provide us the possibility to efficiently detect and image weakly radiative, masked, and optically dark modes. A simple tight-binding model is also formulated to successfully explain the rich plasmon structure and symmetry in the nanoprisms. Furthermore, we discuss a link between the electron-induced light emission and the electromagnetic local density of states associated to the SP modes. Our experimental results are in good agreement with numerical simulations.

References

- [1] N. Yamamoto and K. Araya and F. J. García de Abajo, *Photon emission from silver particles induced by a high-energy electron beam*, Phys. Rev. B, 64, 205419, 2001.
- [2] F. J. García de Abajo, *Optical excitations in electron microscopy*, Rev. Mod. Phys., 82, 209–275, 2010.
- [3] N. Yamamoto, *Development of high-resolution cathodoluminescence system for STEM and application to plasmonic nanostructures*, Microscopy, 65, 282–295, 2016.

On the mechanisms of plasmon-enhanced chiroptical response

T. Weiss^{1*} and E. A. Muljarov²

¹ *4th Physics Institute and Research Center SCoPE, University of Stuttgart, Germany*

² *School of Physics and Astronomy, Cardiff University, United Kingdom*

* t.weiss@pi4.uni-stuttgart.de

We present a rigorous theory based on the resonant state expansion that allows us to analyze all electromagnetic contributions to the plasmonic enhancement of the chiroptical response of chiral media. Potential applications are optimized optical sensors for molecular handedness detection.

Detecting the handedness of chiral molecules is of utmost importance for chemical, biological, and pharmaceutical applications, since the handedness of a molecule determines its interaction with the environment. This includes chemical interactions as well as the interaction with light. Therefore, it is possible to determine the handedness of chiral molecules by optical measurements, but the chiroptical response of such molecules is usually rather weak. Therefore, conventional approaches require using large numbers of chiral molecules.

Plasmonic nanoantennas can enhance the chiroptical response of chiral media. We have recently shown that the electromagnetic enhancement of the circular dichroism, which manifests itself as the difference in absorption of left- and right-handed circularly polarized light, can be as high as three orders of magnitude [1]. Hence, plasmon-enhanced circular dichroism spectroscopy is a promising approach for determining the handedness of few molecules. However, little is known about the underlying enhancement mechanisms.

To address this problem, we have recently extended the so-called resonant state expansion to chiral media [2]. The basic idea of the resonant state expansion is to determine a finite number of resonant states in a reference system, and then to use these resonant states as a basis in order to calculate the resonances in a perturbed system. Furthermore, it is possible to derive the modification of the optical response such as the circular dichroism from the resonant state expansion. Our theory provides analytic expressions for the different contributions to the plasmonic enhancement mechanisms. We find that an optimized design requires a balance between the quality factor and the excitation efficiency of the resonant states, in conjunction with a large field enhancement at the position of the chiral molecules. Furthermore, the plasmonic enhancement of the chiroptical response contains two main contributions: One is proportional to the co-planarity of the incident field and the field components in the plasmonic hot spots, which confirms our previous numerical results [1]. This contribution occurs even in achiral antenna arrangements. The other one is a shift of the resonance frequency, which occurs predominantly in chiral antenna arrangements. It requires that the product of the resonant electric and magnetic fields is non-negative and does not change sign in the regions of the chiral molecules.

References

- [1] M. L. Nesterov, X. Yin, M. Schäferling, H. Giessen, and T. Weiss, *The role of plasmon-generated near fields for enhanced circular dichroism spectroscopy*, ACS Photonics 3, 578-583 (2016).
- [2] E. A. Muljarov and T. Weiss, *Resonant-state expansion for open optical systems: Generalization to magnetic, chiral, and bi-anisotropic materials*, arXiv:1801.08883 (2018).

Atom-Surface Interaction: Theory and Computations

Kurt Busch^{1,2}

¹Humboldt Universität zu Berlin, AG Theoretische Optik & Photonik, 12489 Berlin, Germany

²Max-Born-Institut, 12489 Berlin, Germany

Abstract

Nano-plasmonic and derived systems such as hyperbolic metamaterials promise large and broadband enhancements of the photonic density of states. In turn, these enhancements strongly modify light-matter interaction, notably near plasmonic surfaces. In this talk, recent theoretical advances in equilibrium and non-equilibrium atom-surface interactions such as Casimir-Polder and quantum frictional forces will be discussed with an emphasis regarding their computation in complex nano-plasmonic structures and the role of the material models.

With the advent of nano-scale quantum optical systems, there exists an increased interest in the understanding and subsequent controlling of modified light-matter interactions. Specifically, hybrid systems consisting of cold atoms and nano-photonics/nano-plasmonic structures represent a novel frontier in research with significant application potential for quantum technologies.

Even for simple systems, such as a single atom above a planar surface, there is no full consensus regarding theoretical description of atom-surface interactions. For instance, a recently developed exactly solvable model [1, 2] allows to assess the validity of several often employed approximation schemes, such as the use of the quantum regression theorem or the local thermal equilibrium approximation for equilibrium (e.g., Casimir-Polder forces) and non-equilibrium effects (e.g., quantum friction).

Moreover, based on the above exactly solvable model, further analyses [3] demonstrate the importance of the plasmonic material model. Specifically, for atoms near a plasmonic surface, the atoms can spatially resolve the electron scattering processes within the metal and this effectively mandates that nonlocal material models are employed for the description of atom-surface interactions (for an overview of different material models for metals and their effects on spontaneous emission, see ref. [4]). In fact, such nonlocal effects enhance atom-surface interactions relative to those associated with local material models so that, e.g., quantum frictional forces are enhanced by two to three orders of magnitude for atom-surface distance of the order of a few tens of nanometers. Finally, these theoretical findings raise the question of how to efficiently compute equilibrium and non-equilibrium effects in atom-surface interactions. Specifically, the advantageous properties of the Discontinuous Galerkin Time-Domain (DGTD) approach [5] suggest the adaptation of the DGTD approach for computing atom-surface interactions [6].

- [1] F. Intravaia, R. O. Behunin, C. Henkel, K. Busch, D. A. R. Dalvit, *Failure of Local Thermal Equilibrium in Quantum Friction*, Phys. Rev. Lett. **117**, 100402 (2016).
- [2] F. Intravaia, R. O. Behunin, C. Henkel, K. Busch, D. A. R. Dalvit, *Non-Markovianity in atom-surface dispersion forces*, Phys. Rev. A **94**, 042114 (2016).
- [3] D. Reiche, D. A. R. Dalvit, K. Busch, F. Intravaia, *Spatial dispersion in atom-surface quantum friction*, Phys. Rev. A **95**, 155448 (2017).
- [4] F. Intravaia, K. Busch, *Fluorescence in nonlocal dissipative periodic structures*, Phys. Rev. A **91**, 053836 (2015).
- [5] K. Busch, M. König, J. Niegemann, *Discontinuous Galerkin methods in nano-photonics*, Laser & Photon. Rev. **5**, 773 (2011).
- [6] P. Kristensen, F. Intravaia, K. Busch et al., in preparation, 2018.

The numerical investigation of colliding optical solitons as an all-optical-Gate using the Method of Lines (MoL)

Waldemar Spiller

Micro- and Nanophotonics, FernUniversität Hagen, Hagen, Germany

* Sekretariat.MNP@FernUni-Hagen.de

We have investigated a bidirectional propagation and collision of counter-propagating solitons in a two-level resonant medium. The description of the light pulses: The classical electrodynamics. The description of the medium: A two-level quantum mechanical model. The challenge was the inherent stiffness of the equations.

Summary

We have investigated bidirectional propagation and collision of counter-propagating solitons, ensure their use for all-optical OR- or XOR-switching. The classical electrodynamics was used to describe the light pulse, a two-level quantum mechanical model to describe the atoms of the medium [1], [2]. An extended variant of the Maxwell-Bloch-Equations (EMBE) was obtained in [1]. The solitons had a hyperbolic-secant shaped envelope of 2π area. Collisions for different pulse widths were investigated in the past, [1]. In contrast, our way was a variation of the two pulse widths, to ensure an exploration of the boundary conditions for either a complete annihilation of both solitons (XOR-gate) or a complete annihilation of the left soliton, whereas the right soliton should still continue to propagate (as in the case of an all-optical OR-gate). The EMBEs are inherently stiff and are therefore a challenge in terms of the numerical stability of the solutions. The solutions thus obtained were verified with respect to the results in [1]. Then we considered the case of a simultaneous proportional increase of the two pulse widths (both different, OR-gate) (Fig. 1). The goal was, in particular, to consider accuracy limitations due to the simulation for the annihilation of the left soliton. We have found that the significant increase of the pulse width by a factor of 1.8 still does not represent a limit for the OR-gate accuracy. Then, in a further investigation, our way was a simultaneous variation of the two equal pulse widths, to ensure an exploration of the boundary conditions for a complete annihilation of both solitons (XOR-gate). Our results show that an almost complete annihilation takes place in the whole range of the conceivable pulse widths. The biggest pulse width was limited by the spatio-temporal stability of the soliton. On the other hand, the shortest pulse width was obviously limited methodologically, by the approach of the 'slowly varying envelope approximation', here approx. 50 cycles of the carrier.

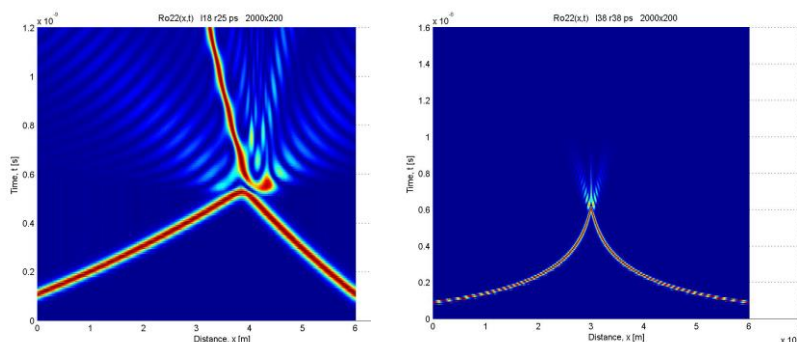


Fig. 1: Collision of optical solitons: OR-and XOR-gate (different scale), respectively.

References

- [1] M. Hutzler, *Collisions of optical solitons in two-level media*, Master's Thesis, FernUniversitaet Hagen, (2014)
- [2] W. Milonni, J. Eberly, *Laser Physics*, John Wiley and Sons Inc. (2010)

All-Optical Digital Amplification in Nonlinear Photonic Crystal Waveguides

Vakhtang Jandieri ^{1*}, Ramaz Khomeriki ², Daniel Erni ¹, Weng Cho Chew ³

¹ *General and Theoretical Electrical Engineering (ATE), Faculty of Engineering, University of Duisburg-Essen, and CENIDE – Center for Nanointegration Duisburg-Essen, Germany*

² *Department of Physics, Tbilisi State University, Georgia*

³ *Electrical and Computer Engineering, Urbana, Illinois, USA*

* yakhtang.jandieri@uni-due.de

Abstract – Within this conceptual study digital all-optical signal pulse amplification is explored within the framework of two coupled photonic crystal W1 waveguides experiencing a Kerr-type nonlinearity. The feasibility of the concept (and potential applications) are demonstrated using analytical formulations as well as full-wave computational electromagnetics.

Photonic crystals (PhCs) are periodically modulated dielectric (or metallic) structures in which any electromagnetic wave propagation is forbidden within a fairly large frequency range (i.e. the photonic band-gap). PhCs are one of the most promising candidates to enable dense integration of distinct optical signal processing functions on a photonic chip, such as e.g. spectral filtering, dispersion compensation, power combining, localization, sensing and fast all-optical switching. For the realization of true all-optical signal processing, the optical system needs to have nonlinear properties. In optically nonlinear media, the index of refraction is modified by the presence of a light signal and this modification can be exploited to influence another light signal, thereby performing an all-optical signal processing operation. In our recent papers, we have proposed a realistic model of an all-optical amplifier using coupled linear W1 photonic crystal waveguides (PCWs) [1]. However, the linear mechanism is based on specific superposition effects yielding therefore linear amplification of relative signal values regarding the input signal. Laser sources, on the other hand, provide sufficiently high light intensities to modify the optical properties of the underlying materials while enabling true all-optical interaction of light waves. This scenario is investigated in the present work [2], where two weakly coupled nonlinear W1 PCWs are proposed as an efficient all-optical digital amplifier.

The realization of all-optical digital amplifiers is demonstrated based on both, an analytical formulation and corresponding detailed numerical studies. Within this conceptual study we consider the coupled nonlinear rod-type PCWs, which is implemented into a 2-D square lattice of the dielectric rods made from a pure Kerr-type material embedded in free space (as the host medium). The underlying idea of digital all-optical amplification is based on the phenomenon of band-gap transmission [3] in periodic nonlinear media. This effect takes place when the frequency of the injected signal is very close to the band edge of the PhC. In the linear case no transmission occurs. However, in the nonlinear case above some threshold value of the signal amplitude, the propagation of solitons takes place as associated eigen-solutions of the specific nonlinear coupled PCW problem. The amplification coefficient is calculated for different amplitudes of the input signal, and the applicability as well as the efficiency of the coupled nonlinear PCWs as all-optical digital amplifier is vividly demonstrated. It is now easier to transfer the proposed idea to PCWs that are embedded in more realistic PhC structures, such as e.g. a planar hole-type PhC with a nonlinear background material. Travelling light amplification in air-hole type nonlinear PCWs is now under our intensive investigation aiming at the realization of all-optical logic gates for future photonic circuits [4]. Another application could focus on plasmonic waveguides, however such densely integrated nonlinear devices are facing considerable challenges such as the inherent losses as well as the high spatial resolution required for the underlying fabrication technology.

References/Notes

- [1] V. Jandieri and R. Khomeriki, "Linear amplification of optical signal in coupled photonic crystal waveguides," *IEEE Photonics Technology Letters*, vol. 27, 639-641, 2015.
- [2] V. Jandieri acknowledges financial support from Alexander von Humboldt Foundation.
- [3] V. Jandieri, R. Khomeriki, D. Erni and W. C. Chew, "Realization of all-optical digital amplification in coupled nonlinear photonic crystal waveguides," *Progress in Electromagnetics Research*, vol.158, pp.63-72, 2017.
- [4] V. Jandieri, R. Khomeriki and D. Erni, "Realization of true logic gates using coupled photonic crystal waveguides based on bandgap transmission phenomenon," *Proceedings of the 12th European Conference on Antennas and Propagation (EuCAP 2018)*, London, United Kingdom, April, 2018 (accepted).

A New Definition for the Kerr Nonlinearity Parameter

Izzatjon Allayarov¹, Swaathi Upendar¹, Markus A. Schmidt^{2,3}, and Thomas Weiss¹

¹ 4th Physics Institute and Research Center SCoPE, University of Stuttgart, Germany

² Leibniz Institute of Photonic Technology, Germany

³ Otto Schott Institute of Material Research, Friedrich Schiller University of Jena, Germany

i.allayarov@pi4.uni-stuttgart.de

We present a new and more general definition for the Kerr nonlinearity coefficient based on the resonant state expansion. It extends conventional approaches to radiating modes, giving rise to new and unexpected phenomena.

The propagation of beams as or pulses in guiding geometries such waveguides and fibers can be described by the nonlinear Schroedinger equation. The nonlinearity enters this equation in the form of a single parameter. The exact form of this Kerr nonlinearity parameter depends on the underlying approximations [1], but it always requires an appropriate normalization of the considered modes. For truly guided modes that decay exponentially with distance to the center of the guiding geometry, the normalization can be carried out by integrating the absolute square value of the electric fields over the entire plane perpendicular to the direction of propagation. However, there is an another class of modes called leaky or radiating modes, for which energy leaks from the core to the cladding and radiates perpendicular to the direction of propagation. Consequently, the corresponding propagation constant has a nonvanishing imaginary part that constitutes the radiative loss to the cladding. Moreover, the Helmholtz equation in the surrounding requires that the electromagnetic fields of these fiber modes grow exponentially with distance to the guiding geometry. A lot of possibilities are discussed in the literature on how to calculate the normalization and, thus, the Kerr nonlinearity parameter for such modes, but an analytical expression for the normalization has been missing so far.

Here, we present for the first time an analytical normalization of these radiating modes that is based on the resonant state expansion [2]. Our approach follows ab initio from Maxwell's equations and requires modifications in the derivation of the nonlinear Schroedinger equation, which – in addition to the correct normalization – result in a modified definition of the Kerr nonlinearity parameter. In the case of truly guided modes, our approach coincides with previous formulations [1] with the advantage that our formulation does not require integration of the fields over the entire plane perpendicular to the direction of propagation. It suffices to integrate over a finite area that contains all spatial inhomogeneities, thus lowering the computational effort. For radiating modes, it turns out that the Kerr nonlinearity parameter has in general a nonvanishing imaginary part that can act as a nonlinear loss or gain for attenuating pulses in a fiber. This unexpected finding might have an impact in potential application such as supercontinuum generation and four-wave mixing.

References

- [1] S. Afshar V. and T. M. Monro, *A full vectorial model for pulse propagation in emerging waveguides with subwavelength structures part I: Kerr nonlinearity*, Optics Express 17, 2298, 2009.
- [2] T. Weiss et al., *Analytical normalization of resonant states in photonic crystal slabs and periodic arrays of nanoantennas at oblique incidence*, Physics Review B 96, 045129, 2017.

Theory and concepts for all-dielectric biosensing

F. Michelotti¹, N. Danz², A. Sinibaldi¹, E. Sepe¹, P. Munzert²

1) SAPIENZA University, Department of Basic and Applied Sciences for Engineering, Roma, Italy

2) Fraunhofer Institute for Applied Optics and Precision Engineering IOF, Jena, Germany

Optical label-free bio-sensing is considered to be among the most promising tools for high throughput detection of biomolecules. Surface Plasmon resonance (SPR), operating in a variety of configurations, is commonly used in biology and pharmaceutical laboratories. Among other label-free optical approaches those based on the excitation of electromagnetic modes at the surface of one dimensional photonic crystals (Bloch Surface Waves - BSW) were demonstrated as a practical route to enhanced resolution and constitute an attractive alternative to SPR [1]. The main advantages of BSW for bio-sensing, in comparison to SPR, lie in the favourable properties of the 1DPC such as the small absorption of the dielectric materials and the tunability of the layer thicknesses to operate in any wavelength range. Besides, the use of BSW in fluorescence-based bio-sensing does not suffer from quenching of the fluorophore's emission at the 1DPC surface.

Here we report on the basic properties of BSW sustained by 1DPC, such as dispersion, polarization, quality factor, sensitivity with respect to a physical perturbation of the surface index [2], BSW coupling of fluorescent emitters in proximity of the surface [3], and the design of real devices taking into account the fabrication tolerances [4].

Finally, we demonstrate the application in a pre-clinical context of a new biosensing platform making use of plastic and disposable BSW biochips operating simultaneously in both label-free (LF) and fluorescence (FLR) modes. Experimental results of cancer biomarkers detection assays in complex biological matrices will be shown [5].

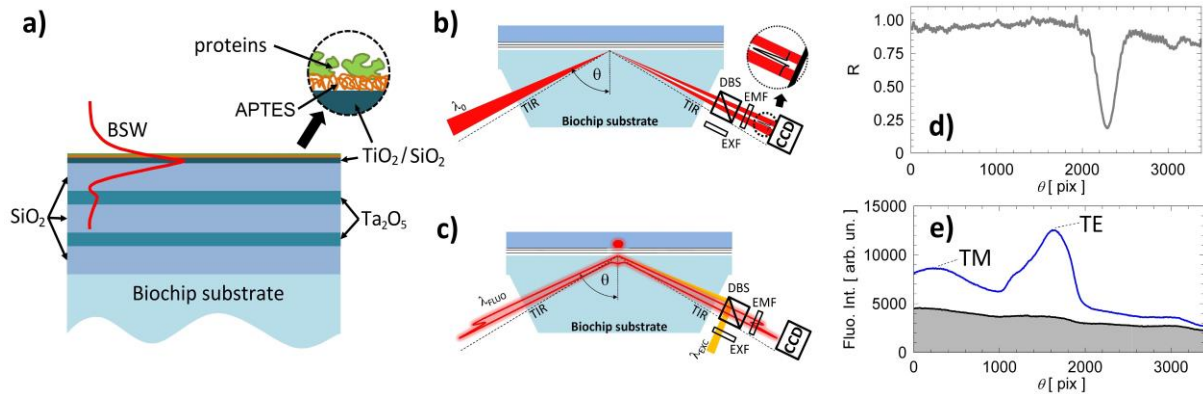


Figure 1. a) Cross section of the BSW biochip. b,c) Sketch of the optical reading layout operating in either the LF (b) or FLR (c) detection mode. d,e) LF and FLR angularly resolved signals.

References:

- [1] A. Sinibaldi, N. Danz, E. Descrovi, P. Munzert, U. Schulz, F. Sonntag, L. Dominici, F. Michelotti, Direct comparison of the performance of Bloch surface wave and surface plasmon polariton sensors, *Sens. Act. B. Chem.* 174, 292 (2012).
- [2] R. Rizzo, N. Danz, F. Michelotti, E. Maillart, A. Anopchenko, C. Wächter, Optimization of angularly resolved Bloch surface wave biosensors, *Optics Express*, Vol. 22(19), pp.23202-23214 (2014)
- [3] F. Michelotti, R. Rizzo, A. Sinibaldi, P. Munzert, C. Wächter, and N. Danz, Design rules for combined label-free and fluorescence Bloch surface wave biosensors, *Opt. Lett.*, Vol. 42(14), 2798 (2017)
- [4] A. Anopchenko, A. Occhicone, R. Rizzo, A. Sinibaldi, G. Figliozzi, N. Danz, P. Munzert, F. Michelotti, Effect of thickness disorder on the performance of photonic crystal surface wave sensors, *Optics Express* 24, 7728 (2016).
- [5] A. Sinibaldi, C. Sampaoli, N. Danz, P. Munzert, L. Sibilio, F. Sonntag, A. Occhicone, E. Falvo, E. Tremante, P. Giacomini, F. Michelotti, *Biosensors and Bioelectronics*, 92, 125 (2017).

Multifunctional Plasmonic Photonic Crystal Fiber Biosensor

Mohammad Y. Azab¹, Mohamed Farhat. O. Hameed^{1,2,3}, Abed M. Nasr¹ and S. S. A. Obayya^{1,3}

¹Faculty of Engineering, Mansoura University, Mansoura, Egypt, Mansoura, 35516, Egypt

²Nanotechnology Engineering Program, University of Science and Technology, Zewail City of Science and Technology, October Gardens, 6th of October City, Giza, Egypt. (Email: mfarahat@zewailcity.edu.eg)

³Centre for Photonics and Smart Materials, Zewail City of Science and Technology, October Gardens, 6th of October City, Giza, Egypt. (Email: sobayya@zewailcity.edu.eg)

In this paper, a novel design of compact surface plasmon resonance multifunctional biosensor based on alcohol mixture photonic crystal fiber (PCF) is proposed and studied. The suggested sensor can be used for temperature and analyte refractive index sensing via the coupling between the core guided modes in the central hole and the surface plasmon modes around a nano gold rod. The reported multifunctional alcohol mixture PCF sensor achieves high temperature sensitivity of $13.1 \text{ nm}/^\circ\text{C}$ with high analyte refractive index sensitivity of $12700 \text{ nm}/\text{RIU}$ which are higher than those reported in the literature.

Design and Numerical Results

Figure 1(a) shows cross section of the suggested multifunction photonic crystal fiber surface plasmon (SP) based biosensor. The proposed design is based on infiltrating the central hole with alcohol mixture which operates as temperature dependent material. In addition, the core mode characteristics are affected by the change in the refractive index of the analyte in the right adjacent hole. Moreover, a gold nanowire is attached to the inside surface of the analyte hole so as to produce SP modes to couple with the core guided modes. Figure 1(b) shows the variation of the effective index of the transverse electric (TE) core guided mode and the TE SP mode with the wavelength. Further, the wavelength dependent confinement losses of the TE core guided mode are shown in Fig. 1 (b). It may be seen from this figure that phase matching between the core mode and SP mode occurs at $\lambda=962 \text{ nm}$ where maximum losses occur. The resonance wavelength is shifted by changing the temperature or analyte refractive index which results in high wavelength sensitivity of $13.1 \text{ nm}/^\circ\text{C}$ and $12700 \text{ nm}/\text{RIU}$ for temperature and analyte refractive index variations, respectively.

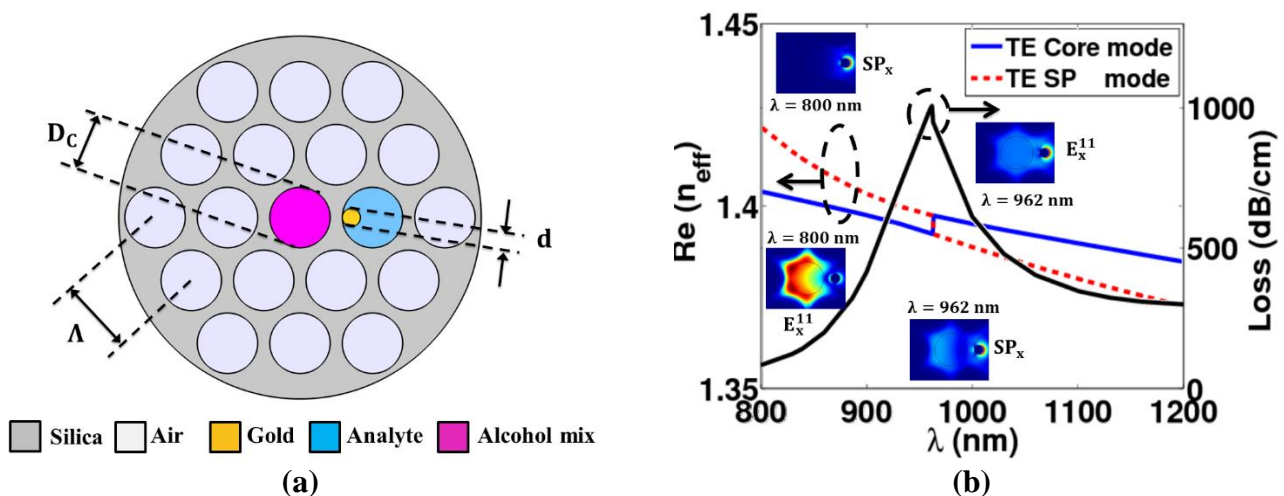


Fig.1 (a) Cross section of the multifunctional SPR-PCF biosensor and (b) Variation of the wavelength dependent effective indices of the quasi TE core mode and SP mode. The confinement losses variation of the quasi TE core mode with the wavelength is also shown in Fig. 1(b). Inset: Field plots of the quasi TE core mode and TE SP mode at different wavelengths.

Reversed phase propagation for hyperbolic surface waves

Taavi Repän¹, Andrey Novitsky¹, Morten Willatzen¹, Andrei Lavrinenko¹,

¹ DTU Fotonik, Technical University of Denmark, Ørsteds Plads 343, DK-2800 Kongens Lyngby, Denmark
tarap@fotonik.dtu.dk

Magnetic properties can be used to control phase propagation in hyperbolic metamaterials. However, in the visible spectrum magnetic properties are difficult to obtain. We discuss hyperbolic surface waves allowing for a similar control over phase, achieved without magnetic properties.

Hyperbolic metamaterials (HMMs) are strongly anisotropic structures, exhibiting metallic properties on one direction while having dielectric properties in the other. This ability of HMMs to allow propagation of waves with short effective wavelengths (i.e. high-k waves) has sparked interest in HMM based devices for subwavelength imaging: hyperlenses [1]. However, broadening due to losses present in a realistic implementation of HMMs is an obstacle for imaging applications. We have recently shown that by employing magnetic properties, this broadening can be significantly reduced by adding a region with reversed phase propagation due to μ -negative HMMs [2].

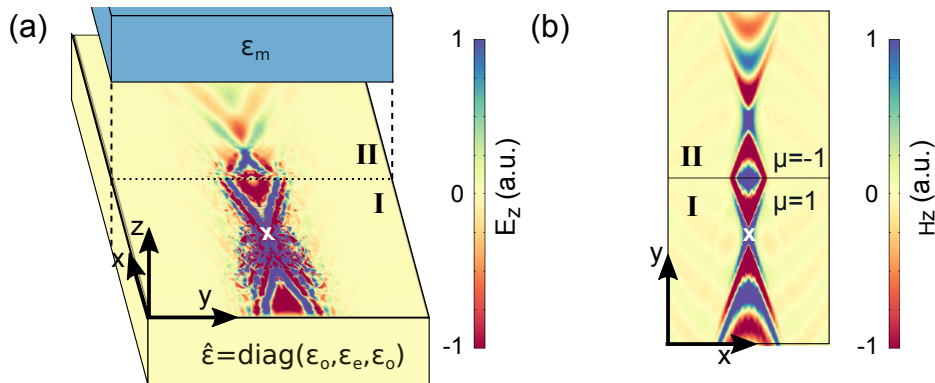


Fig. 1. (a) Geometry of the system, showing both two- and three-layer parts. A point dipole near the surface is used to excite the hyperbolic surface waves. (b) 2D simulation of an analogous case for bulk HMM, with a line source and μ -positive and -negative HMMs. Regions with normal (I) and reversed (II) phase propagation are marked, along with positions of point sources.

The required control over phase propagation can be achieved without magnetic properties in case of surface waves, by using two- and three-layer systems as a counterpart to μ -positive and -negative HMMs, respectively. We study a system composed of an anisotropic metal and a dielectric layer, which supports hyperbolic surface waves (with normal phase propagation). To have region with reversed phase propagation we use a three-layer system, with an additional isotropic metal layer. The system along with numerical simulations is shown in fig. 1. We see that in phase-reversed part the fields are restored towards the original point source. Note that due to lossy media the reconstruction is not perfect.

References

- [1] Zubin Jacob, Leonid V. Alekseyev, and Evgenii Narimanov. Optical hyperlens: Far-field imaging beyond the diffraction limit. *Optics Express*, 14(18):8247, 2006.
- [2] Taavi Repän, Andrey Novitsky, Morten Willatzen, and Andrei V. Lavrinenko. Pseudocanalization regime for magnetic dark-field hyperlenses. *Physical Review B*, 96(19), 2017.

“Cartesian” light: Unconventional propagation of light in a 3D crystal of bandgap cavities

Sjoerd A. Hack^{1,2*}, Jaap J.W. van der Vegt², Willem L. Vos¹

¹ *Complex Photonic Systems, University of Twente, Enschede, The Netherlands*

² *Mathematics of Computational Science, University of Twente, Enschede, The Netherlands*

* s.a.hack@utwente.nl

We explore the unconventional propagation of light in a three-dimensional (3D) crystal of bandgap cavities. Our calculations show that light hops only in the Cartesian x-y-z directions and in the xz-diagonal directions, which differs fundamentally from the conventional spatially-extended Bloch wave propagation.

Ever since the emergence of the field of nanophotonics, it is well-known that fruitful analogies can be drawn between the behavior of photons at the nanoscale on the one hand, and on the other hand the physics of electrons, spins and phonons in condensed matter. In this work, we explore – for the first time ever – the propagation of light in a 3D periodic superstructure of coupled resonant cavities in a 3D photonic-band-gap crystal (Fig. 1). Such a 3D crystal of cavities is the photonic implementation of the Anderson model for spins and electrons, in the limit of zero disorder [1].

Using the plane-wave expansion method, we calculate the dispersion relation of the superstructure. We observe a peculiar diffraction effect, namely that the bandwidth of the dispersion is significantly larger in the xz-diagonal directions than in the other directions in 3D. To understand the underlying physics, we employ the tight-binding method [2]. We find that the light hops only in the Cartesian x-y-z directions and in the xz-diagonal directions (Fig. 2). This situation – 3D hopping of light – differs fundamentally from the conventional spatially-extended Bloch wave propagation.

Recently, our group has started to fabricate 3D crystals of cavities in inverse woodpile photonic crystals [3]. We predict how the modes of a finite superstructure can be observed in our optical experiments, by employing wavefront shaping [4].

References

- [1] P.W. Anderson, *Absence of diffusion in certain random lattices*, Phys. Rev. **109**, 1492-1505 (1958)
- [2] A. Yariv, Y. Xu, R.K. Lee, A. Scherer, *Coupled-resonator optical waveguide: proposal and analysis*, Opt. Lett. **24**, 711-713 (1999)
- [3] D.A. Grishina, C.A.M. Hartevelde, L.A. Woldering, W.L. Vos, *Method for making a single-step etch mask for 3D monolithic nanostructures*, Nanotechnology **26**, 505302 (2015)
- [4] A.P. Mosk, A. Lagendijk, G. Lerosey, M. Fink, *Controlling waves in space and time for imaging and focusing in complex media*, Nat. Photon. **6**, 283-292 (2012)

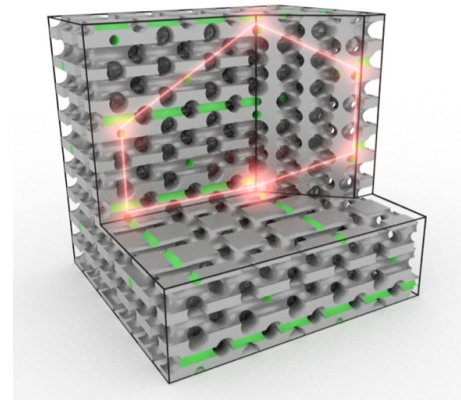


Fig. 1: Cartoon of light hopping in a 3D crystal of cavities

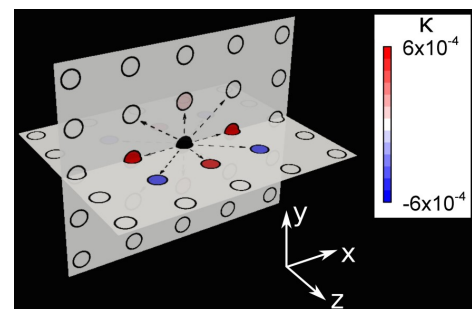


Fig. 2: hopping rates of light from the central cavity to the neighbouring cavities. The sign indicates the bonding character of the two coupled cavities

Design of Apodized and Chirped Bragg Gratings in Subwavelength Grating Metamaterial Waveguides

Jiří Čtyroký^{1*}, Pavel Kwiecien², Ivan Richter², Jens H. Schmid³, Juan Gonzalo Wangüemert-Pérez⁴,
 Íñigo Molina-Fernández⁴, Alejandro Ortega-Moñux⁴, Pavel Cheben³, Ján Litvik⁵, Milan Dado⁵

¹ CAS Institute of Photonics and Electronics, Prague, Czech Republic

² Faculty of Nuclear Sciences and Physical Engineering, Czech Technical University, Prague, Czech Republic

³ National Research Council Canada, Ottawa, Canada

⁴ Universidad de Málaga, Dpto. de Ingeniería Comunicaciones, ETSI Telecomunicación, Málaga, Spain

⁵ University of Žilina, Faculty of Electrical Engineering, Žilina, Slovakia

* ctyrok@ufe.cz

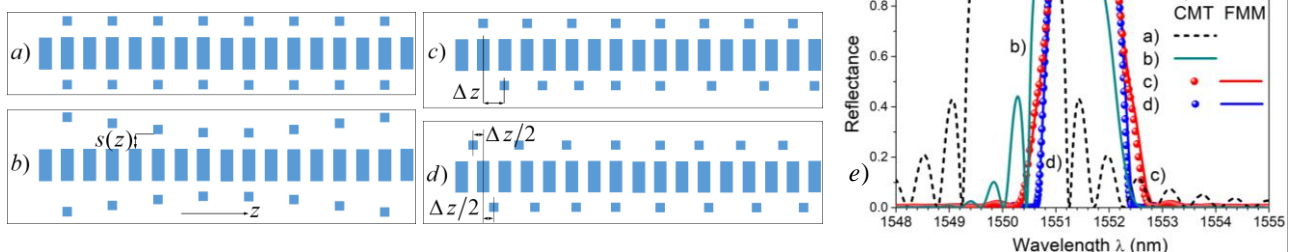
Recently we presented the design of narrow-band Bragg gratings in subwavelength grating metamaterial waveguide and showed that the coupled-mode theory is fully adequate for their analysis. In this contribution we discuss the effects of apodization and chirp of such gratings.

Introduction, motivation, results

Subwavelength grating metamaterial waveguides (SWG) based on silicon-on-insulator (SOI) platform have become important building blocks in silicon photonics devices. SWG refractive index engineering brings unprecedented flexibility to the design of SOI waveguide components without excessive technological demands. We have recently published the first systematic study of narrowband reflection and transmission spectral filters in SOI SWG waveguides comprising Bragg gratings with lateral loading segments [1]. The design was based on assumption that the period of the Bragg grating is twice larger than the period of the SWG core waveguide. As a part of this study we showed that the standard coupled mode theory (CMT) can be successfully applied to the analysis of such gratings, too. Two general approaches toward apodization of such Bragg gratings were also briefly discussed. In this contribution we analyze apodization possibilities in more detail using both the “rigorous” Fourier modal method (FMM) and the CMT. An unintended result of this analysis is that the period of the Bragg grating can be chosen under rather non-restrictive conditions independently of the fundamental period of the SWG waveguide, giving thus the full flexibility to the design of apodized and chirped Bragg gratings on SWG waveguides.

Examples of apodized Bragg gratings in SWG waveguides

An unapodized and three differently apodized Bragg filters in SWG waveguides are schematically depicted in the following figure, together with their spectral reflectances.



Uniform Bragg grating (a) and three designs of cosine-apodized Bragg gratings (b-d) in the SWG waveguide, e) their spectral reflectances calculated by FMM and/or CMT. Design d) gives best results.

References

- [1] J. Čtyroký, J. G. Wangüemert-Pérez, P. Kwiecien, I. Richter, J. Litvik, J. H. Schmid, Í. Molina-Fernández, A. Ortega-Moñux, M. Dado, and P. Cheben, *Opt. Express* 26(1), 179-194. (2018).

Quantum Physics with Plasmons in Graphene and other Atomic-Scale Systems

F. Javier García de Abajo

ICFO-Institut de Ciències Fotoniques, The Barcelona Institute of Science and Technology, 08860 Castelldefels (Barcelona), Spain

javier.garciadeabajo@nanophotonics.es

Plasmons in atomic-scale structures exhibit intrinsic quantum phenomena related to both the finite confinement that they undergo and the small number of electrons on which they are supported. Their interaction with two-level emitters is also evidencing strong quantum effects. In this talk I will discuss several salient features of plasmons in graphene and other atomic-scale materials, and in particular their ability to mediate ultrafast heat transfer [1], the generation of high harmonics [2, 3], their interaction with molecules and quantum emitters [4], and their extreme nonlinearity down to the single-photon level.

References

- [1] R. Yu, A. Manjavacas, and F. J. García de Abajo. Ultrafast radiative heat transfer. *Nat. Commun.*, 8:2, 2017.
- [2] J. D. Cox, A. Marini, and F. J. García de Abajo. Plasmon-assisted high-harmonic generation in graphene. *Nat. Commun.*, 8:14380, 2017.
- [3] J. D. Cox, R. Yu, and F. J. García de Abajo. Analytical description of the nonlinear plasmonic response in nanographene. *Phys. Rev. B*, 96:045442, 2017.
- [4] F. J. García de Abajo and A. Manjavacas. Plasmonics in atomically thin materials. *Faraday Discuss.*, 178:87–107, 2015.

Modelling capture of pump power in the core using deformed step index fibre

D.S. Kumar¹, S.C. Creagh², S. Sujecki¹, T.M. Benson^{1*},

¹ *George Green Institute for Electromagnetics Research, Faculty of Engineering*

² *School of Mathematical Sciences*

University of Nottingham, University Park, Nottingham, NG7 2RD, UK

**trevor.benson@nottingham.ac.uk*

Light propagation in a deformed step index fibre (SIF) is modelled using pixelated phase space. Deformations introduce chaotic trajectories in the fibre that uniformly distribute the power. This improves pump power absorption in the core of proposed rare-earth ion doped SIF lasers and amplifiers for mid-infrared wavelengths.

Mid-infrared (MIR) fibre lasers and amplifiers have been proposed for many applications including imaging, and remote sensing. Such light sources using rare-earth (RE) ions doped in chalcogenide glasses call for schemes in which pump power is efficiently absorbed by the RE ions. In this paper, a passive SIF with deformed core and cladding is modelled with the aim of improving the pump power absorption in the core. The light is propagated using a Poincaré surface of section (phase space) method [1], with the analysis being extended for the first time to include 3D trajectories in the fibre in a pixelated phase space (Figure 1(a)). The phase space transport of the trajectories occurs through both regular and chaotic paths. A phase space is constructed for each inward and outward facing core boundary (core ext. phase space and core int. phase space in Figure 1(a) respectively), and the inward facing outer cladding boundary. Total internal reflection at the outer cladding boundary ensures the propagating light is trapped in the fibre, assuming only classical trajectories. Figure 1(a) shows the phase spaces of a circular chalcogenide glass pair SIF (first row), and that of a similar but deformed SIF (second row). Additional chaotic trajectories are introduced by the fibre deformations and these help spread the power uniformly. The deformations contract the regular regions in the phase space and allow more power to be transported through the chaotic regions. Comparison between a circular SIF and a deformed one shows an improvement in the absorbed power in the latter (Figure 1(b)).

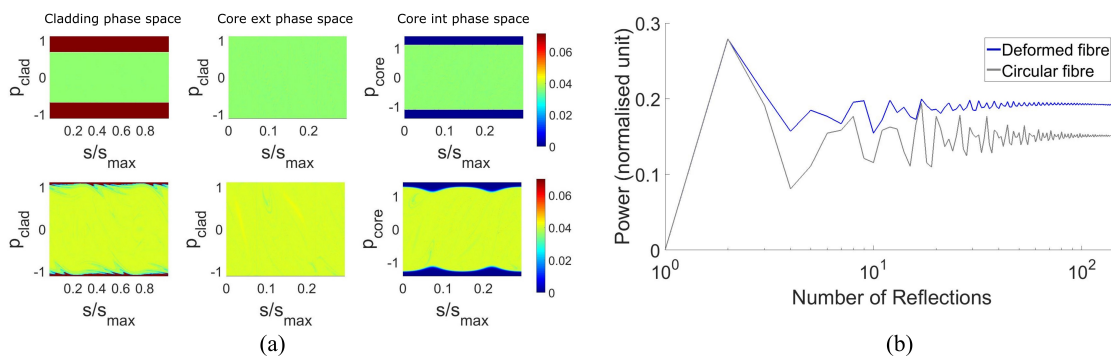


Figure 1. (a) Phase spaces of the cladding and core boundaries of circular (first row) and deformed (second row) SIF; ($n_{core} = 2.7$, $n_{clad} = 2.55$). Chaotic regions of the phase space (green/yellow in the pixelated phase space false colour map) expand with the introduction of the deformation; the regular regions (red/blue) contract. (b) Captured power in the core of a circular SIF and an equivalent deformed SIF following uniform excitation in the cladding phase space.

References

- [1] J. U. Noeckel and A. D. Stone, “Ray and wave chaos in asymmetric resonant optical cavities,” *Nature*, vol. 45, p. 4, 1998. [Online]. Available: <http://arxiv.org/abs/chao-dyn/9806017>

Efficient Optimization of the Trajectory of Photonic Wire Bonds

F. Negredo^{1*}, M. Blaicher³, A. Nestic³, P. Kraft⁴, J. Ott⁴, W. Döfler⁴, C. Koos³, and C. Rockstuhl^{1,2}

¹Institut für Theoretische Festkörperphysik, Karlsruher Institut für Technologie, Germany

²Institut für Nanotechnologie, Karlsruher Institut für Technologie, Germany

³Institut für Photonik und Quantenelektronik, Karlsruher Institut für Technologie, Germany

⁴Fakultät für Mathematik, Karlsruher Institut für Technologie, Germany

*fernando.negredo@kit.edu

We demonstrate a fast and reliable method to estimate losses of single-mode waveguides with an arbitrary 2D trajectory. The method is implemented with the purpose to optimize the trajectory of a photonic wire bond that connects an input and output port of an opto-electronic microchip; in perspective in real-time.

Fundamental Mode Approximation

Photonic Wire Bonds (PWB) [1] are freeform dielectric three-dimensional waveguides. They can be created by 3D Direct Laser Writing Lithography, which provides tremendous flexibility in their fabrication, by enabling arbitrary 3D trajectories and cross-sections. Thus, depending on where output and input ports are located and depending as well on their orientations, obstacles, and height differences, adapted trajectories can be designed.

The challenge is to find an optimum trajectory for the PWB that maximizes the power transmitted through the waveguide. Bending and transition losses are the two key loss factors to consider, from the design point of view. Moreover, such trajectory should be found in a few seconds once the input and output ports are identified. Therefore, we develop a methodology that reliably computes the aforementioned waveguide losses, in a fraction of a second. We rely on the Fundamental Mode Approximation (FMA). It consists in pre-computing the eigenmodes, i.e. their propagation constant and the modal field distribution. Then, transition losses occurring at the interface among waveguides with different curvatures can be readily pre-calculated, and bending losses can be extracted directly from the imaginary part of the propagation constant. Thus, the total loss of a PWB can reliably and quickly be computed, as shown in figure 1.

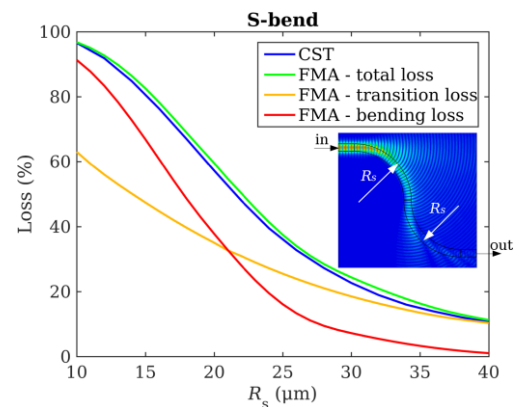


Figure 1. An example of the implementation of the method, where we compare the results obtained using our method and the result obtained via CST Microwave Studio. The S-bend rectangular waveguide considered has core and cladding refractive index of 1.57 and 1.34, respectively. Here, excellent agreement is found from both methods.

Finally, after introducing the methodology for 2D trajectories we discuss an extension of the FMA towards arbitrary 3D trajectories. Having this computational tool at hand is a giant leap to consider photonic wire bonds in the actual fabrication of future opto-electronic integrated systems.

References

- [1] N. Lindenmann, G. Balthasar, D. Hillerkuss, R. Schmogrow, M. Jordan, J. Leuthold, W. Freude, and C. Koos, *Photonic wire bonding: a novel concept for chip-scale interconnects*, *Opt. Express* **20**, 17667-17677, 2012

Spatial separation of electric and magnetic field in toroidal metamaterial

Maria V. Cojocari^{1,2,*}, Alexey A. Basharin,^{1,2,3}

¹ National University of Science and Technology "MISiS", department of Theoretical Physics and Quantum Technology, Moscow, Russian Federation, e-mail address

² Laboratory "Superconducting metamaterials", Moscow, Russian Federation

³ Politecnico di Torino, Department of Electronic and Telecommunications, Torino, Italy

* masha_cojocari@mail.ru

In this paper, we propose a metamaterial with the advantage of spatial field separation, which is determined by combining resonances of two planar metamaterials: one with electric and another with magnetic field strong localizations.

Introduction

Magnetic response of the majority of materials is known to be orders weaker than electrical one. Naturally, such mismatch leads to the suppression of magnetic moments contribution to the light-matter interaction. Stronger capturing of magnetic field was attained by replacing natural materials with metamaterials showing driven permeability. Metamaterials with toroidal dipolar response allow the demonstration of a number of special properties such as novel type of EIT, optical activity, extremely strongly localized fields and anapole.

Metamaterial description

The suggested metamaterial is based on a special structure of high Q-factor planar toroidal metamolecule and its inverted and rotated version. Their unit cells represent two epsilon letters facing each other, resembling torus cross-section: currents excited by incident plane electromagnetic wave start flowing among them asymmetrically. The difference is that in the first type of metamaterials epsilon letters are metallic, while in the second type they are cut out in a piece of metal. First metamaterial supports extremely strong localization of electric field. From the multipole expansion of the metamaterial it can be seen, that the observed sharp resonance of transmission characteristics is determined by the interaction between electric dipole and toroidal moment. In the secondly described metamaterial magnetic field is "captured" in the central wire of the metamolecule. It also supports high Q-factor resonance in the transmission spectrum, which appears as a result of toroidal and magnetic quadrupole moments interaction. In hybrid structure consisted of "electric" and "magnetic" metamolecules there is mutual interference of multipole moments, which leads to the appearance of coupling response in the metamaterial. This response is caused by toroidal moment. It leads to the spatial distribution of the fields, which is supported by a narrow peak in the sample transmission characteristics, which demonstrates full transmission of the incident plane wave through the metamaterial.

Conclusion

To conclude, we proposed a metamaterial, suitable for separation of electric and magnetic field. Its advantage is also high Q-factor resonance, accompanied by low losses in metal. Respectively to the above-mentioned properties, it can be applied to the antennas, qubits and phase shifters.

References

- [1] Basharin, A. A., Chuguevsky, V., Volsky N., Kafesaki, M., Economou E.N., *Extremely high Q-factor metamaterials due to anapole excitation*, Physical Review B, 95 (3), 2017

 **TRR 142**
Tailored Nonlinear Photonics

 **Phoenix Software**
Solutions for Micro and Nano Technologies

JCM | wave

CST
 *joins*  **SIMULIA**